2015

Hugo M. Guzmán Jiménez

Doctoral Thesis

UNIVERSIDAD DE MÁLAGA

Doctoral Thesis

"EXTENSION OF FINITE-CONTROL SET MODEL-BASED PREDICTIVE CONTROL TECHNIQUES TO FAULT-TOLERANT MULTIPHASE DRIVES: ANALYSIS AND CONTRIBUTIONS"

PhD Candidate:
Hugo M. Guzmán Jiménez

Supervisor:
Dr. Mario Javier Durán Martínez
Dr. Federico José Barrero García

Doctoral Program:
Mechatronic Engineering

Electrical Engineering Department, University of Málaga

Málaga, 2015

UNIVERSIDAD DE MÁLAGA

ANDALUCÍA TECH
Campus de Excelencia Internacional
Campus of International Excellence

Doctoral Thesis

"EXTENSION OF FINITE-CONTROL SET MODEL-BASED PREDICTIVE CONTROL TECHNIQUES TO FAULT-TOLERANT MULTIPHASE DRIVES: ANALYSIS AND CONTRIBUTIONS"

PhD Candidate:

Hugo M. Guzmán Jiménez

Supervisor:

Dr. Mario Javier Durán Martínez

Dr. Federico José Barrero García

Doctoral Program: Mechatronic Engineering

A Dissertation Submitted to the Faculty of Electrical Engineering of the University of Málaga in Partial Fulfillment of the Requirements for the Degree of

DOCTOR OF PHILOSOPHY

Electrical Engineering Department, University of Málaga
C/ Doctor Ortiz Ramos s/n. Málaga 29071. Spain.

Málaga, 2015

AUTOR: Hugo Mauricio Guzmán Jiménez
http://orcid.org/0000-0001-8564-2421

EDITA: Publicaciones y Divulgación Científica. Universidad de Málaga

D. Mario Javier Durán Martínez (DNI: 25716851E), profesor titular de Universidad adscrito al Dpto. de Ingeniería Eléctrica de la Universidad de Málaga y tutor/cotutor del doctorando D. Hugo Mauricio Guzmán Jiménez (NIE: X9262205J).

D. Federico José Barrero García (DNI: 28885068N), profesor titular de Universidad adscrito al Dpto. de Ingeniería Electrónica de la Universidad de Sevilla y tutor/cotutor del doctorando D. Hugo Mauricio Guzmán Jiménez (NIE: X9262205J).

CERTIFICAN

Que el trabajo denominado "EXTENSION OF FINITE-CONTROL SET MODEL-BASED PREDICTIVE CONTROL TECHNIQUES TO FAULT-TOLERANT MULTIPHASE DRIVES: ANALYSIS AND CONTRIBUTIONS", cuyo autor es D. Hugo Mauricio Guzmán Jiménez es un trabajo de investigación original, realizado por el alumno como Tesis Doctoral para la obtención del grado de Doctor en Ingeniería

Para que conste a los efectos de presentación y tramitación de la Tesis Doctoral, firmamos la presente el 15 de mayo de 2015.

Fdo.: Mario J. Durán
Profesor titular de Universidad

Fdo.: Federico Barrero
Profesor titular de Universidad

ABSTRACT

Nowadays the world is in the constant need to develop new technologies that are capable of changing from the traditional oil-based energy scheme to a more environmentally friendly energy economy. Research and development projects throughout the world aim to generate new and more efficient systems, capable of either generating energy by renewable energies or to electrify different transportation systems.

Three-phase electrical drives have been traditionally used in energy generation systems and are considered a mature technology. Nonetheless, the inclusion of new energy generation systems and its more recent implementation for transportation means, have posed new challenges regarding the amount of energy they can manage, their efficiency and their reliability. Among the technologies proposed to cope with these challenges, multiphase machines have been recognized in the last few years as a viable solution for applications where the reduction in the total power per phase, the higher overall system reliability and the ability to continue operation under faulty conditions are required. Electric vehicles and railway traction, all-electric ships, more-electric aircraft or wind power generation systems are examples of up-to-date real applications using multiphase machines, most of them taking advantage of the ability to maintain post-fault operation. Among the available multiphase machines topologies, asymmetrical six phase machines and five-phase induction machines with sinusoidally distributed stator windings are the most frequently considered, and a significant amount of research work has been done in the last few years aiming to exploit their advantages and make them an interesting option for industrial applications.

Moreover, the development of more powerful digital signal processors has made possible the adoption of more complex control techniques capable of considering different constraints, working conditions and larger systems. This is the case of predictive controllers, which have been recently proposed for multiphase drive control, considering systems with different number of phases and topologies, for drive operation under torque, speed or current control, common-mode voltage reduction and sensorless operation, among many others.

The purpose of this Doctoral Thesis work is to extend predictive control schemes for multiphase drives, more specifically finite-control set model-based predictive control, to the fault-tolerant operation, exploiting the fault tolerance that multiphase drives possess and ensure efficient and controlled post-fault operation. Although the research of this Thesis is suitable for any type of multiphase drive, the study has been particularized for a five-phase induction motor with sinusoidally distributed windings and fed by a two-level inverter. Two main types of faults are studied, namely, the open-phase fault and the IGBT-gating failure. Due to the nature of predictive controllers, an accurate system model under the different working conditions is necessary in order to properly select the best control action (voltage vector) to be applied to the power converter. Consequently, the electrical drive modeling equations have been studied and the effect of the different types of faults on the electrical machine and the power converter are considered.

This Doctoral Thesis contribution is divided in three journal papers published in the *IEEE Transactions on Industrial Electronics*. The first journal paper discusses the proposed open-phase fault-tolerant scheme based on finite-control set model based predictive control and the electrical drive modeling under an open-phase fault. The controllers' performance is verified through a set of experimental tests, subjecting the electrical drive to different working conditions, considering pre-fault operation, the transition between normal and post-fault operation and finally, post-fault operation considering different criteria such as reducing copper losses or ensuring minimum drive derating. The second journal paper considers an IGBT-gating fault in both semiconductors of the same phase, leading to a non-controlled current in the five-phase drive. The effect that such type of fault has on the electrical drive and on the proposed open-phase predictive controller is assessed, demonstrating that the proposed fault-tolerant scheme is capable of managing this type of fault at the expense of a negligible extra torque derating. Finally, an experimental comparison between a fault-tolerant linear control scheme based on proportional-resonant regulators and the proposed predictive fault-tolerant scheme is presented in the third journal paper. As in previous papers, the controller's performance is evaluated and compared under different working conditions and criteria, providing further insight on the specific benefits of each control scheme.

The journal papers discussed in this Doctoral Thesis are:

1. H. Guzman, M.J. Duran, F. Barrero, B. Bogado, S. Toral, "Speed Control of Five-Phase Induction Motors With Integrated Open-Phase Fault Operation Using Model-

Based Predictive Current Control Techniques," *IEEE Transactions on Industrial Electronics*, vol. 61, no. 9, pp. 4474-4484, Sept. 2014.

2. H. Guzman, F. Barrero, M. Duran, "IGBT-Gating Failure Effect on a Fault-Tolerant Predictive Current Controlled 5-Phase Induction Motor Drive," *IEEE Transactions on Industrial Electronics*, vol. 62, no. 1, pp. 15-20, Jan. 2015.
3. H. Guzman, M. J. Duran, F. Barrero, L. Zarri, B. Bogado, I. Gonzalez Prieto, M. R. Arahal. "Comparative Study of Predictive and Resonant Controllers in Fault-Tolerant Five-Phase Induction Motor Drives", *IEEE Transactions on Industrial Electronics*, DOI: 10.1109/TIE.2015.2418732.

ACKNOWLEDGMENTS

I would like to specially thank my parents, sister and grandparents whose support has been unconditional, their kind words when needed and their love, made possible the culmination of this work.

To Tatiana for accompanying me in this journey and helping me to discern between what's important and what's not.

To Vite and Joel. I'll always look forward to see you. Thank you for your friendship, your support and all the moments we enjoyed.

To my friends in this second home, Spain. All of you that have accompanied us since the beginning up until the end. You that made us feel welcome in Seville and in Málaga. Who shared your life with us and tried to make us feel at home.

To my friends in Colombia, who always stood by my side and received me with a big smile.

To Federico and Mario, who guided me through this work. You where my advisors when needed, and always my friends. You pushed me continuously to do better and together we succeeded. Thank you for welcoming us into your families and sharing with us your life.

TABLE OF CONTENTS

Abstract ..... **I**

Acknowledgements ..... **IV**

Table of Contents ..... **V**

List of Figures ..... **IX**

Chapter 1:

1 Motivation, Objectives and Document Organization **1**

1.1 Motivation Behind this Work **1**

1.2 Objectives **2**

1.2.1 General Objectives **2**

1.2.2 Specific Objectives **2**

1.3 Document Organization **2**

Chapter 2:

2 Multiphase Drives: Generalities, Modeling and Control **4**

2.1 Introduction **4**

2.2 Modeling **8**

2.2.1 Multiphase Induction Machine Modeling **9**

2.2.1.1 Phase Variable Model **10**

2.2.1.2 Stationary Reference Frame **12**

2.2.1.3 Rotating Reference Frame **17**

2.2.2 Multiphase Power Converter Modeling **19**

2.3 Standard Control Techniques **23**

2.3.1 Field Oriented Control **24**

2.3.2 Direct Torque Control **28**

2.4 Predictive Control 32

2.4.1 Finite-Control Set Model-Based Predictive Control 34

2.4.1.1 Predictive Current Control 39

2.4.1.2 Predictive Torque Control 40

2.4.1.3 Restrained Search Predictive Control 42

2.5 Fault-Tolerance in Multiphase Drives 43

2.5.1 Multiphase Machine Faults 45

2.5.1.1 Stator Faults 46

2.5.1.2 Rotor Faults 46

2.5.1.3 Eccentricity Faults 47

2.5.1.4 Bearing Faults 47

2.5.1.5 Bent Shaft Faults 47

2.5.2 Sensor Faults 47

2.5.3 Power Converter Faults 49

2.5.4 Fault-Tolerant Control Techniques 50

2.5.4.1 Drive Derating 51

2.5.4.2 Post-Fault Machine Modeling 53

2.5.4.3 Post-Fault Current Reference 54

2.5.4.4 Post-Fault Control Techniques 56

2.5.4.4.1 Hysteresis Controllers 57

2.5.4.4.2 Robust Controllers 58

2.5.4.4.3 Proportional-Integral Controllers 58

2.5.4.4.4 Proportional-Resonant Controllers 60

2.6 Summary 61

2.7 References 62

Chapter 3:

3 Contributions 72

3.1 Introduction 72

3.2 Fault-Tolerant FCS-MPC for Multiphase Drives Under an Open-Phase Fault 73

3.3 IGBT-Gating Fault Effect in Fault-Tolerant Multiphase Induction Drives 76

3.4 Performance Analysis of Fault-Tolerant FCS-MPC and Linear Control Techniques 79

3.5 Journal Papers 82

Journal Paper 1 83

Journal Paper 2 95

Journal Paper 3 101

3.6 Summary 113

Chapter 4:

4 Conclusions and Future Work 115

4.1 Conclusions 115

4.1.1 Summary of Additional Research Work 116

4.2 Future Work 117

Capítulo 5:

5 Resumen en Español de la Tesis Doctoral 119

5.1 Motivación de la Tesis Doctoral 119

5.2 Objetivos 120

5.2.1 Objetivo General 120

5.2.2 Objetivos Específicos 120

5.3 Organización del Documento 121

5.4 Accionamientos Multifásicos: Generalidades, Modelado y Control 121

5.5 Contribuciones 125

5.5.1 Control Tolerante a Fallos Basado en FCS-MPC para Accionamientos Multifásicos Ante un Fallo de Fase Abierta 126

5.5.2 Fallo en el Disparo de los IGBT's en Accionamientos de Inducción Multifásicos Tolerantes a Fallos 128

5.5.3 Análisis Comparativo entre Controles Tolerantes a Fallos Basados en FCS-MPC y Controles Lineales 130

5.6 Conclusiones 132

5.7 Resumen de Trabajos de Investigación Adicionales.....134

5.8 Trabajo Futuro.....135

LIST OF FIGURES

2.1 Five-phase two-level induction motor drive scheme 8

2.2 Five-phase induction machine scheme 9

2.3 Five-phase induction machine equivalent circuit in the (α, β, x, y) planes 16

2.4 Park rotating reference frame 18

2.5 Five-phase induction machine equivalent circuit in the (d, q, x, y) planes 19

2.6 Five-phase two-level drive load configuration scheme 21

2.7 Space Vector Diagrams in the α–β (left side) and x–y (right side) planes 22

2.8 Rotating reference frame aligned to the rotor components 25

2.9 Field Oriented Control scheme for five-phase drive 26

2.10 Direct Torque Control scheme for five-phase drive 29

2.11 Modified DTC scheme with two lookup tables for five-phase drive 31

2.12 Modified DTC scheme with virtual vector lookup table for five-phase drive 31

2.13 Predictive control methods 32

2.14 Finite-Control Set Model-Based Predictive Control scheme 34

2.15 FCS-MPC flow diagram 35

2.16 FCS-MPC prediction horizon principle 36

2.17 FCS-MPC based Predictive Current Control with an outer speed control loop 39

2.18 FCS-MPC based Predictive Torque Control with an outer speed control loop 41

2.19 FCS-MPC based Restrained Search Predictive Control 43

2.20 Multiphase drive types of faults 45

2.21 Post-fault control scheme based on hysteresis controllers 58

2.22 Post-fault control scheme based on PI controllers 59

2.23 Post-fault control scheme based on PI and PR controllers 60

3.1 Pre- and post- fault drive topology and proposed control scheme based on an outer speed and flux loop and an inner open-phase fault-tolerant FCS-MPC current control 74

3.2 Mapping of the α–β components for the five-phase system under normal (a) and open-phase fault operation implementing the traditional Clarke transformation (b) and the modified Clarke transformation (c) 75

3.3 Electrical drive topology reconfiguration under IGBT-Gating failure and control scheme based on an outer speed and flux loop and an inner fault-tolerant FCS-MPC current control 78

3.4 Pre- and post- fault drive topology and implemented control scheme based on an outer speed and flux loop and an inner open-phase fault-tolerant PR controller 81

CHAPTER: 1

MOTIVATION, OBJECTIVES AND DOCUMENT ORGANIZATION

1.1 MOTIVATION BEHIND THIS WORK

Electrical machines constitute one of the cornerstones of renewable energies and electric vehicle propulsion. The constant necessity for higher power ratings in order to either generate more energy or to provide electromechanical force for larger vehicles, has motivated research and development activities in multiphase drives. The ability to manage more power with lower torque pulsation and lower current harmonic content and achieve higher fault-tolerance capability, than conventional three-phase drives [1], makes them an ideal candidate for applications where reliability is of special interest for economical and/or safety reasons.

Although up until now multiphase drives implementation in industry applications is not widely spread, it is foreseeable that with the development of larger wind energy turbines and the advances on more electric aircrafts, ships and vehicles, with higher fault-tolerance standards and requirements, multiphase machines will gain significant interest. Recent research work on multiphase drives aims to exploit multiphase machines special characteristics and present them to the industry as a viable solution for different applications, regarding its higher number of phases not as an increase on its implementation complexity, but as a higher control and design degrees of freedom, that can improve overall reliability and performance. Consequently, different control techniques aiming for high speed or high torque operation, fault resiliency under different types of faults, types of winding and multi-drive and multi-motor connections, have been proposed.

The following Doctoral thesis work is focused on the study of multiphase machines under different fault conditions and the development/comparison of control strategies that are capable of ensuring post-fault operation.

1.2 OBJECTIVES

The general and specific objectives of this Doctoral Thesis work are:

1.2.1 GENERAL OBJECTIVE

The extension of predictive control schemes for multiphase drives, more specifically finite-control set model-based predictive control, to the fault-tolerant operation, exploiting the fault-tolerance capability that multiphase drives possess and ensure efficient and controlled post-fault operation.

1.2.2 SPECIFIC OBJECTIVES

- Research on multiphase motors, their advantages, disadvantages and their industrial application in electric vehicle propulsion and wind energy generation systems.
- Analyze the effect of different types of faults on the electrical drive and develop new and interesting mathematical models for multiphase drives under different fault conditions.
- Study of multiphase drives control techniques under pre- and post-fault working conditions.
- Identify the post-fault system limitations and constraints, considering a five-phase induction drive with two level voltage source inverters, and propose different fault-tolerant management techniques in order to ensure the maximum energy optimization.
- Study and analyze conventional three-phase predictive control strategies and extend them to multiphase drives and fault-tolerance.
- Implement, compare and assess the performance of fault-tolerant linear and predictive control techniques under different working conditions operation.

1.3 DOCUMENT ORGANIZATION

This Doctoral thesis is organized following the directives given by the University of Málaga for an article compendium thesis. The document is divided in three main parts. In the first part, the motivation and objectives of this doctoral research work are presented (Chapter 1), along with the generalities and the state of the art of multiphase drives (Chapter 2), where a thorough study of the available scientific publications on multiphase drives modelling and control techniques under pre-

and post-fault operation are presented. Subsequently, the thesis contributions and its analysis is then presented in the second part (Chapter 3). The first two contributions are based on the proposal (Journal paper 1) of a fault-tolerant model-based predictive controller for five-phase induction machines under open-phase faults and the subsequent study (Journal paper 2) of such controller under an IGBT-gating failure. The third contribution is based on a comparative analysis of the proposed fault-tolerant predictive controller with a fault-tolerant proportional resonant controller, further clarifying the main advantages and disadvantages of each controller under an open-phase fault situation (Journal paper 3). Finally, a summary of the journal papers, conference works, patents and research projects behind this doctoral thesis (which were not included as the main contributions), along with conclusions and future work, are presented in the third part of the document (Chapter 4).

CHAPTER: 2

MULTIPHASE DRIVES: GENERALITIES, MODELING AND CONTROL

2.1 INTRODUCTION

In this chapter a thorough literature review on five-phase induction machines and power converters modeling equations is presented. Correspondingly some of the standard linear, nonlinear and predictive control techniques, available in the literature for multiphase drives operation are discussed.

Multiphase motor drives, based on electrical machines with more than three phases, were proposed nearly 50 years ago. However, they have only gained special attention of the research community during the past few years after the development of high power and high switching frequency semiconductor devices, like IGBT's, and powerful microelectronic control units, like DSP's and FPGA's [1], enabling efficient and proper control of multiphase machines. This has led researchers to propose multiphase drives technology for high performance, high power and fault-tolerant applications such as wind energy generation [2], aerospace [3] and vehicle propulsion [4, 5]. Regarding industrial implementations, multiphase drives can be found in i) ultra-high speed elevators [6], using a nine-phase permanent-magnet machine controlled by three three-phase power converters, ii) ship propulsion [7, 8], where an Alstom "Advanced Induction Motor" of 20 MW, fifteen-phase with three independent neutral points and controlled by three five-phase power converters, was implemented in a US Navy electric ship prototype and iii) the refrigeration string of a Liquefied Natural Gas (LNG) installation as reported in [8], where a 45 MW, 7200 volts, twelve-phase motor, with four independent neutral points, controlled by four IGBT based, three-phase cascaded multilevel converters was designed and constructed. Previous uses prove that multiphase drives are a viable solution for high power, safety critical applications and capable of meeting industry standards.

Some of the advantages of multiphase drives when compared with standard three-phase motor

drives [1, 9, 10, 11] are:

1. Improved spatial distribution of the Magneto Motive Force (MMF) in the machine air gap [9], reducing rotor copper losses.
2. Lower harmonic content in the stator excitation currents.
3. Lower torque pulsations. Multiphase machines are less susceptible to torque pulsations at low frequencies, the lowest torque pulsation frequency in an n-phase machine is caused by harmonics of the order $(2n \pm 1)$.
4. Less harmonic content in the DC-Link currents.
5. Improved power distribution. For a given nominal power, the current rating through each phase decreases as the number of phases increases.
6. Higher number of control degrees of freedom, allowing:
    a. High torque density drives: In multiphase machines with concentrated windings, it is possible to use the lower current harmonic components (third harmonic in a five-phase machine, third and fifth harmonics in a seven-phase machine, and so on) to increase torque production capability [12, 13].
    b. Multimotor drives. By connecting in series the stator windings of a set of distributed windings multiphase machines, different number of machines can be independently controlled with only one power converter [14, 15].
    c. Fault-Tolerant Drives: More reliable than their three-phase counterparts. In a three phase machine in case of an open-phase fault, the machine can still work as a one-phase machine but it would need external equipment in order to start up the machine and control torque oscillations. On the other hand, an n-phase machine with one or more of its phases in fault condition (depending on its total number of phases (n) and its constructive characteristics), could continue developing a rotating field as long as the number of open-circuited phases is no more than $(n - 3)$, at the expense of lower torque and current ratings, without requiring external equipment.

Multiphase machines are traditionally classified depending on the winding distribution as concentrated or distributed windings' machines and on the winding arrangement like symmetrical or asymmetrical machines. Concentrated windings' multiphase machines generate a high harmonic field flux content when a sinusoidal stator voltage is applied, which can be used to enhance the electrical

torque production. However, this flux harmonic content only generates electromagnetic losses in the machine if the distributed winding topology is used. On the other hand, symmetrical machines are formed by consecutive phase windings equally displaced $2\pi/n$, while asymmetrical machines are formed by independent set of windings displaced π/n.

Moreover, multiphase machines can be further classified by the number of odd or even phases they possess [17, 18, 19] and if the number of phases is multiple of three [20, 21, 22]. Among machines with an even number of phases, six-phase machines are the most common ones in scientific literature. These type of machines can be found with asymmetrical (30°) or symmetrical (60°) winding distribution and single or dual neutral points. However, the most commonly used structure is based on two three-phase asymmetric windings and two independent neutral points, also called dual three-phase machines. A considerable body of knowledge has been developed regarding the modeling of these machines [22], and their control techniques (based on field oriented [23, 24, 25, 26], direct torque [27, 28], or predictive control [29, 30]) or modulation strategies [31, 32, 33]. On the other hand, machines with an odd number of phases are sometimes preferred for their inherent symmetric structure. These types of machines are constructed in star-winding connection, with a single neutral and can be found either with concentrated or distributed windings. This is the case of five-phase machines, where several modulation and control techniques have been proposed in the literature, based on carrier-based pulse width modulation and space vector modulation [34, 35, 36], field oriented control [13, 37, 38], direct-torque control [39, 40] and predictive control [41, 42], aimed to exploit the advantages multiphase machines possess, maintaining sinusoidal or non-sinusoidal stator voltages, depending on the winding distribution.

Furthermore, depending on whether the number of phases it possesses is a prime number or not, different winding dispositions can be obtained, resulting in machines with single neutral, multiple neutral points or with polygon configuration. The effect of the winding configuration during different working states has been analyzed in [43, 44, 45], where it has been shown that properly changing the stator winding configuration can benefit torque/speed operation. An n-phase machine stator windings can be connected in $((n+1)/2)$, different configurations. For instance a five-phase drive can be connected in star, pentagon or pentacle configuration, where for the same DC-Link voltage and drive power rating, the voltage across the winding is higher in the pentacle configuration, followed by the pentagon and star connection and conversely phase currents are higher in star connection followed by pentagon and pentacle configurations. As a result, star winding configuration will provide higher

torque with lower speed operation, while pentagon winding connection will provide less torque but slightly more speed and finally pentacle connection will provide high speed operation at lower torque.

As was demonstrated in [46, 47], it is possible to control multiple series connected multiphase machines from a single power converter by connecting each of the machines stator windings in series with a particular phase transposition in order to decouple the effect of the currents producing torque and flux of one machine in the other set of machines. Multimotor drive configuration has been studied implementing five- and six-phase machines [48, 49, 50], as well as topologies consisting of machines with different number of phases or different types of machines [51, 52]. By implementing multiple Field Oriented Control (FOC) loops, one for each pair of currents in the Vector Space Decomposition (VSD) frame, it is possible to properly exploit the additional degrees of freedom that multiphase drives possess and control for example in a five-phase drive, two machines independently. Phase winding transposition is made in order to ensure that one machines d-q currents represent the x-y currents of the remaining machine, and therefore do not influence the torque production. Consequently, the d-q current components are used to control torque and flux production of the first machine and the x-y current components are used to control, in a similar way, torque and flux components of the second machine. Nonetheless, multimotor drive topology results in an increase of copper losses and does not provide fault-tolerant operation capability, due to the fact that the additional degrees of control freedom exploited, in multiphase drives, for fault-tolerance are used in order to independently control each machine. Furthermore, multimotor drive configuration is not feasible with concentrated winding machines due to the fact that x-y current components influence torque production and consequently independent control of each multiphase machine is not possible.

As can be seen, multiphase drives are an interesting technology, formed by a considerable number of machines and power converter topologies. Their special benefits and capabilities have made them attractive within research community and some industrial applications, stating their future importance as transportation and energy generation increase their power ratings. Thus the need for continuous research on the subject is justified in order to meet industry and safety standards while exploiting multiphase machines benefits at reasonable costs.

2.2 MODELING

The general scheme of the multiphase drive used in this doctoral thesis is presented in Fig. 2.1. The system consists of a two-level IGBT based power converter and a five-phase induction machine. In first place, the modeling equations for the distributed winding five-phase induction machine will be described and the physical model of the machine in phase variables will be studied. Then, in order to reduce the model complexity and the number of state variables necessary to control the machine, the model is analyzed in the stationary (α, β, x, y) reference frame using the Clarke transformation. Next, for control purposes, the machine model will be analyzed in the rotating $(d\text{-}q)$ reference frame, by means of the Park transformation. Finally, the power converter modeling will be addressed. The phase and line voltages dependent on the inverter switching state will be studied, the available voltage space vectors in the (α, β, x, y) planes and drive load configuration will be depicted and the effect of voltage vectors in the common-mode voltage will be presented.

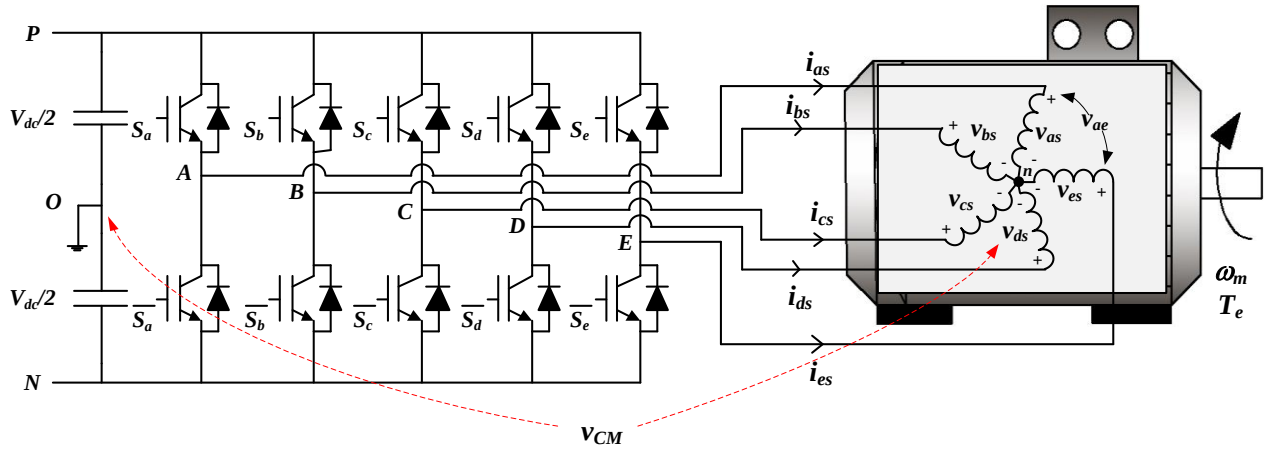

Fig. 2.1.: Five-phase two-level induction motor drive scheme.

The induction machine under study is based on a 30-slots, three-phase induction machine with 2-pairs of poles (P) whose stator has been rewound to obtain a five-phase ($n = 5$) induction machine with 3 pairs of poles. The stator is formed by five windings evenly distributed around the stator circumference with an electrical displacement of $\vartheta = 2\pi/5 = 72°$ and the rotor has a squirrel cage single-neutral topology, equivalent to five windings evenly distributed with an electrical displacement of 72°, as shown in Fig. 2.2.

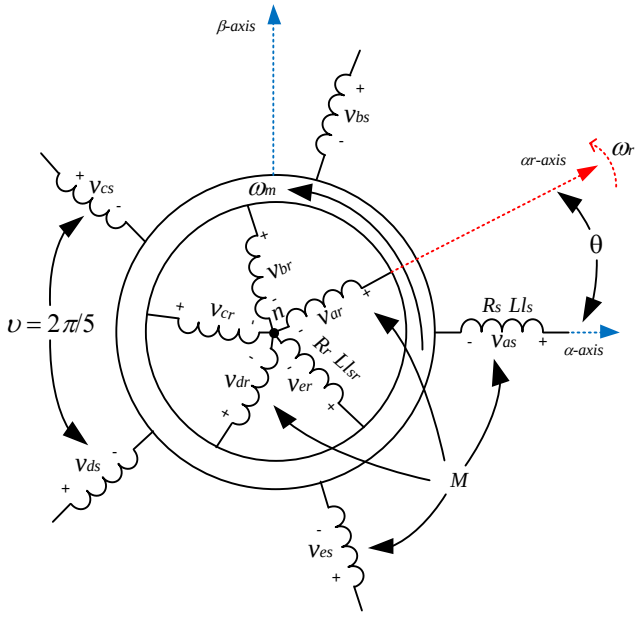

Fig. 2.2.: Five-phase induction machine scheme.

Two different approaches can be considered when modeling electrical machines namely, the phase variable model [10] and the vector space decomposition. The VSD method [31, 53] considers the machine variables in a stationary reference frame or in a dynamic or rotating reference frame. In what follows, VSD is applied to obtain the machine's model, considering the machines variables in the stationary reference frame and implementing the Clarke transformation matrix. The machine has been also modeled assuming the following hypotheses:

1. The machine is constituted by identical windings equally distributed around the stator and rotor. The rotor has a squirrel cage topology.
2. The magnetic field saturation, mutual leakage inductances and the core losses due to parasite currents are neglected.
3. The machine air gap is considered constant.
4. The machine reluctance is independent of the rotor position.
5. The effect of non-null spatial harmonics on the flux and torque is a non-modeled effect that is considered a perturbation.

2.2.1 MULTIPHASE INDUCTION MACHINE MODELING

Let us in the first place analyze the electrical model of the machine in healthy operation. This topic has been widely analyzed in the literature [1, 9] and constitutes the point of reference for understanding the effect different fault conditions have on the machines model.

2.2.1.1 PHASE VARIABLE MODEL

The five-phase induction machine can be described by a set of stator and rotor phase voltage equilibrium equations referred to a fixed reference frame linked to the stator as follows (Fig. 2.2).

$$[V_s] = [R_s][I_s] + \frac{d}{dt}[\lambda_s] = [R_s][I_s] + [L_{ss}]\frac{d}{dt}[I_s] + \frac{d}{dt}[L_{sr}(\theta)][I_r] \quad (1)$$

$$[V_r] = [R_r][I_r] + \frac{d}{dt}[\lambda_r] = [R_r][I_r] + [L_{rr}]\frac{d}{dt}[I_r] + \frac{d}{dt}[L_{rs}(\theta)][I_s] \quad (2)$$

where θ represents the rotor electrical angular position with respect to the stator, and rotates at the rotor electrical velocity ω_r.

The stator/rotor voltage, flux and current phase vectors are expressed as in (3)-(8), being the voltage rotor components equal to zero due to the rotor squirrel cage topology.

$$[V_s] = [v_{as}\ v_{bs}\ v_{cs}\ v_{ds}\ v_{es}]^T \quad (3)$$

$$[V_r] = [v_{ar}\ v_{br}\ v_{cr}\ v_{dr}\ v_{er}]^T \quad (4)$$

$$[\lambda_s] = [\lambda_{as}\ \lambda_{bs}\ \lambda_{cs}\ \lambda_{ds}\ \lambda_{es}]^T \quad (5)$$

$$[\lambda_r] = [\lambda_{ar}\ \lambda_{br}\ \lambda_{cr}\ \lambda_{dr}\ \lambda_{er}]^T \quad (6)$$

$$[I_s] = [i_{as}\ i_{bs}\ i_{cs}\ i_{ds}\ i_{es}]^T \quad (7)$$

$$[I_r] = [i_{ar}\ i_{br}\ i_{cr}\ i_{dr}\ i_{er}]^T \quad (8)$$

The transformation relationship between stator-rotor components depends on the number of turns in the stator (N_s) and the number of turns in the rotor (N_r), as stated by (9). Taking this into account the rotor electrical parameters referred to the stator can be defined by (10)-(13).

$$k_w = \frac{N_s}{N_r} \quad (9)$$

$$[I_r'] = \frac{1}{k_w}[I_r] \quad (10)$$

$$[V_r'] = k_w[V_r] \quad (11)$$

$$[\lambda_r'] = k_w[\lambda_r] \quad (12)$$

$$[R_r'] = {k_w}^2[R_r] \quad (13)$$

The stator/rotor resistance and inductance matrices are defined as:

$$[R_s] = \begin{bmatrix} R_s & 0 & 0 & 0 & 0 \\ 0 & R_s & 0 & 0 & 0 \\ 0 & 0 & R_s & 0 & 0 \\ 0 & 0 & 0 & R_s & 0 \\ 0 & 0 & 0 & 0 & R_s \end{bmatrix} \quad [R_r] = \begin{bmatrix} R_r & 0 & 0 & 0 & 0 \\ 0 & R_r & 0 & 0 & 0 \\ 0 & 0 & R_r & 0 & 0 \\ 0 & 0 & 0 & R_r & 0 \\ 0 & 0 & 0 & 0 & R_r \end{bmatrix} \quad (14)$$

$$[L_{ss}] = L_{ls}[I_5] + M[\Lambda(\vartheta)] \quad (15)$$

$$[L_{rr}] = L_{lr}[I_5] + M[\Lambda(\vartheta)] \tag{16}$$

$$[\Lambda(\vartheta)] = \begin{bmatrix} 1 & \cos(\vartheta) & \cos(2\vartheta) & \cos(3\vartheta) & \cos(4\vartheta) \\ \cos(4\vartheta) & 1 & \cos(\vartheta) & \cos(2\vartheta) & \cos(3\vartheta) \\ \cos(3\vartheta) & \cos(4\vartheta) & 1 & \cos(\vartheta) & \cos(2\vartheta) \\ \cos(2\vartheta) & \cos(3\vartheta) & \cos(4\vartheta) & 1 & \cos(\vartheta) \\ \cos(\vartheta) & \cos(2\vartheta) & \cos(3\vartheta) & \cos(4\vartheta) & 1 \end{bmatrix} \tag{17}$$

Due to the machines symmetry, it is assumed that the number of turns in the stator and rotor are the same. Thus, the stator-rotor and rotor-stator mutual inductances are the same and identified by (M) [53], making possible to conclude that:

$$[L_{sr}(\theta)] = [L_{rs}(\theta)]^T = M[\Psi(\theta)] \tag{18}$$

$$[\Psi(\theta)] = \begin{bmatrix} \cos(\Delta_1) & \cos(\Delta_2) & \cos(\Delta_3) & \cos(\Delta_4) & \cos(\Delta_5) \\ \cos(\Delta_5) & \cos(\Delta_1) & \cos(\Delta_2) & \cos(\Delta_3) & \cos(\Delta_4) \\ \cos(\Delta_4) & \cos(\Delta_5) & \cos(\Delta_1) & \cos(\Delta_2) & \cos(\Delta_3) \\ \cos(\Delta_3) & \cos(\Delta_4) & \cos(\Delta_5) & \cos(\Delta_1) & \cos(\Delta_2) \\ \cos(\Delta_2) & \cos(\Delta_3) & \cos(\Delta_4) & \cos(\Delta_5) & \cos(\Delta_1) \end{bmatrix} \tag{19}$$

Notice that $[I_5]$ is the identity matrix of order 5, Δ_i angles are defined as: $\Delta i = \theta + (i-1)\vartheta$, being $i = \{1,2,3,4,5\}$, L_{ls} and L_{lr} are the stator and rotor leakage inductances and $\vartheta = 2\pi/5$ is the windings electrical displacement.

The electromagnetic torque can be calculated by [54]:

$$T_e = \frac{d}{d\theta} W_{co} = \frac{P}{2} \begin{bmatrix} [I_s] \\ [I_r] \end{bmatrix}^T \frac{d}{d\theta} \begin{bmatrix} L_{ss} & L_{sr}(\theta) \\ L_{rs}(\theta) & L_{rr} \end{bmatrix} \begin{bmatrix} [I_s] \\ [I_r] \end{bmatrix} \tag{20}$$

Which further developing can be expressed as:

$$T_e = \frac{P}{2} \cdot \begin{bmatrix} [I_s] \\ [I_r] \end{bmatrix}^T \begin{bmatrix} 0 & \frac{d}{d\theta} L_{sr}(\theta) \\ \frac{d}{d\theta} L_{rs}(\theta) & 0 \end{bmatrix} = \frac{P}{2} \left[[I_s]^T \frac{d}{d\theta} L_{sr}(\theta)[I_r] + [I_r]^T \frac{d}{d\theta} L_{rs}(\theta)[I_s] \right] \tag{21}$$

where $[L_{sr}(\theta)] = [L_{rs}(\theta)]^T$, therefore:

$$[I_r]^T \left[\frac{d}{d\theta} L_{rs}(\theta) \right] [I_s] = [I_s]^T \left[\frac{d}{d\theta} L_{sr}(\theta) \right] [I_r] \tag{22}$$

And the electromagnetic torque will be:

$$T_e = P[I_s]^T \left[\frac{d}{d\theta} L_{sr}(\theta) \right] [I_r] \tag{23}$$

$$\begin{aligned} T_e = -PM[&(i_{as} \cdot i_{ar} + i_{bs} \cdot i_{br} + i_{cs} \cdot i_{cr} + i_{ds} \cdot i_{dr} + i_{es} \cdot i_{er}) \sin(\theta) \\ &+ (i_{as} \cdot i_{br} + i_{bs} \cdot i_{cr} + i_{cs} \cdot i_{dr} + i_{ds} \cdot i_{er} + i_{es} \cdot i_{ar}) \sin(\theta - \vartheta) \\ &+ (i_{as} \cdot i_{cr} + i_{bs} \cdot i_{dr} + i_{cs} \cdot i_{er} + i_{ds} \cdot i_{ar} + i_{es} \cdot i_{br}) \sin(\theta - 2\vartheta) \\ &+ (i_{as} \cdot i_{dr} + i_{bs} \cdot i_{er} + i_{cs} \cdot i_{ar} + i_{ds} \cdot i_{br} + i_{es} \cdot i_{cr}) \sin(\theta - 3\vartheta) \\ &+ (i_{as} \cdot i_{er} + i_{bs} \cdot i_{ar} + i_{cs} \cdot i_{br} + i_{ds} \cdot i_{cr} + i_{es} \cdot i_{dr}) \sin(\theta - 4\vartheta)] \end{aligned} \tag{24}$$

Finally, the machines speed, which depends on the electromagnetic torque will be:

$$J_m \frac{d}{dt}\omega_m = T_e - T_L - B_m\omega_m \tag{25}$$

Notice that ω_m is the rotor mechanical speed, T_L is the load mechanical torque applied to the machine axis, J_m is the rotational inertia and B_m is the rotor-load friction coefficient.

2.2.1.2 STATIONARY REFERENCE FRAME

In order to eliminate the dependence of the coupling inductances with time and divide the model in a set of three independent-orthogonal equations, the Clarke transformation is applied to the machine model [10]. The power invariant decoupling Clarke transformation matrix (T_c) is defined as follows:

$$[T_c] = \sqrt{\frac{2}{5}}\begin{bmatrix} 1 & \cos(\vartheta) & \cos(2\vartheta) & \cos(3\vartheta) & \cos(4\vartheta) \\ 0 & \sin(\vartheta) & \sin(2\vartheta) & \sin(3\vartheta) & \sin(4\vartheta) \\ 1 & \cos(2\vartheta) & \cos(4\vartheta) & \cos(6\vartheta) & \cos(8\vartheta) \\ 0 & \sin(2\vartheta) & \sin(4\vartheta) & \sin(6\vartheta) & \sin(8\vartheta) \\ \frac{1}{\sqrt{2}} & \frac{1}{\sqrt{2}} & \frac{1}{\sqrt{2}} & \frac{1}{\sqrt{2}} & \frac{1}{\sqrt{2}} \end{bmatrix} \; where \; [T_c]^{-1} = [T_c]^T \tag{26}$$

The three independent-orthogonal equations constitute three different planes namely, (α, β), (x, y), (z). The currents involved in the electromechanical conversion are mapped in the (α, β) subspace, the harmonics and the system losses will be mapped in the (x, y) plane and the homopolar components of the system in the z plane which due to the machine windings connection, will be zero.

Multiplying the stator and rotor phase voltage equations (1) and (2), by the transformation matrix (T_c):

$$[T_c][V_s] = [T_c][R_s][T_c]^{-1}[T_c][I_s] + [T_c][L_{ss}][T_c]^{-1}\frac{d}{dt}\left[[T_c][I_s]\right] + \frac{d}{dt}\left[[T_c]L_{sr}(\theta)[T_c]^{-1}[T_c][I_r]\right] \tag{27}$$

$$[0] = [T_c][R_r][T_c]^{-1}[T_c][I_r] + [T_c][L_{rr}][T_c]^{-1}\frac{d}{dt}\left[[T_c][I_r]\right] + \frac{d}{dt}\left[[T_c]L_{rs}(\theta)[T_c]^{-1}[T_c][I_s]\right] \tag{28}$$

where the stator and rotor voltage, current and flux matrices in the α-β-x-y-z reference frames are:

$$\begin{bmatrix} v_{s\alpha} \\ v_{s\beta} \\ v_{sx} \\ v_{sy} \\ v_{sz} \end{bmatrix} = [T_c][V_s] \quad \begin{bmatrix} i_{s\alpha} \\ i_{s\beta} \\ i_{sx} \\ i_{sy} \\ i_{sz} \end{bmatrix} = [T_c][I_s] \quad \begin{bmatrix} \lambda_{s\alpha} \\ \lambda_{s\beta} \\ \lambda_{sx} \\ \lambda_{sy} \\ \lambda_{sz} \end{bmatrix} = [T_c][\lambda_s] \tag{29}$$

$$\begin{bmatrix} v'_{r\alpha} \\ v'_{r\beta} \\ v'_{rx} \\ v'_{ry} \\ v'_{rz} \end{bmatrix} = [T_c][V_r] \qquad \begin{bmatrix} i'_{r\alpha} \\ i'_{r\beta} \\ i'_{rx} \\ i'_{ry} \\ i'_{rz} \end{bmatrix} = [T_c][I_r] \qquad \begin{bmatrix} \lambda'_{r\alpha} \\ \lambda'_{r\beta} \\ \lambda'_{rx} \\ \lambda'_{ry} \\ \lambda'_{rz} \end{bmatrix} = [T_c][\lambda_r] \tag{30}$$

Further developing (27)-(28), the rotor/stator resistance and inductance matrices in the α-β-x-y-z reference frames are given by:

$$[T_c][R_s][T_c]^{-1} = [R_s] \tag{32}$$

$$[T_c][R_r][T_c]^{-1} = [R_r] \tag{31}$$

Defining the stator and rotor inductances as $L_s = L_{ls} + L_m$ and $L_r = L_{ls} + L_m$, repectively, where ($L_m = \frac{5}{2}M$), is the mutual inductance in the (α, β, x, y) reference frame, then:

$$[T_c][L_{ss}][T_c]^{-1} = L_{ls}[I_5] + M\begin{bmatrix} \frac{5}{2} & 0 & 0 & 0 & 0 \\ 0 & \frac{5}{2} & 0 & 0 & 0 \\ 0 & 0 & 0 & 0 & 0 \\ 0 & 0 & 0 & 0 & 0 \\ 0 & 0 & 0 & 0 & 0 \end{bmatrix} = \begin{bmatrix} L_s & 0 & 0 & 0 & 0 \\ 0 & L_s & 0 & 0 & 0 \\ 0 & 0 & L_{ls} & 0 & 0 \\ 0 & 0 & 0 & L_{ls} & 0 \\ 0 & 0 & 0 & 0 & L_{ls} \end{bmatrix} \tag{32}$$

$$[T_c][L_{sr}(\theta)][T_c]^{-1} = L_m\begin{bmatrix} \cos(\theta) & -\sin(\theta) & 0 & 0 & 0 \\ \sin(\theta) & \cos(\theta) & 0 & 0 & 0 \\ 0 & 0 & 0 & 0 & 0 \\ 0 & 0 & 0 & 0 & 0 \\ 0 & 0 & 0 & 0 & 0 \end{bmatrix} \tag{33}$$

$$[T_c][L_{rr}][T_c]^{-1} = \begin{bmatrix} L_r & 0 & 0 & 0 & 0 \\ 0 & L_r & 0 & 0 & 0 \\ 0 & 0 & L_{lr} & 0 & 0 \\ 0 & 0 & 0 & L_{lr} & 0 \\ 0 & 0 & 0 & 0 & L_{lr} \end{bmatrix} \tag{34}$$

$$[T_c] * [L_{rs}(\theta)] * [T_c]^{-1} = L_m\begin{bmatrix} \cos(\theta) & \sin(\theta) & 0 & 0 & 0 \\ -\sin(\theta) & \cos(\theta) & 0 & 0 & 0 \\ 0 & 0 & 0 & 0 & 0 \\ 0 & 0 & 0 & 0 & 0 \\ 0 & 0 & 0 & 0 & 0 \end{bmatrix} \tag{35}$$

As a result the (α, β) subspace stator/rotor voltage equations will be:

$$\begin{bmatrix} v_{s\alpha} \\ v_{s\beta} \end{bmatrix} = \begin{bmatrix} R_s & 0 \\ 0 & R_s \end{bmatrix}\begin{bmatrix} i_{s\alpha} \\ i_{s\beta} \end{bmatrix} + \frac{d}{dt}\left[\begin{bmatrix} L_s & 0 \\ 0 & L_s \end{bmatrix}\begin{bmatrix} i_{s\alpha} \\ i_{s\beta} \end{bmatrix} + L_m\begin{bmatrix} \cos(\theta) & -\sin(\theta) \\ \sin(\theta) & \cos(\theta) \end{bmatrix}\begin{bmatrix} i'_{r\alpha} \\ i'_{r\beta} \end{bmatrix}\right] \tag{36}$$

$$\begin{bmatrix} 0 \\ 0 \end{bmatrix} = \begin{bmatrix} R_r & 0 \\ 0 & R_r \end{bmatrix}\begin{bmatrix} i'_{r\alpha} \\ i'_{r\beta} \end{bmatrix} + \frac{d}{dt}\left[\begin{bmatrix} L_r & 0 \\ 0 & L_r \end{bmatrix}\begin{bmatrix} i'_{r\alpha} \\ i'_{r\beta} \end{bmatrix} + L_m\begin{bmatrix} \cos(\theta) & \sin(\theta) \\ -\sin(\theta) & \cos(\theta) \end{bmatrix}\begin{bmatrix} i_{s\alpha} \\ i_{s\beta} \end{bmatrix}\right] \tag{37}$$

Due to the nature of the electrical machine, the rotor variables are referred to the rotating frame (α', β') that moves at the rotor electrical angular speed. In order to set the rotor and stator electrical variables to the same reference frame (stator reference frame) the following rotating matrix will be applied to the rotor voltage equation [10].

$$[T_r(\theta)] = \begin{bmatrix} \cos(\theta) & -\sin(\theta) & 0 & 0 & 0 \\ \sin(\theta) & \cos(\theta) & 0 & 0 & 0 \\ 0 & 0 & 1 & 0 & 0 \\ 0 & 0 & 0 & 1 & 0 \\ 0 & 0 & 0 & 0 & 1 \end{bmatrix} where\ [T_r(\theta)]^{-1} = [T_r(\theta)]^T = [T_r(-\theta)] \quad (38)$$

Applying the rotating matrix to the rotor electrical variables:

$$\begin{bmatrix} v_{r\alpha} \\ v_{r\beta} \\ v_{rx} \\ v_{ry} \\ v_{rz} \end{bmatrix} = [T_r(\theta)] \begin{bmatrix} v'_{r\alpha} \\ v'_{r\beta} \\ v'_{rx} \\ v'_{ry} \\ v'_{rz} \end{bmatrix} \quad \begin{bmatrix} i_{r\alpha} \\ i_{r\beta} \\ i_{rx} \\ i_{ry} \\ i_{rz} \end{bmatrix} = [T_r(\theta)] \begin{bmatrix} i'_{r\alpha} \\ i'_{r\beta} \\ i'_{rx} \\ i'_{ry} \\ i'_{rz} \end{bmatrix} \quad \begin{bmatrix} \lambda_{r\alpha} \\ \lambda_{r\beta} \\ \lambda_{rx} \\ \lambda_{ry} \\ \lambda_{rz} \end{bmatrix} = [T_r(\theta)] \begin{bmatrix} \lambda'_{r\alpha} \\ \lambda'_{r\beta} \\ \lambda'_{rx} \\ \lambda'_{ry} \\ \lambda'_{rz} \end{bmatrix} \quad (39)$$

Replacing (39) in (36)-(37), the new stator/rotor voltage equations will be:

$$\begin{bmatrix} v_{s\alpha} \\ v_{s\beta} \end{bmatrix} = \begin{bmatrix} R_s & 0 \\ 0 & R_s \end{bmatrix} \begin{bmatrix} i_{s\alpha} \\ i_{s\beta} \end{bmatrix} + \frac{d}{dt} \left[\begin{bmatrix} L_s & 0 \\ 0 & L_s \end{bmatrix} \begin{bmatrix} i_{s\alpha} \\ i_{s\beta} \end{bmatrix} + L_m \begin{bmatrix} i_{r\alpha} \\ i_{r\beta} \end{bmatrix} \right] \quad (40)$$

$$\begin{bmatrix} 0 \\ 0 \end{bmatrix} = [T_r(\theta)] \begin{bmatrix} R_r & 0 \\ 0 & R_r \end{bmatrix} [T_r(-\theta)][T_r(\theta)] \begin{bmatrix} i'_{r\alpha} \\ i'_{r\beta} \end{bmatrix} + [T_r(\theta)] \frac{d}{dt} \left[\begin{bmatrix} L_r & 0 \\ 0 & L_r \end{bmatrix} [T_r(-\theta)] \begin{bmatrix} i_{r\alpha} \\ i_{r\beta} \end{bmatrix} + L_m [T_r(-\theta)] \begin{bmatrix} i_{s\alpha} \\ i_{s\beta} \end{bmatrix} \right] \quad (41)$$

where:

$$[T_r(\theta)][R_r][T_r(-\theta)] = [R_r] \quad (42)$$

$$[T_r(\theta)] \frac{d}{dt} \begin{bmatrix} L_r & 0 \\ 0 & L_r \end{bmatrix} [T_r(-\theta)] \begin{bmatrix} i_{r\alpha} \\ i_{r\beta} \end{bmatrix} = \omega_r \begin{bmatrix} 0 & L_r \\ -L_r & 0 \end{bmatrix} \begin{bmatrix} i_{r\alpha} \\ i_{r\beta} \end{bmatrix} + \begin{bmatrix} L_r & 0 \\ 0 & L_r \end{bmatrix} \frac{d}{dt} \begin{bmatrix} i_{r\alpha} \\ i_{r\beta} \end{bmatrix} \quad (43)$$

Notice that $\omega_r = \frac{d\theta}{dt} = P * \omega_m$.

$$[T_r(\theta)] \frac{d}{dt} \left[L_m [T_r(\theta)] \begin{bmatrix} i_{s\alpha} \\ i_{s\beta} \end{bmatrix} \right] = \omega_r \begin{bmatrix} 0 & L_m \\ -L_m & 0 \end{bmatrix} \begin{bmatrix} i_{s\alpha} \\ i_{s\beta} \end{bmatrix} + \begin{bmatrix} L_m & 0 \\ 0 & L_m \end{bmatrix} \frac{d}{dt} \begin{bmatrix} i_{s\alpha} \\ i_{s\beta} \end{bmatrix} \quad (44)$$

$$\begin{bmatrix} 0 \\ 0 \end{bmatrix} = \begin{bmatrix} R_r & 0 \\ 0 & R_r \end{bmatrix} \begin{bmatrix} i_{r\alpha} \\ i_{r\beta} \end{bmatrix} + \left[\begin{bmatrix} \frac{d}{dt} L_r & L_r \omega_r \\ -L_r \omega_r & \frac{d}{dt} L_r \end{bmatrix} \begin{bmatrix} i_{r\alpha} \\ i_{r\beta} \end{bmatrix} + \begin{bmatrix} \frac{d}{dt} L_m & L_m \omega_r \\ -L_m \omega_r & \frac{d}{dt} L_m \end{bmatrix} \begin{bmatrix} i_{s\alpha} \\ i_{s\beta} \end{bmatrix} \right] \quad (45)$$

Finally, the (α, β) subspace matrix can be written as in (46), which is in accordance with the results available in the literature:

$$\begin{bmatrix} v_{s\alpha} \\ v_{s\beta} \\ 0 \\ 0 \end{bmatrix} = \begin{bmatrix} R_s + \frac{d}{dt}L_s & 0 & \frac{d}{dt}L_m & 0 \\ 0 & R_s + \frac{d}{dt}L_s & 0 & \frac{d}{dt}L_m \\ \frac{d}{dt}L_m & L_m\omega_r & R_r + \frac{d}{dt}L_r & L_r\omega_r \\ -L_m\omega_r & \frac{d}{dt}L_m & -L_r\omega_r & R_r + \frac{d}{dt}L_r \end{bmatrix} * \begin{bmatrix} i_{s\alpha} \\ i_{s\beta} \\ i_{r\alpha} \\ i_{r\beta} \end{bmatrix} \quad (46)$$

And their equivalents in complex vector are:

$$\overrightarrow{v_{s\alpha\beta}} = R_s\overrightarrow{\imath_{s\alpha\beta}} + \frac{d}{dt}\overrightarrow{\lambda_{s\alpha\beta}} \quad (47)$$

$$0 = R_r\overrightarrow{\imath_{r\alpha\beta}} + \frac{d}{dt}\overrightarrow{\lambda_{r\alpha\beta}} - j\omega_r\overrightarrow{\lambda_{r\alpha\beta}} \quad (48)$$

$$\overrightarrow{\lambda_{s\alpha\beta}} = L_s\overrightarrow{\imath_{s\alpha\beta}} + L_m\overrightarrow{\imath_{r\alpha\beta}} \quad (49)$$

$$\overrightarrow{\lambda_{r\alpha\beta}} = L_m\overrightarrow{\imath_{s\alpha\beta}} + L_r\overrightarrow{\imath_{r\alpha\beta}} \quad (50)$$

where the complex electrical vectors are defined as:

$$\overrightarrow{v_{s\alpha\beta}} = v_{s\alpha} + jv_{s\beta} \quad (51)$$

$$\overrightarrow{v_{r\alpha\beta}} = v_{r\alpha} + jv_{r\beta} \quad (52)$$

$$\overrightarrow{\imath_{s\alpha\beta}} = i_{s\alpha} + ji_{s\beta} \quad (53)$$

$$\overrightarrow{\imath_{r\alpha\beta}} = i_{r\alpha} + ji_{r\beta} \quad (54)$$

$$\overrightarrow{\lambda_{s\alpha\beta}} = \lambda_{s\alpha} + j\lambda_{s\beta} \quad (55)$$

$$\overrightarrow{\lambda_{r\alpha\beta}} = \lambda_{r\alpha} + j\lambda_{r\beta} \quad (56)$$

In a similar way, the (x, y) subspace voltage and flux rotor components are obtained through (27)-(28) and represented in matrix and complex vector form, as shown in (57)-(62).

$$\begin{bmatrix} v_{sx} \\ v_{sy} \end{bmatrix} = \begin{bmatrix} R_s + \frac{d}{dt}L_{ls} & 0 \\ 0 & R_s + \frac{d}{dt}L_{ls} \end{bmatrix} \begin{bmatrix} i_{sx} \\ i_{sy} \end{bmatrix} \quad (57)$$

$$\begin{bmatrix} 0 \\ 0 \end{bmatrix} = \begin{bmatrix} R_r + \frac{d}{dt}L_{lr} & 0 \\ 0 & R_r + \frac{d}{dt}L_{lr} \end{bmatrix} \begin{bmatrix} i_{rx} \\ i_{ry} \end{bmatrix} \quad (58)$$

$$\overrightarrow{v_{sxy}} = R_s\overrightarrow{\imath_{sxy}} + \frac{d}{dt}\overrightarrow{\lambda_{sxy}} \quad (59)$$

$$0 = R_r\overrightarrow{\imath_{rxy}} + \frac{d}{dt}\overrightarrow{\lambda_{rxy}} \quad (60)$$

$$\overrightarrow{\lambda_{sxy}} = L_{ls}\overrightarrow{\imath_{sxy}} \quad (61)$$

$$\overrightarrow{\lambda_{rxy}} = L_{lr}\overrightarrow{\imath_{rxy}} \quad (62)$$

where the complex electrical vectors are defined as:

$$\overrightarrow{v_{sxy}} = v_{sx} + jv_{sy} \tag{63}$$

$$\overrightarrow{v_{rxy}} = v_{rx} + jv_{ry} \tag{64}$$

$$\overrightarrow{i_{sxy}} = i_{sx} + ji_{sy} \tag{65}$$

$$\overrightarrow{i_{rxy}} = i_{rx} + ji_{ry} \tag{66}$$

$$\overrightarrow{\lambda_{sxy}} = \lambda_{sx} + j\lambda_{sy} \tag{67}$$

$$\overrightarrow{\lambda_{rxy}} = \lambda_{rx} + j\lambda_{ry} \tag{68}$$

Finally, the (z), subspace obtained through (27)-(28) is:

$$v_{sz} = \left(R_s + \frac{d}{dt}L_{ls}\right) i_{sz} \tag{69}$$

$$v_{rz} = \left(R_r + \frac{d}{dt}L_{lr}\right) i_{rz} \tag{70}$$

Notice that as a result of the VSD applied to the voltage equations, the machine can be electrically modeled by three sets of independent circuits for (α, β), (x, y) and (z) planes, Fig. 2.3.

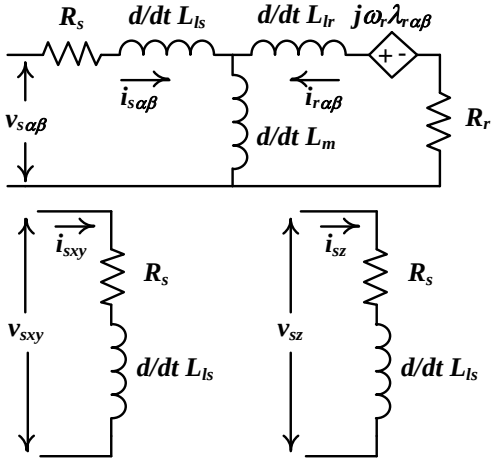

Fig. 2.3.: Five-phase induction machine equivalent circuit in the (α, β, x, y) planes.

The electromagnetic torque can be calculated [54] by equation (23), mapped in the (α, β, x, y) reference frame as follows:

$$T_e = P([I_s]^T_{\alpha\beta xyz}[T_c]\frac{d}{d\theta}L_{sr}(\theta)[T_c]^{-1}[T_r(-\theta)][I_r]_{\alpha\beta xyz}) \tag{71}$$

Notice that:

$$[T_c]\frac{d}{d\theta}[L_{sr}(\theta)][T_c]^{-1} = \frac{d}{d\theta}([T_c] * [L_{sr}(\theta)] * [T_c]^{-1}) = L_m\frac{d}{d\theta}\begin{bmatrix} \cos(\theta) & -\sin(\theta) & 0 & 0 & 0 \\ \sin(\theta) & \cos(\theta) & 0 & 0 & 0 \\ 0 & 0 & 0 & 0 & 0 \\ 0 & 0 & 0 & 0 & 0 \\ 0 & 0 & 0 & 0 & 0 \end{bmatrix} \tag{72}$$

$$\frac{d}{d\theta}([T_c][L_{sr}(\theta)][T_c]^{-1}) = L_m \begin{bmatrix} -\sin(\theta) & -\cos(\theta) & 0 & 0 & 0 \\ \cos(\theta) & -\sin(\theta) & 0 & 0 & 0 \\ 0 & 0 & 0 & 0 & 0 \\ 0 & 0 & 0 & 0 & 0 \\ 0 & 0 & 0 & 0 & 0 \end{bmatrix} \quad (73)$$

As it was expected the (x, y), (z), subspace electric variables are zero; this demonstrates that the electromechanical energy conversion takes place only in the (α, β) subspace components. Taking this into account, the electromagnetic torque can be calculated by:

$$T_e = PL_m[i_{s\alpha} \; i_{s\beta}] \begin{bmatrix} -sin(\theta) & -cos(\theta) \\ cos(\theta) & -sin(\theta) \end{bmatrix} \begin{bmatrix} cos(\theta) & sin(\theta) \\ -sin(\theta) & cos(\theta) \end{bmatrix} \begin{bmatrix} i_{r\alpha} \\ i_{r\beta} \end{bmatrix} = PL_m[i_{s\alpha} \; i_{s\beta}] \begin{bmatrix} 0 & -1 \\ 1 & 0 \end{bmatrix} \begin{bmatrix} i_{r\alpha} \\ i_{r\beta} \end{bmatrix} \quad (74)$$

$$T_e = PL_m(i_{r\alpha} i_{s\beta} - i_{r\beta} i_{s\alpha}) \quad (75)$$

Notice that the electromagnetic torque in the stationary reference frame, can be also expressed in complex vector form in terms of the rotor and stator currents (76), stator flux and current (77), rotor flux and current (78) and rotor flux and stator current (79). This is of special importance for control purposes where different schemes are implemented depending on the selected torque expression.

$$T_e = PL_m(\overrightarrow{\imath_{r\alpha\beta}} \times \overrightarrow{\imath_{s\alpha\beta}}) \quad (76)$$

$$T_e = P(\overrightarrow{\lambda_{s\alpha\beta}} \times \overrightarrow{\imath_{s\alpha\beta}}) \quad (77)$$

$$T_e = P(\overrightarrow{\lambda_{r\alpha\beta}} \times \overrightarrow{\imath_{r\alpha\beta}}) \quad (78)$$

$$T_e = P\frac{L_m}{L_r}(\overrightarrow{\lambda_{r\alpha\beta}} \times \overrightarrow{\imath_{s\alpha\beta}}) \quad (79)$$

2.2.1.3 ROTATING REFERENCE FRAME

The VSD theory applied to the voltage, current and flux equations in the stationary stator reference frame allows a significant simplification of the dynamic modeling equations. Moreover, it is observed that only (α, β) components are involved in torque production and consequently are a priority for control purposes. Under transient conditions these components possess an oscillating nature that must be avoided in order to ensure proper control. To achieve this, voltage, current and flux vectors are mapped in a rotating reference frame $(d\text{-}q)$ at a constant speed (ω_a). Consequently, the d- and q- components of each vector in the common reference frame, are non-oscillating, constant in steady state and varying in transient state [55]. The vector rotation into the $(d\text{-}q)$ reference frame is achieved by means of the Park transformation (80) for stator components (T_{sp}) and (81) for rotor components (T_{rp}), as shown graphically in Fig. 2.4.

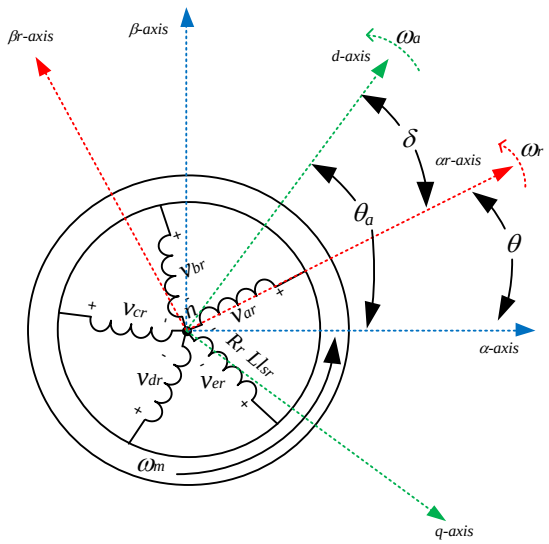

Fig. 2.4.: Park rotating reference frame.

The rotating d- and α_r- axes instantaneous position with respect to the stationary stator α-axis reference frame is denoted by (θ_a) and (θ), respectively. Consequently the rotating α_r-axis position with respect to the d- reference frame (δ), is given by (82). Notice that the (α_r, β_r) vectors are rotating at a speed denoted by (ω_r), related to the mechanical speed by (83) and to their instantaneous position by (84). On the other hand, the $(d\text{-}q)$ plane is rotating at a speed (ω_a) and is related to its instantaneous position by (85).

$$[T_{sp}] = \begin{bmatrix} \cos(\theta_a) & -\sin(\theta_a) \\ \sin(\theta_a) & \cos(\theta_a) \end{bmatrix} \tag{80}$$

$$[T_{rp}] = \begin{bmatrix} \cos(\delta) & -\sin(\delta) \\ \sin(\delta) & \cos(\delta) \end{bmatrix} \tag{81}$$

$$\delta = \theta_a - \theta \tag{82}$$

$$\omega_r = P\omega_m \tag{83}$$

$$\delta = \int_0^t (\omega_a - \omega_r)dt = \int_0^t \omega_{sl} dt \tag{84}$$

$$\theta_a = \int_0^t \omega_a dt \tag{85}$$

As a result, applying (80) and (81) to the (α, β) stator/rotor voltage components, the voltage matrix defined in (46) and the electromagnetic torque (α, β), can be expressed in the rotating reference frame by (86) and (87), respectively. Moreover, the machines equivalent electrical model in the d-q reference frame will be as shown in Fig. 2.5. Observe that the equivalent circuit in the x-y components remain the same as in the stationary reference frame due to the fact that vector rotation is only applied to the (α, β) components.

$$\begin{bmatrix} v_{sd} \\ v_{sq} \\ 0 \\ 0 \end{bmatrix} = \begin{bmatrix} R_s + \frac{d}{dt}L_s & -L_s\omega_a & \frac{d}{dt}L_m & -L_m\omega_a \\ L_s\omega_a & R_s + \frac{d}{dt}L_s & L_m\omega_a & \frac{d}{dt}L_m \\ \frac{d}{dt}L_m & -L_m\omega_{sl} & R_r + \frac{d}{dt}L_r & -L_r\omega_{sl} \\ L_m\omega_{sl} & \frac{d}{dt}L_m & L_r\omega_{sl} & R_r + \frac{d}{dt}L_r \end{bmatrix} * \begin{bmatrix} i_{sd} \\ i_{sq} \\ i_{rd} \\ i_{rq} \end{bmatrix} \quad (86)$$

$$T_e = PL_m(i_{rd}i_{sq} - i_{rq}i_{sd}) \quad (87)$$

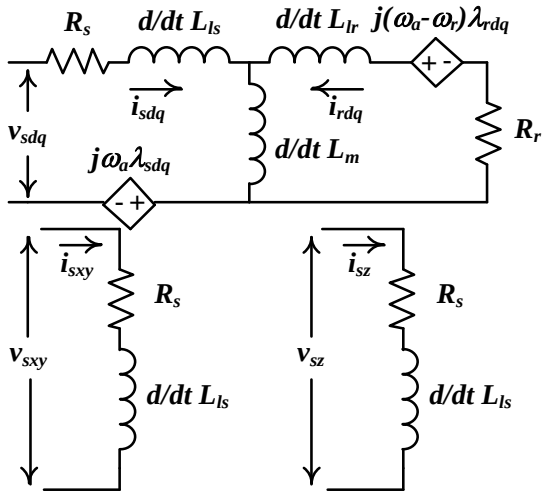

Fig. 2.5.: Five-phase induction machine equivalent circuit in the (d, q, x, y) planes.

Notice that the electromagnetic torque equation can be written in terms of the stator or rotor flux as in (88) and (89), respectively. This is of special importance for control purposes where different schemes can be implemented by setting the d-axis fixed to either the air-gap, stator or rotor flux component, as will be studied further on.

$$T_e = P(\lambda_{sd}i_{sq} - \lambda_{sq}i_{sd}) \quad (88)$$

$$T_e = P\frac{L_m}{L_r}(\lambda_{rd}i_{sq} - \lambda_{rq}i_{sd}) \quad (89)$$

2.2.2 MULTIPHASE POWER CONVERTER MODELING

Power converters are in charge of converting energy from AC to DC or vice versa, controlling its voltage, current and frequency characteristics. Depending on its nature or application requirements, different topologies can be found in the literature, distinguished by the number of phases they possess (single phase, three-phase or multiphase) and the number of voltage levels they use to synthetize the modulated current/voltage (two-level, multilevel). Depending on the electrical ratings of the final application, the power converter can be constructed implementing different semiconductor technologies. For instance, power converters where high switching frequency (1 MHz), low voltage

(up to 1 kV) and low current (around 100 A) is required are commonly based on Metal Oxide Semiconductor Field Effect (MOSFET), however if the voltage and current ratings increase (in the order of kV and kA) Insulated Gate Bipolar Transistor (IGBT), are used at the expense of lower switching frequencies.

The general scheme of the five-phase two-level induction motor drive is depicted in Fig. 2.1. The power converter consists of a voltage source inverter (VSI), based on ten IGBT semiconductors and its corresponding anti-parallel free-wheeling diode, two for each phase, whose electrical ratings are able to withstand the entire DC-Link voltage and the maximum rated current of the induction machine. The DC-Link voltage is provided by an external low-impedance DC source. Each phase IGBT's switching state is denoted by (S_i). Where $S_i = 0$ if the lower switch is ON and the upper switch is OFF, connecting the machine winding to the negative rail of the converter (N) and $S_i = 1$ if the opposite occurs, connecting the phase winding to the positive rail (P). Consequently only two voltage levels are applied namely, $0 - V_{dc}$, when referred to the negative rail of the VSI or $\pm V_{dc}/2$, if referred to the DC-Link mid-point. Accordingly, the leg voltage, referred to the negative rail of the VSI, is given in terms of the semiconductor switching state (S_i) and the DC-Link voltage (90).

$$v_{iN} = S_i V_{dc} \tag{90}$$

During normal operation the sum of the machines phase voltages is zero (91), where each phase voltage (v_{is}), can be written in terms of the voltage between phase (i) and the negative rail of the converter (N) and the voltage between the machines neutral point (n) and the inverters negative rail (92).

$$\sum[v_{is}] = v_{as} + v_{bs} + v_{cs} + v_{ds} + v_{es} = 0 \tag{91}$$

$$v_{is} = v_{iN} - v_{nN} \tag{92}$$

Consequently further developing (91), considering the phase voltage in (92).

$$v_{aN} + v_{bN} + v_{cN} + v_{dN} + v_{eN} - 5v_{nN} = 0 \rightarrow v_{nN} = \frac{1}{5}(v_{aN} + v_{bN} + v_{cN} + v_{dN} + v_{eN}) \tag{93}$$

On the other hand, the machines phase and line voltage matrix can be written as:

$$\begin{bmatrix} v_{aN} \\ v_{bN} \\ v_{cN} \\ v_{dN} \\ v_{eN} \\ 0 \end{bmatrix} = \begin{bmatrix} 1 & 0 & 0 & 0 & 0 & 1 \\ 0 & 1 & 0 & 0 & 0 & 1 \\ 0 & 0 & 1 & 0 & 0 & 1 \\ 0 & 0 & 0 & 1 & 0 & 1 \\ 0 & 0 & 0 & 0 & 1 & 1 \\ -1 & -1 & -1 & -1 & -1 & 0 \end{bmatrix} \begin{bmatrix} v_{as} \\ v_{bs} \\ v_{cs} \\ v_{ds} \\ v_{es} \\ v_{nN} \end{bmatrix} \tag{94}$$

Applying the inverse transformation to (94), the phase voltages can be calculated in terms of the leg voltages by:

$$\begin{bmatrix} v_{as} \\ v_{bs} \\ v_{cs} \\ v_{ds} \\ v_{es} \end{bmatrix} = \frac{1}{5}\begin{bmatrix} 4 & -1 & -1 & -1 & -1 \\ -1 & 4 & -1 & -1 & -1 \\ -1 & -1 & 4 & -1 & -1 \\ -1 & -1 & -1 & 4 & -1 \\ -1 & -1 & -1 & -1 & 4 \end{bmatrix}\begin{bmatrix} v_{aN} \\ v_{bN} \\ v_{cN} \\ v_{dN} \\ v_{eN} \end{bmatrix} \tag{95}$$

Considering that the leg voltage is given in terms of the switching state (S_i) and the DC-Link voltage (90), the stator phase voltage matrix (95), from now on (V_{pre}), can be written as:

$$\begin{bmatrix} v_{as} \\ v_{bs} \\ v_{cs} \\ v_{ds} \\ v_{es} \end{bmatrix} = \frac{V_{dc}}{5}\begin{bmatrix} 4 & -1 & -1 & -1 & -1 \\ -1 & 4 & -1 & -1 & -1 \\ -1 & -1 & 4 & -1 & -1 \\ -1 & -1 & -1 & 4 & -1 \\ -1 & -1 & -1 & -1 & 4 \end{bmatrix}\begin{bmatrix} S_a \\ S_b \\ S_c \\ S_d \\ S_e \end{bmatrix} = V_{pre} \tag{96}$$

From (96) it is possible to see that different load configurations are obtained depending on the five-phase drive switching state. These load configurations will result in phase voltages of 0, $\pm 1/5V_{dc}$, $\pm 2/5V_{dc}$, $\pm 3/5V_{dc}$, $\pm 4/5V_{dc}$, as shown in Fig. 2.6, depending on the number of windings connected to either the positive or the negative rail of the VSI {positive-negative}.

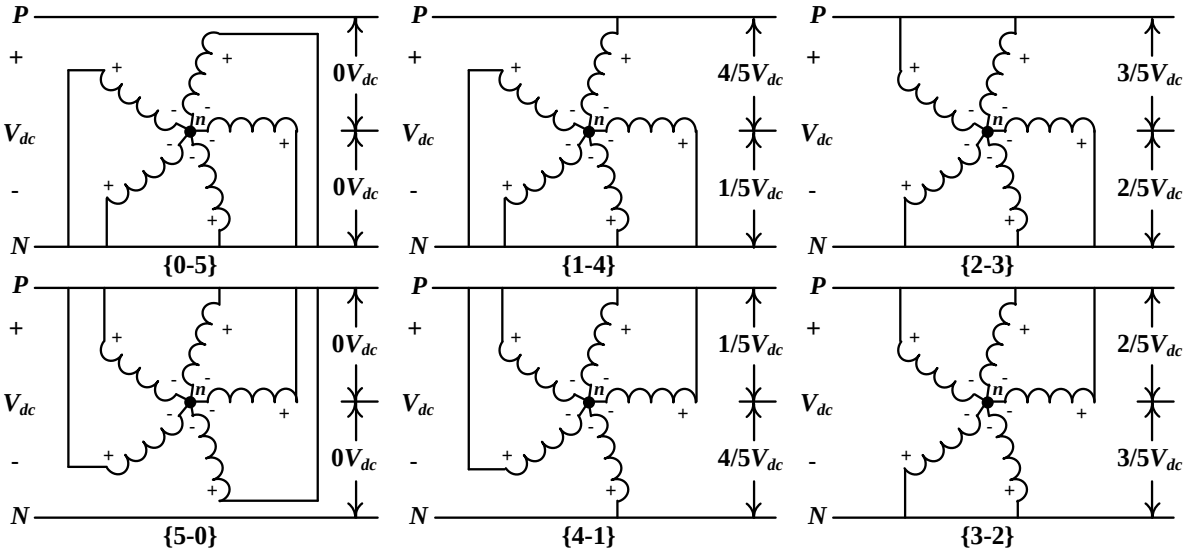

Fig. 2.6.: Five-phase two-level drive load configuration scheme.

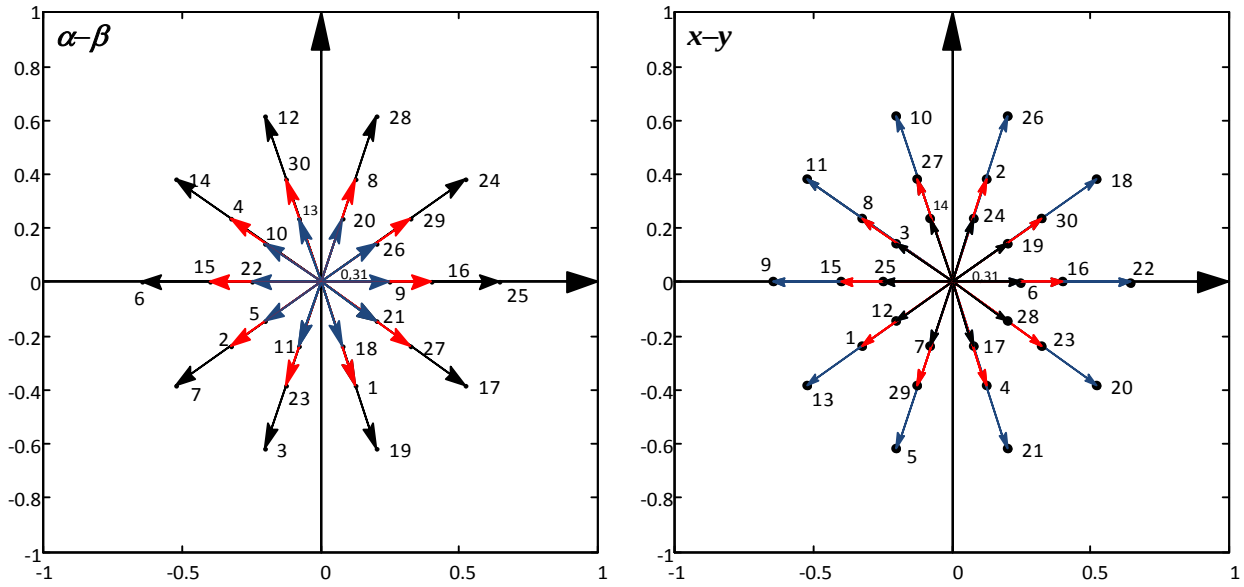

Fig. 2.7.: Space Vector Diagrams in the $\alpha-\beta$ (left side) and $x-y$ (right side) planes.

The two-level five-phase VSI allows $2^5 = 32$ voltage vectors (30 active and 2 zero), which are mapped in the α-β and x-y subspaces (Fig. 2.7), applying the Clarke transformation matrix (26) to the stator phase voltage matrix in (96). Each vector is identified using the decimal number corresponding to the binary code of the switching state of each pair of IGBT's $[Sa; Sb; Sc; Sd; Se]$. Due to the machines winding configuration, the harmonic components of order $5n$, are eliminated. However harmonics of order $(10n + 1)$, $(10n + 3)$, $(10n + 7)$ and $(10n + 9)$ with $n = 0,1,2,3,4,5$, will still appear in the harmonic spectrum. Those harmonic components that contribute to the electromechanical energy conversion are mapped in the α-β plane, while the components that do not generate electrical torque are mapped in the x-y plane. Summarizing, the harmonic spectrum mapped in the α, β, x, y will be:

- α-β Plane: Harmonic components of order $10n \pm 1$.
- x-y Plane: Harmonic components of order $10n \pm 3$.
- z Plane: Harmonic components of order $5n$.

Notice in Fig. 2.7, that the 30 active voltage vectors can be subdivided in three sets of ten vectors namely, large (in black color), medium (in red color) and small (in blue color). Moreover, observe that the large vectors in the α-β plane are mapped as small vectors in the x-y plane, the medium voltage vectors in the α-β plane are also the medium vectors in the x-y plane and finally, that the small vectors in the α-β plane are mapped as large vectors in the x-y plane. Depending on the multiphase drive point of operation, the stator voltage applied to the machine can vary. This stator

voltage vector must be selected according to the desired value in the α-β plane (required electrical torque) without a high increment of the applied component in the x-y plane, which will increase undesired electromagnetic losses.

The common-mode voltage (CMV) relates the motor neutral voltage to the mid-point of the DC-Link [56], as shown in Fig. 2.1, marked as V_{CM}. The expression of the CMV in a five-phase drive is:

$$V_{CM} = \frac{V_{dc}}{5}(S_a + S_b + S_c + S_d + S_e) - \frac{V_{dc}}{2} \quad (97)$$

Notice from (97) that the maximum peak value of the common-mode voltage in a five-phase drive is $|V_{CM}| = V_{dc}/2$, the minimum voltage variation is $\pm V_{dc}/5$ and that there are three different possible voltage levels. Notice also that even though the five-phase drive is based on a two-level VSI, the resultant CMV is multilevel as a consequence of the number of switching states. Considering the possible switching combinations in (97), there are six different sets of common-mode voltage values [56], that can be divided depending on the magnitude of the CMV generated in the α-β subspace [9]:

- Small CMV ($\pm 0.1V_{dc}$): Given by switching state combinations resulting in {2-3} or {3-2} load configurations (Fig. 2.6).
- Medium CMV ($\pm 0.3V_{dc}$): Given by switching state combinations resulting in {1-4} or {4-1} load configurations (Fig. 2.6).
- Large CMV ($\pm 0.5V_{dc}$): Given by switching state combinations resulting in {0-5} or {5-0} load configurations (Fig. 2.6).

2.3 STANDARD CONTROL TECHNIQUES

Multiphase drives control schemes are based mainly on the extension of traditional control techniques originally proposed for three-phase machines, implementing linear and nonlinear regulators such as Proportional Integral (PI) and hysteresis controllers. Proposed control techniques effectively exploit the additional degrees of freedom that multiphase drives possess, ensuring fast response to changes on the velocity and torque references, while maintaining the electrical drive within its maximum current rating. In this way Field Oriented Control (FOC) technique, originally founded in the literature for the three-phase case [57, 58, 59], based on PI and hysteresis controllers, has been extended for the multiphase case [60], successfully decoupling torque and flux control, regardless of the number of phases of the multiphase drive. This is also the case of the Direct Torque

Control (DTC), based on hysteresis regulators proposed for the three-phase case in [61], and extended to the five-phase induction machine in [62].

2.3.1 FIELD ORIENTED CONTROL

Among the control techniques found in the literature, field oriented control or Vector Control, is probably the most widely used in industrial applications. It is based on independently controlling torque and flux production in the decoupled rotating reference frame (d-q), obtained through Clarke-Park transformations, with the d-axis aligned to the air-gap, stator or rotor flux component [63]. Regardless to which component the d-axis is aligned to, the controller is based on eliminating the q– stator or rotor flux component in the electromagnetic torque equation (88)-(89), in order to ensure that torque production is controlled only by stator flux and current (88) or rotor flux and stator current (89). Notice that the proper selection to which flux the rotating reference frame is aligned to, results in control scheme simplifications. For instance, if the rotating reference frame is aligned to the air-gap flux, proper control of the q- component must be provided in order to maintain it at zero. On the other hand if the stator flux is selected both stator flux and current must be controlled resulting in a much complex control scheme than when rotor flux is implemented where rotor flux and stator currents are independently controlled by d- and q- components, respectively. As a result Rotor Field Oriented Control (RFOC) is the most widely used among FOC strategies in industry application [9]. There are two RFOC strategies found in the literature namely, the Indirect Rotor Flux Oriented Control (IRFOC) and the Direct Field Oriented Control (DRFOC). Being the main difference between both methods, the way in which the rotor flux angular position is obtained.

When the RFOC is implemented the rotor flux in the q-axis is null (Fig. 2.8), and the rotor currents can be obtained through the rotor flux equations as follows:

$$\lambda_{rd} = (L_{lr} + L_m)i_{rd} + L_m i_{sd} \rightarrow i_{rd} = \frac{1}{L_r}(\lambda_{rd} - L_m i_{sd}) \quad (98)$$

$$\lambda_{rq} = 0 = (L_{lr} + L_m)i_{rq} + L_m i_{sq} \rightarrow i_{rq} = -\frac{L_m}{L_r} i_{sq} = -k_r i_{sq} \quad (99)$$

Substituting the rotor currents (98)-(99) in the d-q reference frame voltage equations in (86), the machine modeling equations take the following form:

$$\lambda_{rd} + \tau_r \frac{d}{dt}\lambda_{rd} = L_m i_{sd} \quad (100)$$

$$\omega_{sl}\tau_r \lambda_{rd} = L_m i_{sq} \quad (101)$$

$$T_e = P\frac{L_m}{L_r}\lambda_{rd} i_{sq} = P k_r \lambda_{rd} i_{sq} \quad (102)$$

$$\tau_r = \frac{L_r}{R_r} \quad (103)$$

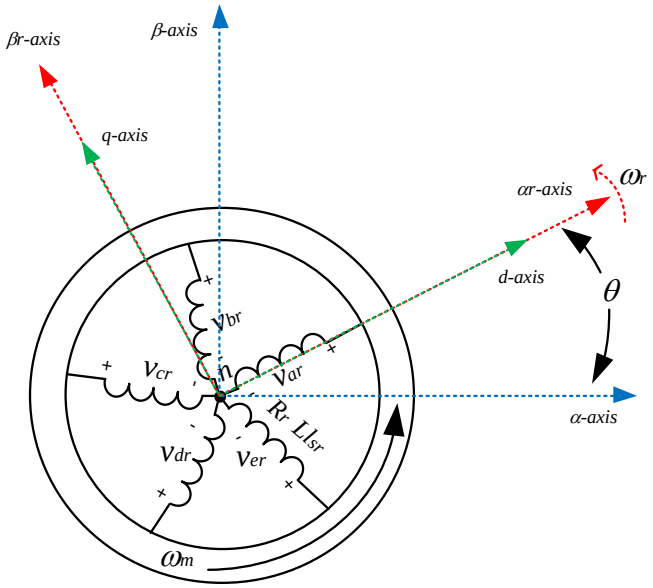

Fig. 2.8.: Rotating reference frame aligned to the rotor components.

An important aspect of IRFOC is that it is highly dependent on the machines parameters. FOC strategies can be implemented using PI or hysteresis based controllers. The main drawback of hysteresis controllers is that due to their variable operating frequency, higher and unpredictable voltage and current harmonic components [64] are generated.

From (100)-(102) it is possible to conclude that the d-current component will control the rotor flux while q-current component will control torque production. The IRFOC control scheme for a five-phase drive is shown in Fig. 2.9. It consists of four independent control loops for speed, flux, x- and y-current control. The d-current is controlled through a PI regulator based on the rotor flux error. On the other hand q-current control is achieved by and outer speed PI regulator cascaded with an inner current PI controller. Finally the x- and y-current components are controlled through single PI regulators.

Depending on the specific drive application the system delay time must be considered in the control loop. For instance in low voltage applications, where power dissipation due to switching losses is not a constraint, high switching frequencies can be managed and the system delay effect can be neglected from the current controller. However in medium and high voltage applications, where power dissipation capability is a major constraint, VSI's are operated at low switching frequencies

(under 1 kHz) in which system time delay directly affects the electrical drive performance and consequently must be considered in the controller design [63, 64].

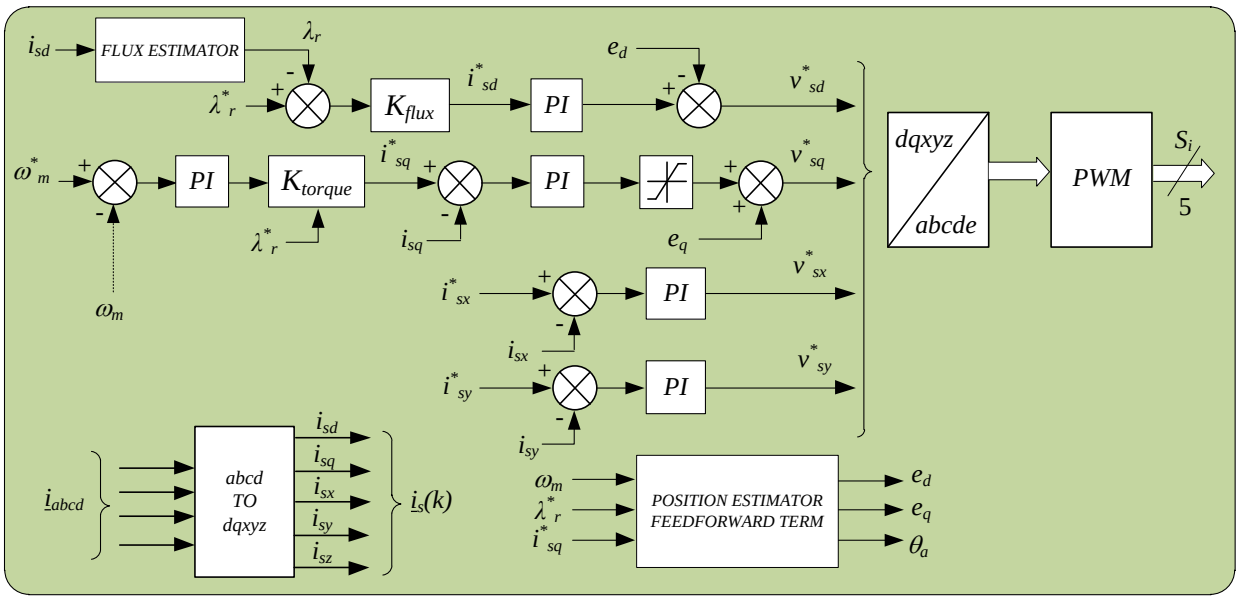

Fig. 2.9.: Field Oriented Control scheme for five-phase drive.

As discussed earlier, the VSD of the machines currents into the α-β-x-y planes is done through the Clarke transformation matrix (T_c) in (26). Subsequently, the α-β current components are rotated to the d-q reference by (80) and the position estimator (85), that now corresponds to the rotor flux angle and takes the following form:

$$\theta_a = \int (\omega_r + \omega_{sl})\, dt = \int \left(\omega_r + \frac{L_m i_{sq}^*}{\tau_r \lambda_{rd}^*} \right) dt \tag{104}$$

Notice that the slip speed (ω_{sl}) is estimated by (101) considering the stator q- reference current and the rotor q- reference flux.

Feedforward terms e_d and e_q (105)-(106), respectively, are included in order to improve the controller performance, eliminating the influence of motion induced voltage in the stator components and consequently reducing cross-coupling between d- and q- components [63].

$$e_d = \sigma L_s i_{sq}^* \omega_a \tag{105}$$

$$e_q = L_s \frac{\lambda_{rd}^*}{L_m} \omega_a \tag{106}$$

Notice that feedforward terms highly depend on the accuracy of the estimated machines parameters. Moreover it has been stated that the effect of feedforward terms in the reduction of cross-coupling is affected by the VSI's switching frequency, showing that for low switching frequencies feedforward terms are not capable of decoupling d- and q-components [63].

Notice also that there are two more current components available for control purposes in the five-phase system. Due to the fact that the electrical drive is based on a distributed winding machine, the x- and y-current components do not generate electrical torque and must be minimized in order to reduce losses. As a consequence their reference current is set to zero. This is not the case when concentrated winding machines are used, where it is possible to enhance torque production by properly injecting the third harmonic current component in the stator currents [13, 65].

Once the control action is determined for every component loop, *i.e.* the voltages v_{sd}, v_{sq}, v_{sx} and v_{sy} are established, they are transformed to phase variables in order to be applied by the selected Pulse Width Modulation (PWM) strategy to the power converter. PWM technique is based on establishing and controlling the time duration of the turn-on gate pulses applied to the IGBT semiconductors of each converter phase and consequently controlling the frequency and magnitude of the inverter output voltage.

Traditional PWM strategies, which can be found in the literature as Carrier Based Pulse Width Modulation (CBPWM) and Space Vector Pulse Width Modulation (SVPWM), have also been extended to the multiphase case [16, 66, 65, 67, 68, 69, 70]. CBPWM is realized by comparing the reference voltage waveform (which has the desired magnitude and frequency) and a triangular signal (whose frequency corresponds to the desired power converter switching frequency). While SVPWM is realized by averaging the time that different voltage space vectors (with adjacent switching states) are applied to the power converter semiconductor [66].

Ideally, the implemented SVPWM strategy should ensure that i) each semiconductor can only commutate from ON to OFF state or vice versa, twice in each period, maintaining a constant switching frequency, ii) the RMS value of the modulated phase voltage are obtained from v_{sd}-v_{sq} references, iii) a complete DC-Link voltage utilization is possible and iv) minimum low-order harmonic components, in order to maintain near sinusoidal voltages, are applied to the machine windings [67]. This is achieved by properly selecting the application times of large and medium voltage vectors. Depending on the selected SVPWM method, sinusoidal phase voltages at the expense of not fully utilizing the DC-Link voltage or complete DC-Link bus utilization at the expense of the appearance of small low order harmonic components (quasi-sinusoidal stator phase voltages operation) is achieved [67].

2.3.2 DIRECT TORQUE CONTROL

Direct Torque Control (DTC) was originally proposed for three-phase drives in the 80's, as a control technique capable of offering fast torque and flux control performance as the one obtained with FOC [61], and different schemes have been proposed for the three-phase drives case [71]. Subsequently, it was extended to the multiphase drive case considering different types of machines [12, 71], neutral point connections [72, 73] and speed sensorless drives [74]. Moreover, comparison between FOC and DTC techniques is also found in the literature for three- and five-phase drives [75, 13]. Contrary to FOC techniques, its dependency on machine parameters is lower and does not contain current control loops. Then, the transformation of stator and rotor phase currents to a rotating reference frame is not performed, reducing the controllers' implementation complexity and computational cost, and assuming the specific application the necessity for using position sensors [76].

The main drawbacks of DTC are its high torque and flux ripple, mainly due to the "all or nothing" nature of hysteresis controllers maintaining semiconductors at a fixed switching state position, its variable switching frequency, which depends on the speed/load torque operating point and the bandwidth of the hysteresis regulators, and the fact that its performance highly depends on the electrical drive topology [62, 76].

Traditionally, DTC schemes for electrical drives are based solely on an outer PI speed controller followed by two internal hysteresis regulators for torque and stator flux components, Fig. 2.10. Based on the available voltage space vectors, a look-up table is determined off-line, containing the different switching states and its effect on the stator flux and torque. The appropriate voltage vector is selected each sampling period in order to follow the controller references, given by hysteresis regulators, choosing the voltage vector that increases or reduces torque production following the stator flux reference.

To estimate the five-phase drive torque and flux, measured phase currents are first mapped into the stationary reference frame by the Clarke transformation (26). If the voltage variation across the stator resistance in a small sample period (T_s) is neglected, the stator phase flux can be obtained through (47) by:

$$\overrightarrow{\lambda_{s\alpha\beta}} = \int_0^t \left(\overrightarrow{v_{s\alpha\beta}} - R_s \overrightarrow{\imath_{s\alpha\beta}}\right) dt = \overrightarrow{v_{s\alpha\beta}} T_s \tag{107}$$

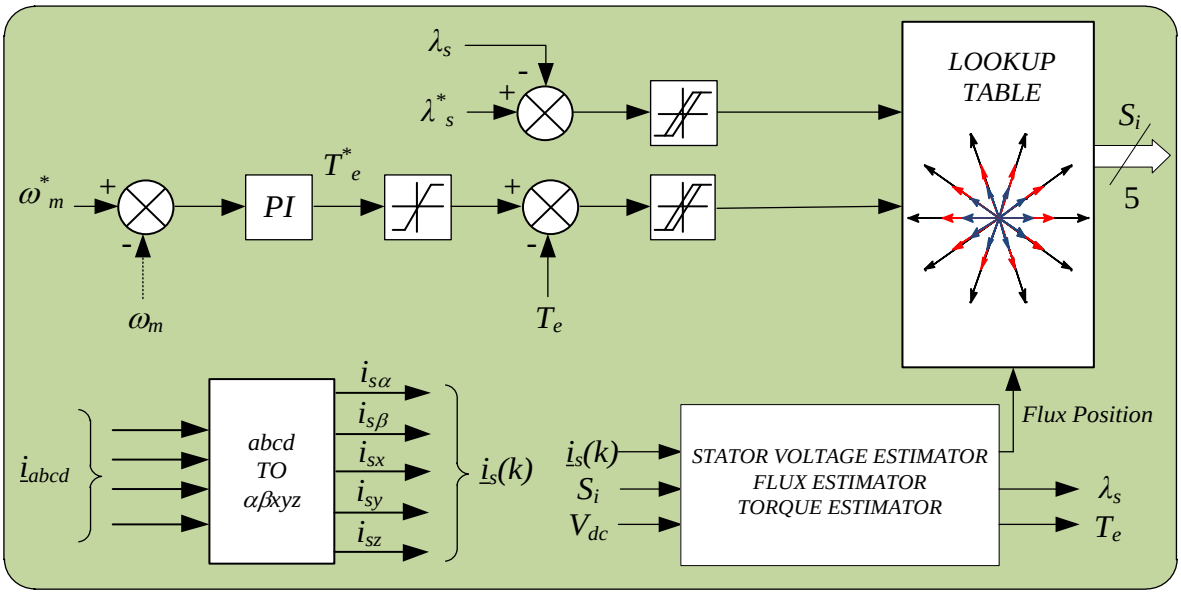

Fig. 2.10.: Direct Torque Control scheme for five-phase drive.

Notice that the increment of the stator flux component directly depends on the stator voltage vector, which can also be determined through the converter switching states (108), avoiding the necessity to implement voltage sensors to determine phase voltages. Nonetheless, if the DC-Link voltage is not constant, it is necessary to measure its value in order to properly determine the stator voltage vector in the stationary reference frame.

$$\overrightarrow{v_{s\alpha\beta}} = \frac{2}{5}V_{dc}\left[S_a + S_b e^{j\frac{2\pi}{5}} + S_c e^{j\frac{4\pi}{5}} + S_d e^{-j\frac{4\pi}{5}} + S_e e^{-j\frac{2\pi}{5}}\right] \quad (108)$$

The electromagnetic torque in the complex vector form and in the stationary reference frame (76), can be also expressed in terms of the stator flux and rotor flux as:

$$T_e = \frac{5}{2}\frac{Pk_r}{\sigma L_s}\left(\overrightarrow{\lambda_{r\alpha\beta}} \times \overrightarrow{\lambda_{s\alpha\beta}}\right) \quad (109)$$

$$\sigma = 1 - \left(\frac{L_m^2}{L_s L_r}\right) \quad (110)$$

Notice that the stator and rotor flux are related through (111). Given that the stator current is multiplied by a constant term with a small value, if the instantaneous stator current change is limited, the difference between stator and rotor flux is negligible, thus it can be assumed that both components have the same value ($\overrightarrow{\lambda_{s\alpha\beta}} = \overrightarrow{\lambda_{r\alpha\beta}}$) [62]. Considering this, and finding the derivative of (109) in order to establish the change of the electromagnetic torque with respect to time:

$$\overrightarrow{\lambda_{s\alpha\beta}} = k_r\overrightarrow{\lambda_{r\alpha\beta}} + \sigma L_s\overrightarrow{\imath_{s\alpha\beta}} \rightarrow \overrightarrow{\lambda_{s\alpha\beta}} = \overrightarrow{\lambda_{r\alpha\beta}} \quad (111)$$

$$\frac{\sigma L_s}{Pk_r}\frac{d}{dt}T_e = \left[\left(\overrightarrow{\lambda_{r\alpha\beta}} \times \overrightarrow{v_{s\alpha\beta}}\right) - R_m T_e - \omega_r \lambda_{s\alpha\beta}^2\right] \quad (112)$$

$$R_m = \frac{R_s}{Pk_r} + \frac{\sigma L_s}{Pk_r\tau_r} + \frac{L_m}{P\tau_r} \quad (113)$$

As a result, torque production is directly related to the stator flux (which is independently controlled to a constant value) and the applied voltage vector, thus proper selection of the voltage vector will increase or decrease produced torque.

Notice that depending on the electrical drive topology, the number of available voltage vectors varies. As a result DTC offers better performance as the number of phases of the electrical drive and/or as the number of voltage levels of the power converter increases, resulting in higher number of available voltage vectors and consequently reducing flux and torque ripple at the expense of a more complex look-up table [62, 76]. For instance a five-phase drive has 32 available voltage vectors (Fig. 2.7), offering improved control flexibility when compared with drives with fewer number of phases. Those vectors mapped in the α-β plane that tend to the same direction, have the same control effect on the machines torque and flux, however the controllers response depends on the amplitude of the selected vector, where large vectors (Fig. 2.7 in black color) provide faster response, followed by medium and small vectors. Proper selection of voltage vectors highly influences the electrical drive operation, for instance when a step change in torque or flux reference is applied to the controller, large voltage vectors will be selected at first, trying to achieve a fast response, however due to the absence of current control loops, this will lead to high phase currents. Consequently additional control measures have been proposed in the literature such as maximum torque saturation [75], use of improved switching tables and vector selection [77]. An additional effect that is compensated by improving the methods used for proper voltage vector selection is the flux weakening observed when working at low speed, where traditional DTC predominantly selects zero voltage vectors, reducing the machine flux [75].

In order to further compensate DTC drawbacks different modifications to its structure have been proposed in the literature. Research presented in [77] implements a modified DTC scheme for five-phase drives (Fig. 2.11), based on two look-up tables, containing the effect of the different voltage vectors on the α-β and x-y planes. Consequently the selected voltage vector will be the one that maximizes torque and flux and also has a small impact in the x-y plane, reducing low order harmonics. Moreover the use of DTC schemes with PI controllers and SVPWM strategies [78, 79] have been also proposed, in order to compensate the variable switching frequency and torque/flux ripple.

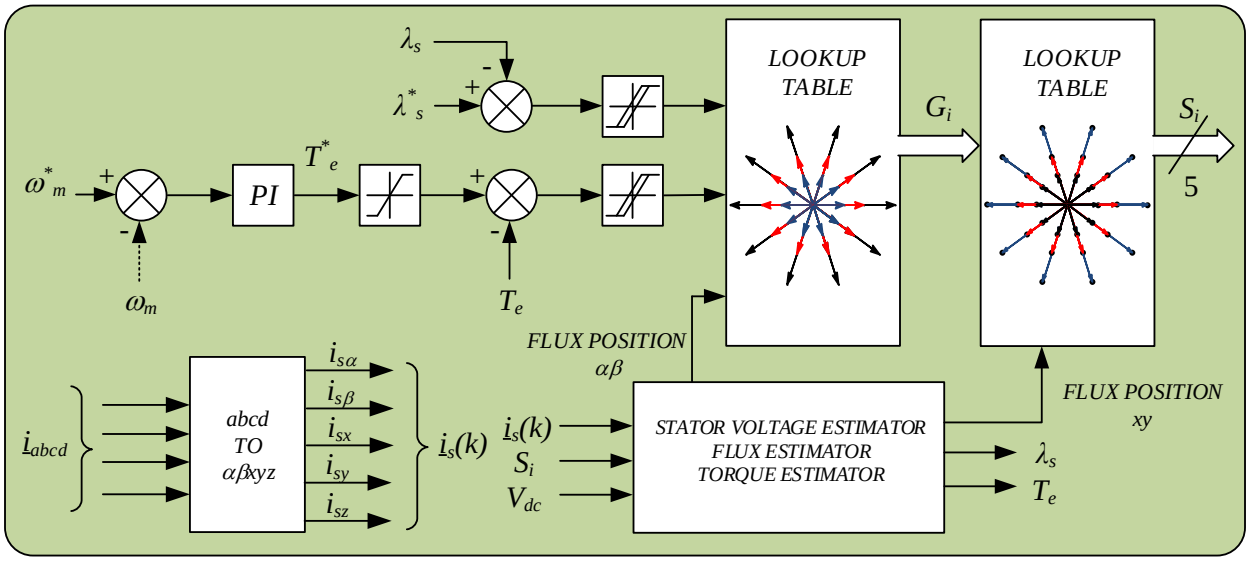

Fig. 2.11.: Modified DTC scheme with two lookup tables for five-phase drive.

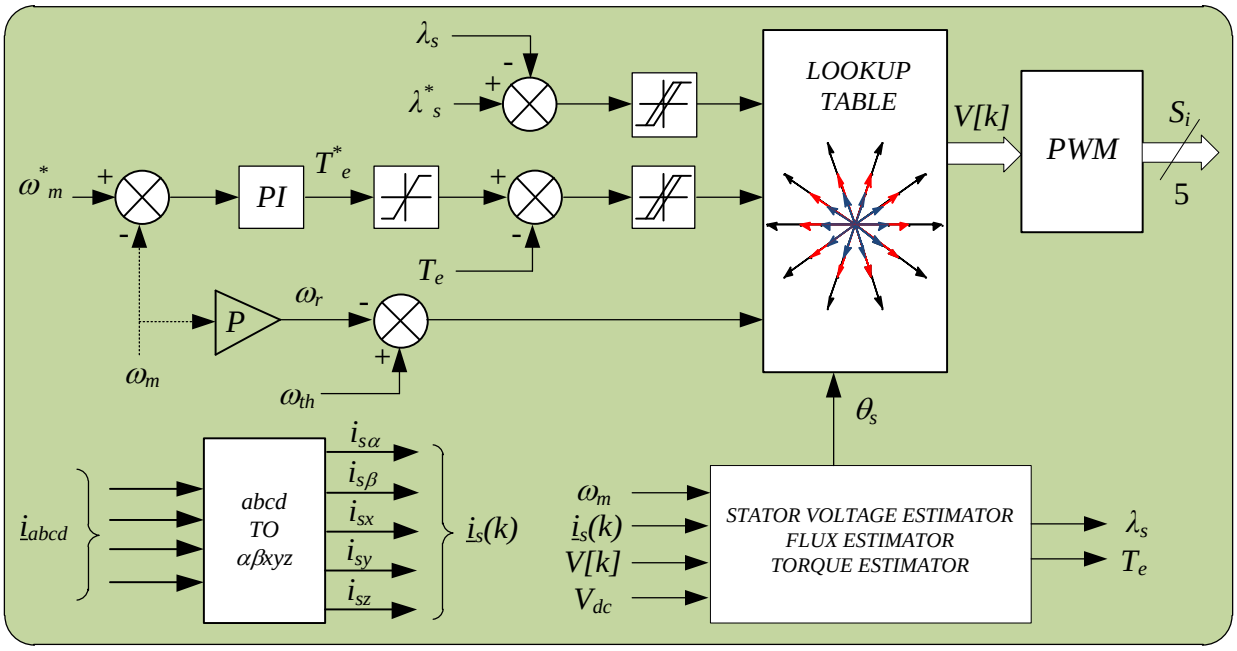

Fig. 2.12.: Modified DTC scheme with virtual vector lookup table for five-phase drive.

More recently, modified schemes have been proposed including new capabilities to traditional DTC such as sensorless drive control [80], where only phase currents and DC-Link voltage are measured in order to calculate the stator flux position and load angle, necessary to estimate the machines position and speed, achieving speed sensorless operation. Correspondingly, research presented in [40], also achieves speed sensorless operation, while avoiding the demagnetizing effect at low speed operation and eliminating low frequency current harmonics, through the inclusion of ten virtual voltage vectors in a modified lookup table, increasing control capabilities. Finally, based on

the virtual voltage vectors proposed in [40], a DTC with common-mode voltage reduction capability is proposed in [81], Fig. 2.12, where the additional virtual voltage vectors are selected in order to avoid zero voltage vectors.

2.4 PREDICTIVE CONTROL

Predictive controllers can be defined as any algorithm that is based on the model of the controlled system to predict its future behavior and selects the most suitable control action in order to correctly follow the control criteria. Different predictive controllers are available in the literature and have been thoroughly studied in [82, 83], presenting the general subdivision shown in Fig. 2.13. Further on, depending on their operating principle, available techniques have been classified into classical predictive control and Finite-Control Set Model-Based Predictive Control (FCS-MPC) [84].

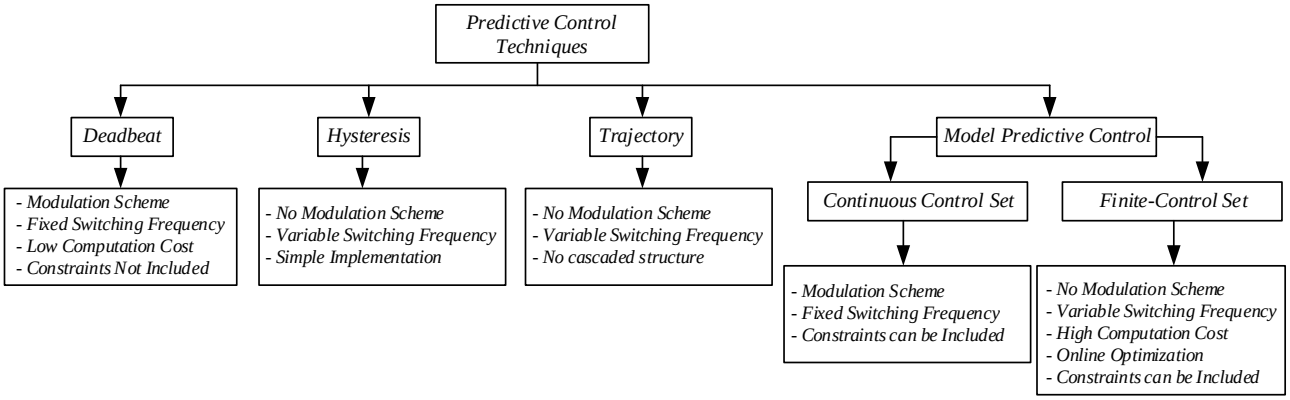

Fig. 2.13.: Predictive control methods.

Deadbeat Predictive Control (DBPC) is classified as a classical predictive controller and is based on an accurate model of the system to estimate the required voltage to achieve the reference value of the controlled variable. The required reference voltage is imposed to the electrical drive through modulation strategies, thus operating with a fixed switching frequency. This is one of the main differences between DBPC and hysteresis, trajectory and FCS-MPC strategies. This scheme has been applied for three- and five- phase drives in [85, 86, 87, 88].

Hysteresis Predictive Control (HPC), also classified as a classical controller, is based on maintaining the control variables between predefined boundaries, given by the hysteresis regulator. When the controlled variable reaches the limit of the control boundary, a new switching state is determined, by predicting the time intervals required in order for the controlled vector to reach the hysteresis boundary [82].

Trajectory Predictive Control (TPC) techniques consist on forcing the controlled variables to follow a pre-calculated trajectory, by applying a pre-defined set of switching states, classified depending on the effect they have on the electrical drive, either increasing or decreasing torque production, as presented in [89], where Direct Self Control (DSC) is developed for a three-phase drive.

Model Predictive Control (MPC) consists of an accurate model of the system that is used to predict the future behavior of the state variables through time, depending on the applied voltage vector. Each sampling period an error between the controlled variables and the ones predicted in the model are evaluated in a cost function. The switching state that ensures a lower cost function is selected to be applied during the next cycle. Among the benefits of MPC control is the capability to include systems nonlinearities and consider at the same time different constraints, such as current ratings, common-mode voltage and low order harmonics reduction. On the other hand, the main drawback of MPC is the high amount of calculations needed in order to solve the optimization problem online. This limits the implementation because sampling times must be big enough in order to ensure proper algorithm calculation. In order to compensate this drawback, three different modifications to the traditional MPC have been presented in the literature:

A. Solving the optimization problem off-line: Implementing the MPC online as a search tree, consequently reducing the time needed by the controller to select a proper control action [90].
B. Generalized Predictive Control (GPC): A linear controller is obtained by solving the optimization problem analytically. However this makes the inclusion of systems nonlinearities and different constraints in the basic MPC much more difficult [91].
C. Finite-Control Set Model-Based Predictive Control (FCS-MPC): Based on the discrete/finite number of switching states of the power converters. The optimization problem is reduced to the estimation of the electrical drive behavior due to available switching states, selecting the switching state that minimizes the implemented cost function [92].

The present doctoral thesis presents a novel fault-tolerant control strategy based on FCS-MPC techniques. Consequently the following literature review is based solely on FCS-MPC control techniques.

2.4.1 FINITE-CONTROL SET MODEL-BASED PREDICTIVE CONTROL

FCS-MPC techniques [92], have become an interesting alternative to the standard FOC and DTC approaches in the development of high-performance three- and multiphase drives [29, 41, 84, 93], and have been proposed with different types of power converters [94, 95].

The basic scheme of FCS-MPC is presented in Fig. 2.14. In this case in order to present a simple FCS-MPC, the external control loop is neglected, however depending on the implemented external loop, current references are provided by speed and flux controllers.

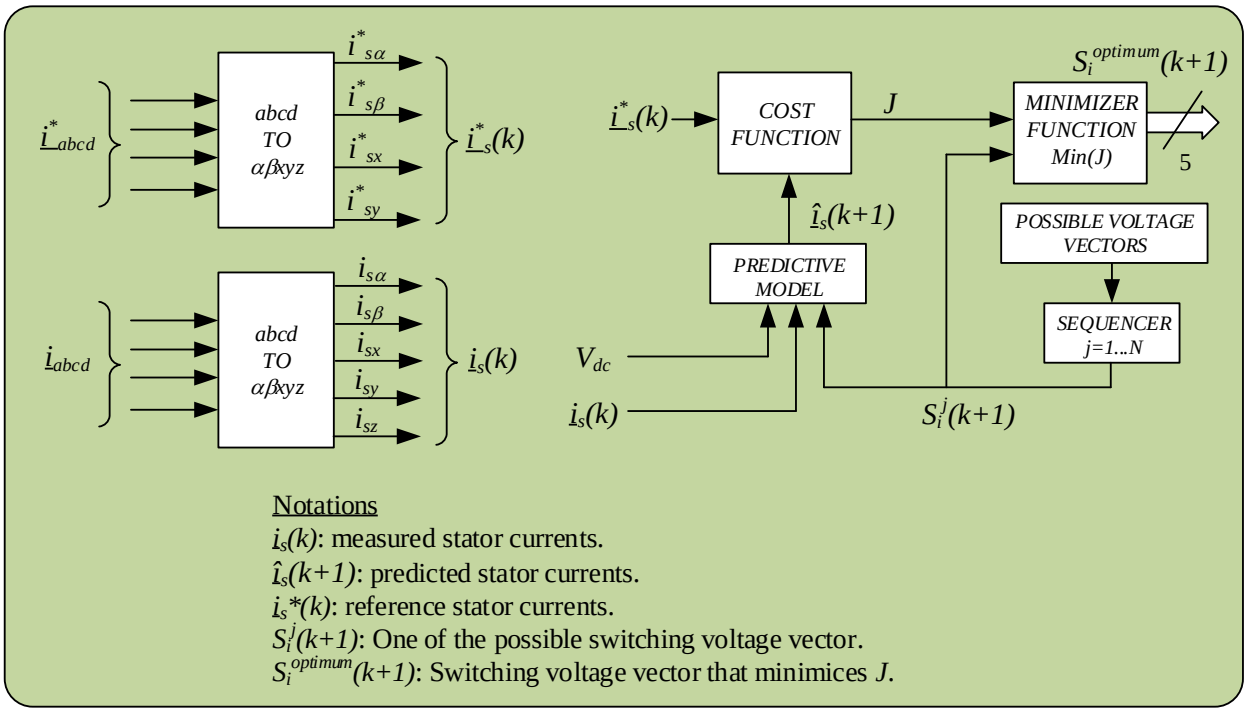

Fig. 2.14.: Finite-Control Set Model-Based Predictive Control scheme.

Every sampling period, the reference ($\underline{i}_s^*(k)$) and measured phase currents ($\underline{i}_s(k)$) are mapped in the stationary reference frame. Then, the machine state-space model is used, to predict current evolution ($\hat{\underline{i}}_s(k+1)$), depending on the different possible switching states ($S_i^j(k+1)$) and considering the VSI DC-Link voltage and measured phase currents ($\underline{i}_s(k)$). Subsequently, a cost function (J) is evaluated, considering each predicted current and the reference current ($\underline{i}_s^*(k)$). Finally, the switching vector that provides the lowest value of the cost function (J), is applied to the power converter during the next sampling period ($S_i^{optimum}(k+1)$). This process is depicted in the flow

diagram in Fig. 2.15.

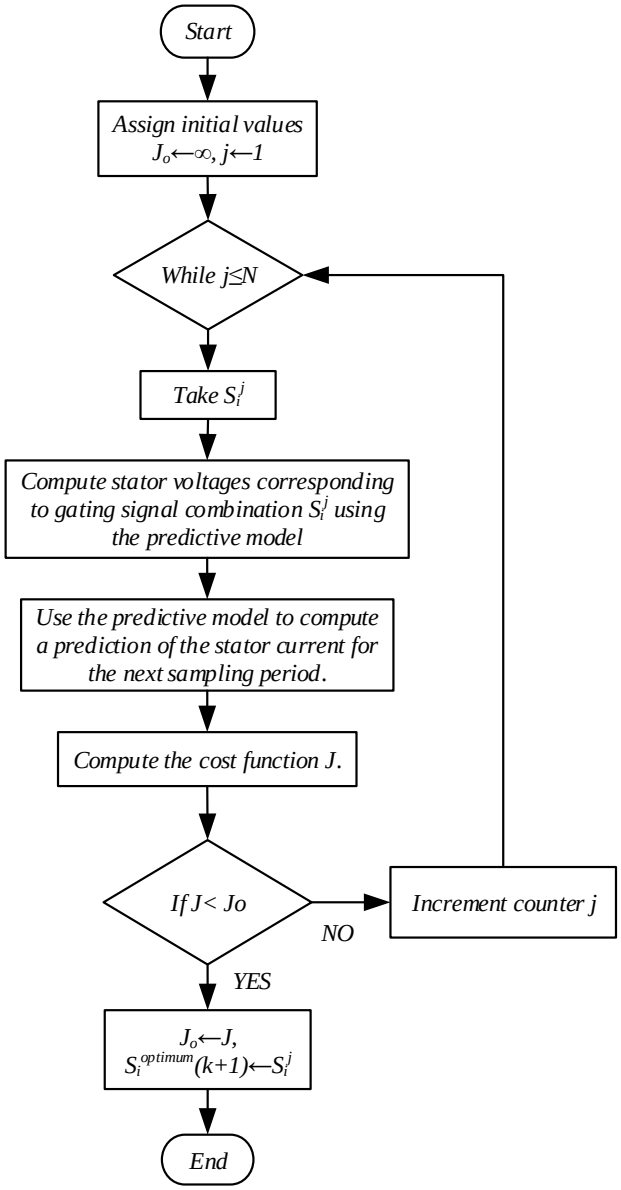

Fig. 2.15.: FCS-MPC flow diagram.

Notice that different cost functions (114) can be defined depending on the specific application in order to include different control constraints (C_i). For instance in a conventional FCS-MPC current controller, the cost function may only depend on the reference and predicted currents in the stationary reference frame, however when a FCS-MPC torque control is implemented, the cost function is defined not only by predicted current but also by predicted torque and flux. Furthermore, different control criteria aimed to optimize the multiphase drive performance, such as DC-Link voltage balancing, switching stress minimization, common-mode voltage reduction and stator current

harmonic minimization, can be included. Each of the constraints considered in the cost function can be assigned a different degree of importance on the overall controller objective, through the proper definition of weight factors (W_i). Being this one of the advantages of FCS-MPC, where different constraints can be considered without an increase in its implementation complexity.

$$J = W_1 C_1 + W_2 C_2 + \cdots + W_i C_i \quad (114)$$

FCS-MPC can be classified in two categories depending on the prediction horizon (N_p) they implement, in either large or short prediction horizon [84]. Prediction horizon can be defined as the number of future states in time that the controller predicts in order to select the most suitable control action. Short prediction horizon is defined as ($N_p = 1$), where measured variables are determined in the instant (k), then the optimum switching state is calculated for ($k + 1$) and applied at ($k + 1$). On the other hand large prediction horizon ($N_p \geq 2$), further predict the behavior of the electrical drive for future instants ($k + 2, k + 3$ ...) and selects the optimum VSI switching state to be applied on ($k + 1$), respectively (Fig. 2.16). It has been demonstrated that larger prediction horizon results in better performance [95], however the increase in the prediction horizon, results in higher computational costs making its implementation not suitable [96]. Notice that FCS-MPC does not provide a fixed switching frequency, due to the fact that it does not necessarily apply a switching vector to the VSI each sampling period.

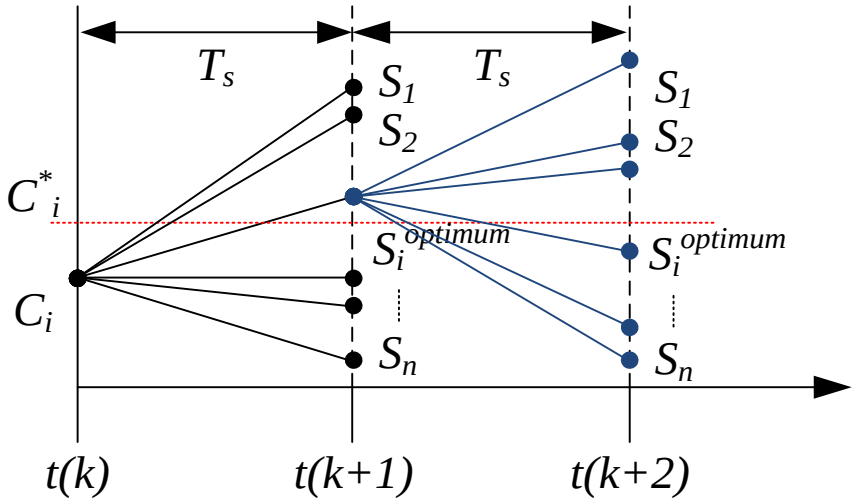

Fig. 2.16.: FCS-MPC prediction horizon principle.

In order to implement the FCS-MPC in a Digital Signal Processor (DSP), the machine modeling equations must be represented in a discrete-time state-space form [97, 98]. In this case the

stator phase currents and rotor flux, in the stationary reference frame, are assumed as state variables [97]. As a result the machine modeling equations can be expressed as:

$$\frac{d}{dt}\overrightarrow{i_{s\alpha\beta}} = -\left(\frac{1}{\sigma\tau_s} - \frac{1-\sigma}{\sigma\tau_r}\right)\overrightarrow{i_{s\alpha\beta}} + \frac{1-\sigma}{\sigma\tau_r L_m}\overrightarrow{\lambda_{r\alpha\beta}} - \frac{1-\sigma}{\sigma L_m}\omega_r\overrightarrow{\lambda_{r\alpha\beta}} + \frac{1}{\sigma L_s}\overrightarrow{v_{s\alpha\beta}} \tag{115}$$

$$\frac{d}{dt}\overrightarrow{i_{sxy}} = -\frac{1}{\tau_{ls}}\overrightarrow{i_{sxy}} + \frac{1}{L_{ls}}\overrightarrow{v_{sxy}} \tag{116}$$

$$\frac{d}{dt}\overrightarrow{i_{sz}} = -\frac{1}{\tau_{ls}}\overrightarrow{i_{sz}} + \frac{1}{L_{ls}}\overrightarrow{v_{sz}} \tag{117}$$

$$\frac{d}{dt}\overrightarrow{\lambda_{r\alpha\beta}} = \frac{L_m}{\tau_r}\overrightarrow{i_{s\alpha\beta}} - \frac{1}{\tau_r}\overrightarrow{\lambda_{r\alpha\beta}} - j\omega_r\overrightarrow{\lambda_{r\alpha\beta}} \tag{118}$$

$$\overrightarrow{\lambda_{s\alpha\beta}} = \sigma L_s\overrightarrow{i_{s\alpha\beta}} + k_r\overrightarrow{\lambda_{r\alpha\beta}} \tag{119}$$

Being k_r, τ_r, σ, τ_s and τ_{ls} as defined in (102), (103), (110), (120) and (121), respectively.

$$\tau_s = \frac{L_s}{R_s} \tag{120}$$

$$\tau_{ls} = \frac{L_{ls}}{R_s} \tag{121}$$

Rewriting (115)-(119) in terms of their real and imaginary components in matrix form:

$$\frac{d}{dt}[x] = [A][x] + [B][u] \tag{122}$$

$$[y] = [C][x] \tag{123}$$

where:

$$[x] = \left[i_{s\alpha}\ i_{s\beta}\ i_{sx}\ i_{sy}\ i_{sz}\ \lambda_{r\alpha}\ \lambda_{r\beta}\right]^T \tag{124}$$

$$[u] = \left[v_{s\alpha}\ v_{s\beta}\ v_{sx}\ v_{sy}\ v_{sz}\ \right]^T \tag{125}$$

$$[y] = \left[\lambda_{s\alpha}\ \lambda_{s\beta}\right]^T \tag{126}$$

$$[A] = \begin{bmatrix} -\left(\frac{1}{\sigma\tau_s} - \frac{1-\sigma}{\sigma\tau_r}\right) & 0 & 0 & 0 & 0 & \frac{1-\sigma}{\sigma\tau_r L_m} & \frac{1-\sigma}{\sigma L_m}\omega_r \\ 0 & -\left(\frac{1}{\sigma\tau_s} - \frac{1-\sigma}{\sigma\tau_r}\right) & 0 & 0 & 0 & -\frac{1-\sigma}{\sigma L_m}\omega_r & \frac{1-\sigma}{\sigma\tau_r L_m} \\ 0 & 0 & -\frac{1}{\tau_{ls}} & 0 & 0 & 0 & 0 \\ 0 & 0 & 0 & -\frac{1}{\tau_{ls}} & 0 & 0 & 0 \\ 0 & 0 & 0 & 0 & -\frac{1}{\tau_{ls}} & 0 & 0 \\ \frac{L_m}{\tau_r} & 0 & 0 & 0 & 0 & -\frac{1}{\tau_r} & -\omega_r \\ 0 & \frac{L_m}{\tau_r} & 0 & 0 & 0 & \omega_r & -\frac{1}{\tau_r} \end{bmatrix} \tag{127}$$

$$[B] = \begin{bmatrix} \frac{1}{\sigma L_s} & 0 & 0 & 0 & 0 \\ 0 & \frac{1}{\sigma L_s} & 0 & 0 & 0 \\ 0 & 0 & \frac{1}{L_{ls}} & 0 & 0 \\ 0 & 0 & 0 & \frac{1}{L_{ls}} & 0 \\ 0 & 0 & 0 & 0 & \frac{1}{L_{ls}} \\ 0 & 0 & 0 & 0 & 0 \\ 0 & 0 & 0 & 0 & 0 \end{bmatrix} \tag{128}$$

$$[C] = \begin{bmatrix} \sigma L_s & 0 & 0 & 0 & 0 & k_r & 0 \\ 0 & \sigma L_s & 0 & 0 & 0 & 0 & k_r \end{bmatrix} \tag{129}$$

Notice in (127) that matrix $[A]$ has components that depend on the instantaneous value of the mechanical speed (ω_m) and consequently it is not possible to calculate all its terms off-line. However it is possible to divide matrix $[A]$ into a constant matrix $[A_c]$ and a speed dependent $[A_\omega]$ matrix, allowing to estimate off-line all matrix $[A]$ constant components and online only those components dependent on the mechanical speed, as follows:

$$[A] = [A_c] + [A_\omega] \tag{130}$$

Next, the machine state-space equations (122)-(123) are discretized with a sample period (T_s), assuming constant input and constant matrices during the whole sampling period [98]:

$$x[k+1] = [\Phi]x[k] + [\Gamma]u[k] \tag{131}$$

$$y[k+1] = [C]x[k+1] \tag{132}$$

$$[\Phi] = e^{[A]T_s} = e^{([A_c]+[A_\omega])T_s} = e^{[A_c]T_s} \cdot e^{[A_\omega]T_s} \tag{133}$$

$$[\Gamma] = \int_0^{T_s} e^{[A]\tau}\,[B]d\tau = e^{[A_c]T_s}[B]T_s \tag{134}$$

Consequently matrix [Φ], consists of a constant term ($e^{[A_c]T_s}$), calculated off-line and a time varying term ($e^{[A_\omega]T_s}$), which by applying the Cayley-Hamilton theorem, can be defined as [98]:

$$e^{[A_\omega]T_s} = \begin{bmatrix} 1 & 0 & 0 & 0 & 0 & L_m\frac{1-cos(\omega_r T_s)}{\sigma L_s L_r} & L_m\frac{sin(\omega_r T_s)}{\sigma L_s L_r} \\ 0 & 1 & 0 & 0 & 0 & -L_m\frac{sin(\omega_r T_s)}{\sigma L_s L_r} & L_m\frac{1-cos(\omega_r T_s)}{\sigma L_s L_r} \\ 0 & 0 & 1 & 0 & 0 & 0 & 0 \\ 0 & 0 & 0 & 1 & 0 & 0 & 0 \\ 0 & 0 & 0 & 0 & 1 & 0 & 0 \\ 0 & 0 & 0 & 0 & 0 & cos(\omega_r T_s) & -sin(\omega_r T_s) \\ 0 & 0 & 0 & 0 & 0 & sin(\omega_r T_s) & cos(\omega_r T_s) \end{bmatrix} \tag{135}$$

In the following subsections some of the FCS-MPC schemes implemented in multiphase drives will be presented. Notice that the proposed techniques are based on fast inner FCS-MPC controllers with outer slower PI regulators, offering higher control bandwidth compared with cascaded PI controllers [84].

2.4.1.1 PREDICTIVE CURRENT CONTROL

Predictive Current Control (PCC) based on FCS-MPC uses only the predicted stator currents in the stationary reference frame in order to control the multiphase drive. Current references are obtained in the rotating reference frame, from an outer PI based speed control loop and a constant d-component current and then mapped in the stationary reference frame in order to be used in the cost function, as shown in Fig. 2.17. This simple predictive controller scheme has been implemented in multiphase drives, with different number of windings, neutral points and power converters [29, 30, 41].

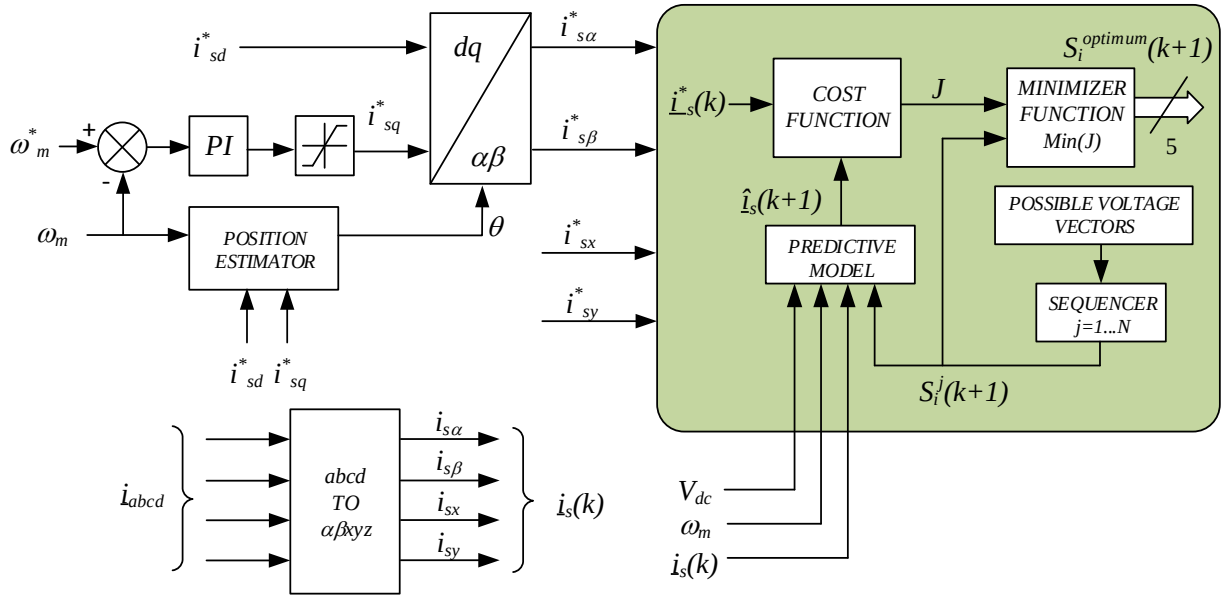

Fig. 2.17.: FCS-MPC based Predictive Current Control with an outer speed control loop.

The overall control aim is to generate a desired electric torque which implies sinusoidal stator current references in a-b-c-d-e phase coordinates. In the stationary α-β-x-y reference frame, the control aim is traduced into a reference stator current vector in the α-β plane, which is constant in magnitude but changing its electrical angle following a circular trajectory, and depending on the implemented multiphase machine, either null or non-null reference stator current vector in the x-y plane. For instance, if a five-phase machine with distributed windings is implemented, the α-β stator

current components contribute to torque production while x-y stator current components do not, thus a zero reference is set for the x-y current components. The weight factors in the cost function (136) are adjusted in order to favor those switching states (32, for a five-phase two-level VSI), that maximize α-β currents and at the same time provide minimum x-y currents.

$$J = A|\overline{\overline{\iota_{s\alpha}}}| + B\left|\overline{\overline{\iota_{s\beta}}}\right| + C|\overline{\overline{\iota_{sx}}}| + D\left|\overline{\overline{\iota_{sy}}}\right| \quad (136)$$

where each α-β-x-y current term is defined as:

$$\overline{\overline{\iota_{s\alpha}}} = i^*_{s\alpha}(k+1) - \hat{\imath}_{s\alpha}(k+1),\ \overline{\overline{\iota_{s\beta}}} = i^*_{s\beta}(k+1) - \hat{\imath}_{s\beta}(k+1) \quad (137)$$

$$\overline{\overline{\iota_{sx}}} = i^*_{sx}(k+1) - \hat{\imath}_{sx}(k+1),\ \overline{\overline{\iota_{sy}}} = i^*_{sy}(k+1) - \hat{\imath}_{sy}(k+1) \quad (138)$$

In [41], a predictive current controller in the rotating reference frame was implemented for a five-phase two-level induction motor drive with a modified cost function (139) and its performance was compared against an IRFOC, in different operating points. In this case a weight factor has only been provided for *x-y* currents in order to favor currents produced in the *d-q* plane. It was concluded that the PCC controller provided better transient state performance and low order harmonic minimization, while the IRFOC ensured better steady-state operation and offered lower phase current ripple regardless of the operating frequency, at the expense of higher switching stress.

$$J = \overline{\overline{\iota_{sd}}} + \overline{\overline{\iota_{sq}}} + W_{xy}\left[\overline{\overline{\iota_{sxy}}}\right] \quad (139)$$

where each d-q-x-y current term is defined as:

$$\overline{\overline{\iota_{sd}}} = \left(i^*_{sd}(k+2) - i_{sd}(k+2)\right)^2,\ \overline{\overline{\iota_{sq}}} = \left(i^*_{sq}(k+2) - i_{sq}(k+2)\right)^2 \quad (140)$$

$$\overline{\overline{\iota_{sxy}}} = \left[\left(i^*_{sx}(k+2) - i_{sx}(k+2)\right)^2 + \left(i^*_{sy}(k+2) - i_{sy}(k+2)\right)^2\right] \quad (141)$$

2.4.1.2 PREDICTIVE TORQUE CONTROL

The general scheme of the Predictive Torque Control (PTC) based on FCS-MPC for five-phase two-level induction motor drives presented in [42] is shown in Fig. 2.18. It is formed by an outer PI based speed control and an inner PTC, whose controlled variables are the stator flux and the produced torque. The basic PTC cost function is defined as in (142), where (T_n^2) and (λ_{sn}^2) represent the weight factor of torque and stator flux components and their value corresponds to their rated values at base speed operation. In order to improve PTC performance in [42] a modified cost function was presented, aimed to not only control stator flux and produced torque but also limit the maximum

achievable α-β stator currents to ($i_{\alpha\beta-MAX}$) and reducing harmonic components in the x-y plane (143).

$$J = \frac{1}{T_n^2}\left(T_e^*(k) - T_e(k+1)\right)^2 + \frac{1}{\lambda_{sn}^2}\left(\lambda_s^*(k) - \lambda_s(k+1)\right)^2 \quad (142)$$

$$J = \frac{1}{T_n^2}\overline{\overline{T_e}} + \frac{1}{\lambda_{sn}^2}\overline{\overline{\lambda_s}} + K_{\alpha\beta}\left(\left|i_{s\alpha\beta}[k+1]\right| > i_{\alpha\beta-MAX}\right) + \frac{1}{i_{sn}^2}\left|i_{sxy}[k+1]\right|^2 \quad (143)$$

where torque and flux terms are defined as:

$$\overline{\overline{T_e}} = \left(T_e^*(k) - T_e(k+1)\right)^2, \overline{\overline{\lambda_s}} = \left(\lambda_s^*(k) - \lambda_s(k+1)\right)^2 \quad (144)$$

Torque reference is provided by an external PI, based on the speed error, while the stator flux reference has been set at its nominal value for base speed operation. For each of the 32 voltage vectors available in a five-phase two-level drive, the predictive model estimates the electromagnetic torque, stator flux and stator currents in the stationary reference frame. Then the cost function (143) is evaluated and the switching state with lower cost (J) is applied to the VSI.

Predictive torque control has been compared with FOC and DTC control techniques for the three- and five-phase case in [42, 84, 99], where it has been concluded that, PTC offers faster torque and speed response, with lower overshoot than both FOC and DTC, phase currents possess more ripple than FOC and DTC due to the variable switching frequency nature of FCS-MPC techniques and torque ripple is lower than in DTC.

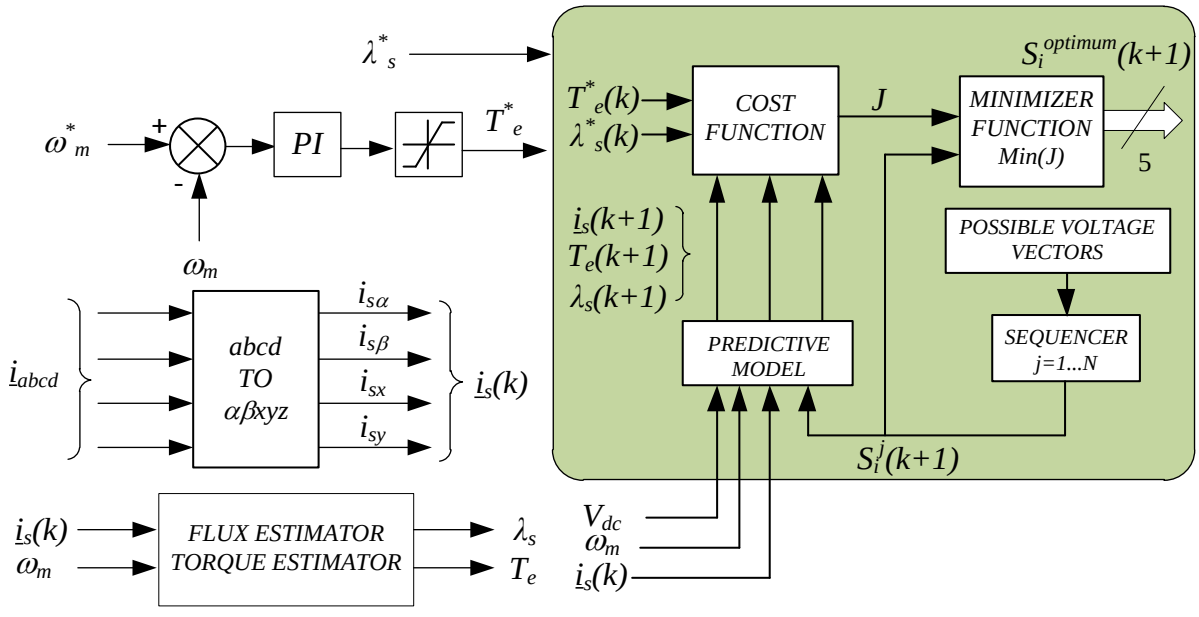

Fig. 2.18.: FCS-MPC based Predictive Torque Control with an outer speed control loop.

2.4.1.3 RESTRAINED SEARCH PREDICTIVE CONTROL

One of the main drawbacks of FCS-MPC is the high computational cost that is needed in order to estimate the state variables for all the available switching states for a given prediction horizon. This effect is further aggravated as multiphase drives and/or multilevel power converters are implemented, increasing the number of available voltage vectors and consequently the number of algorithm iterations. Restrained Search Predictive Control (RSPC) reduces the amount of voltage vectors used in the state variables prediction, based on constraints (A) or (B) and (C), which are evaluated each sampling period [100], as shown in Fig. 2.19. As a result discarded vectors are not selected off-line, but instead are dynamically selected, each sample period, using the following rules:

A. The subset of voltage vectors must include those that involve one commutation or less.
B. The subset of voltage vectors must include those that involve two commutations or less.
C. Any VSI leg must not commute in two consecutive switching periods.

Notice that condition (A) and (B) reduce the amount of commutations of the power converter, being (A) much more restrictive than (B), while condition (C) reduces the amount of commutations in each power converter leg.

The proposed RSPC implemented in [100] is based on a two-level six-phase drive, with 64 available voltage vectors. The controller is based on the predictive current control, previously presented (Fig. 2.17), and a cost function defined as (145).

$$J = \frac{1}{R_{\alpha\beta}}\left[\overline{\overline{i_{s\alpha}}} + \overline{\overline{i_{s\beta}}}\right] + \lambda_{xy}\left[i_{sx}(k+1)^2 + i_{sy}(k+1)^2\right] \quad (145)$$

where α-β current terms are defined as:

$$\overline{\overline{i_{s\alpha}}} = \left(i^*_{s\alpha}(k+1) - i_{s\alpha}(k+1)\right)^2,\ \overline{\overline{i_{s\beta}}} = \left(i^*_{s\beta}(k+1) - i_{s\beta}(k+1)\right)^2 \quad (146)$$

As a result of the constraints (A), (B) and (C), from the 64 available voltage vectors, only 6 voltage vectors are available if conditions (A) and (C) are adopted, while if conditions (B) and (C) are assumed, 16 voltage vectors are available in case one power converter leg is switched in the previous switching period and 11 if two legs are switched in the previous switching period. As a result, both set of condition (A and C) or (B and C), highly reduce the amount of calculations needed in order to select an appropriate switching state, being condition (A and C) much more restrictive than (B and C). This results in better dynamic performance of the RSPC implementing conditions (B and C), when compared to (A and C), being the first one similar to the performance obtained when all 64 switching states are evaluated, but with lower total current harmonic distortion. Furthermore it is

observed that the sampling period when RSPC is implemented, with conditions (B and C), can be reduced up to a (50%) of the sampling period with traditional FCS-MPC, in order to obtain a similar switching frequency [100].

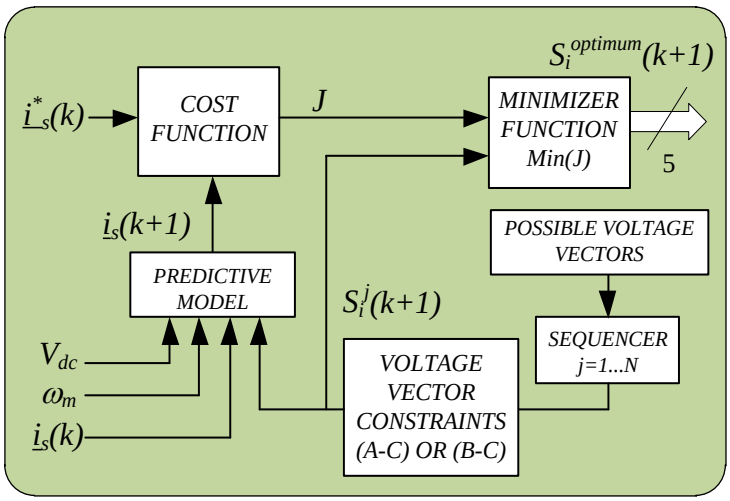

Fig. 2.19.: FCS-MPC based Restrained Search Predictive Control.

2.5 FAULT-TOLERANCE IN MULTIPHASE DRIVES

In order to increase the use of electrical drives in different high-demand applications, the development of cost-effective robust and reliable systems has become one of the latest challenges in electrical drives design [101]. Fault-tolerant capability, i.e. the ability to ensure proper speed or torque reference tracking under abnormal conditions, has been considered in three-phase electrical drives taking into account different design and research approaches, including redundant equipment and over dimensioned designs, leading to effective and viable fault standing but costly solutions. As recent research suggests, fault-tolerance in three-phase drives for different types of faults is viable, ensuring drive performance and control capability only at the expense of extra equipment [101]. This is not the case of multiphase drives which, due to the higher number of phases they possess, present higher fault-tolerant capability than conventional three-phase drives, without the need of extra electrical equipment and only requiring proper post-fault control techniques in order to continue operating [102]. For instance, multiphase drives with single neutral machines are capable of maintaining operation as long as three healthy phases are remaining [103]. This inherent fault-tolerance without the need of extra hardware is specially appreciated in traction and aerospace applications for security reasons and also in offshore wind farms where corrective maintenance can result in extra costs and

be difficult under bad weather conditions [3, 104, 105, 106].

As in pre-fault operation, post-fault achievable torque depends on the specific characteristics of the electrical drive, which include the machines characteristics, number of windings and windings angle displacement [105].

Fault management is divided in four different states namely, fault occurrence, fault detection (FD), fault isolation (FI) and finally post-fault control or fault-tolerant control (FTC) operation. Different fault detection techniques have been proposed based on the specific characteristics the electrical drive presents once a fault has occurred. Subsequently, depending on the electrical drive topology and type of fault, the fault isolation is done in order to ensure proper post-fault behavior. As a result there are commonly found in the literature, strategies that address both fault detection and isolation (FDI). Finally, a proper post-fault control needs to be implemented in order to maintain correct reference tracking. This includes considering the applicable electrical drive derating and suitable post-fault control references.

Abnormal or faulty operation of an electrical drive generally results in asymmetrical current, voltage and flux components, producing torque and speed oscillation and leading to certain fault-dependent frequency components which can be used in order to develop different fault detection algorithms [107]. Fault detection and isolation is not considered in this thesis work and consequently a thorough study is not done within the document.

In this section, a survey analysis on the different types of faults in electrical drives will be presented. The available detection and isolation methods will be slightly commented and the proposed post-fault control techniques, for multiphase drives, will be studied. For this purpose, the electrical drive, such as the one in Fig. 2.20, is divided in four main groups namely, the power converter, electronic sensors (current, temperature, speed and voltage), main electronic control unit and electrical machine. Faults due to errors in the main electronic control unit will be associated to the effect they produce in the power converter (i.e. like the IGBT-gating failure effect leaving the semiconductor either in ON or OFF state), thus they will not be studied independently. As it is expected, fault types are not dependent on the electrical drive number of phases. However, the fault management highly depends on the drive power converter configuration and electrical machine type. Moreover, it must be considered that different types of faults may result in the same abnormal machine behavior (i.e. an open-phase fault due to a machine winding rupture or the damage of two semiconductors of one phase in the power converter).

Multiphase drive faults can be classified depending on their nature (electrical or mechanical), location or on the effect they have on the overall system (open-phase, sensor loss, etc.).

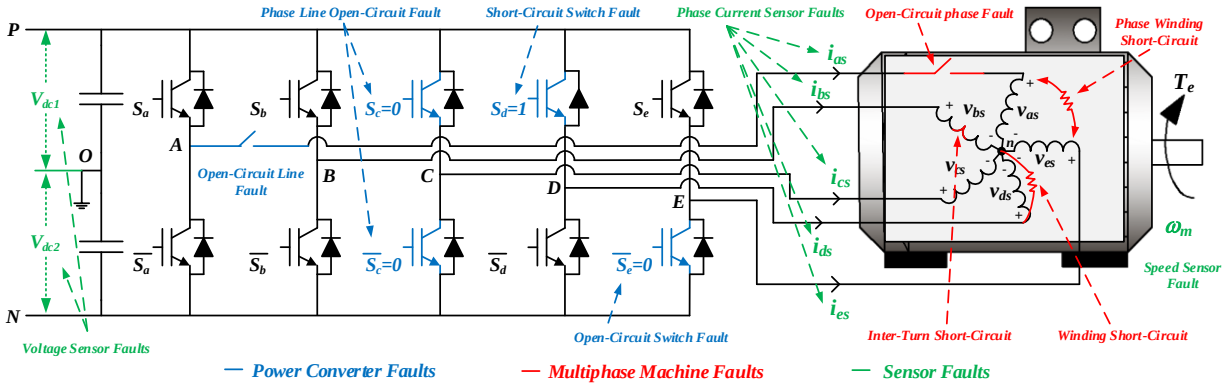

Fig. 2.20.: Multiphase drive types of faults.

In this thesis, faults will be classified depending on the location of its occurrence as shown in Fig. 2.20:

1. Multiphase Machine Faults.
2. Sensor Faults.
3. Power Converter Faults.

2.5.1 MULTIPHASE MACHINE FAULTS

Electrical machine faults can be caused by either electrical or mechanical problems/stress and can be classified as [107, 108, 109, 110, 111]:

1. Stator Faults:
    a. Open-circuit of one or more stator phase windings.
    b. Short-circuit of one or more stator phase windings.
2. Rotor Faults:
    a. Shorted rotor field winding.
    b. Broken rotor bars.
    c. Cracked rotor end-rings.
3. Eccentricity or Air-gap irregularities:
    a. Static.
    b. Dynamic.
4. Bearing Faults.
5. Bent shaft.

As stated in [107, 108, 109], the most common faults in electrical machines are the bearing failures, stator winding faults, broken rotor bar, shaft and coupling faults, cracked rotor end-rings and air-gap eccentricity. Leading to unbalanced stator currents and voltages, the appearance of specific harmonics in the phase currents, overall torque oscillation and reduction, machines vibration, noise, overheating and efficiency reduction [110, 111]. These abnormal operating characteristics have been considered by researchers in order to detect and determine a fault occurrence in the electrical drive, leading to different diagnostic methods based on monitoring the variation in the machines electromagnetic field, temperature, radio frequency emission, noise, vibration and current signature [110, 112].

2.5.1.1 STATOR FAULTS

Stator faults are mostly due to mechanically damaged connections caused by insulation failure due to the machines constructive characteristics (non-appropriate core lamination, slot wedges or joints or leakage in cooling systems), electrical operating conditions (high temperatures in the stator core or winding coils, starting stresses, over or under voltage operation, electrical discharges, unbalanced stator voltages) and ambient conditions (dirt, oil and moisture contamination) [110, 111, 113]. Leading to inter-turn [113], winding, stator-winding [114], and different phase windings short circuits [110, 111], which may further result in open-phase faults of one or more phase windings [115, 116].

Open-phase fault detection methods are based on analyzing the additional *x-y* current components available in multiphase drives and generating specific indices based on the pattern *x-y* currents would follow in normal and faulty condition, allowing to determine not only the fault occurrence but also its location [102, 113, 117, 118]. On the other hand, short circuit fault detection is based either on the analysis of the axial flux component by means of an external flux sensor wound around the machines shaft [119] or on motor current signature analysis techniques based on the unbalanced phase currents that appear in the machine after the fault occurrence due to the asymmetric impedance terms [120].

2.5.1.2 ROTOR FAULTS

Rotor faults are composed by both electrical faults (shorted rotor windings) and mechanical faults (broken bars and cracked rotor rings). These types of faults are mainly caused by thermal stress

due to the drive operation under overload and unbalanced load conditions, electromagnetic stress, manufacturing problems, dynamic stress from shaft torque, environmental conditions and fatigued mechanical parts [110, 111].

2.5.1.3 ECCENTRICITY FAULTS

Eccentricity is caused by manufacturing and constructive errors that cause an unequal air gap between the stator and the rotor, leading to unbalanced radial forces and possible rotor-stator contact [110]. Eccentricity can be further classified as static (where the position of the air gap inequality is fixed) and dynamic (where the rotor center is not properly aligned at the rotation center and the position of the air gap inequality rotates). Eccentricity detection methods are mostly based on phase current and vibration analysis [110, 121, 122].

2.5.1.4 BEARING FAULTS

Bearing faults are mainly caused by assembling errors, where the bearings may be misaligned or forced into the shaft/housing. This results in bearing vibration and may be detected by the machines phase currents analysis [121].

2.5.1.5 BENT SHAFT FAULTS

Bent shaft faults are similar to dynamic eccentricity faults [110], and are mainly due to force unbalance or machine-load misalignment, resulting on machine vibration and further machine failure [111].

2.5.2 SENSOR FAULTS

Speed, DC-Link voltage and current sensors are commonly used in electrical drives for control and protection purposes (Fig. 2.20). Such is the case of FOC and predictive techniques where speed and at least two (for a three-phase drive) and four (for a five-phase drive) current measurements are needed in order to ensure proper control behavior. In case of faulty sensor operation, inexistent, noisy or deviated measured signals can downgrade the system performance or result in a complete drive failure [123, 124, 125, 126]. Sensor faults have been mainly analyzed for three-phase drives and recent work has addressed this type of fault for the multiphase case [80, 127, 128]. The following reviewed articles consider also the three-phase case as a mean to present this type of fault, which depending on

the faulty sensor (i.e. DC-Link voltage, current or speed), may have the same effect in drives with higher number of phases.

Research has been mainly focused on handling only one faulty sensor due to the small probability of more than one sensor fault [129]. Post-fault operation techniques after sensor faults, are commonly based on switching between different control techniques depending on the type of sensor fault, reconfiguring from a closed-loop control to an open-loop strategy [130, 131, 132, 133, 134, 135], downgrading the electrical drive dynamic performance, or on implementing different independent observers, for either DC voltage, phase current or speed and maintaining closed-loop control operation [123, 132].

For instance, when a voltage sensor fault occurs its effect results, regardless of the number of drive phases, on either a very small or much higher voltage measurement with respect to the expected value. This is of special importance in electric vehicle applications where the DC-Link voltage is constantly changing and an accurate measure is needed [136]. Proposed techniques for DC-Link voltage estimation, susceptible of implementation in the multiphase case, are based on the modulation index and estimated phase voltage [123].

Current sensor faults are among the most critical faults in electrical drive applications. This is due to the fact that most closed-loop control techniques are based on current measurement and consequently any variation on the measured current may result in instantaneous power demanding control actions, leading the whole system to possible electrical stress. Current sensor faults are most commonly detected and handled by estimating the expected current values, based on the machines electrical parameters, Luenberger observers based on the remaining current sensor information and on adaptive and extended Kalman filters [123, 126, 129, 137, 138, 139, 140, 141], which can be extended to multiphase drives.

Similar to current sensor faults, speed sensor faults affect closed-loop speed control techniques leading to rotor field disorientation and power demanding control actions imposed by the controller aiming to maintain the speed reference [123]. These types of faults are mainly due to vibration and temperature issues and are effectively detected and handled, in the three-phase case, by using speed estimation techniques based on Luenberger observers and extended Kalman filters [126, 142, 143, 144]. Regarding multiphase drives, speed sensorless operation has been analyzed in a five-phase drive under normal operation with a DTC scheme [80], estimating the rotor speed/position based on the position of the stator flux linkages and under an open-phase fault [128], implementing a FOC scheme

with proportional-resonant controllers and estimating the machine speed using a rotor flux-based model reference adaptive system.

2.5.3 POWER CONVERTER FAULTS

Power converter faults are among the most non-predictable and common types of faults of industrial electrical drives [145]. These types of faults are mainly due to the semiconductor driver failure, leaving the semiconductor either in constant ON or OFF state or to the burn out of the semiconductor. Power converter faults are presented graphically in Fig. 2.20, and can be classified as [102]:

1. Single short-circuit switch fault.
2. Single open-circuit switch fault.
3. Phase-leg short-circuit fault.
4. Phase-leg open-circuit fault.
5. Open-circuit line fault.

These faults may lead the converter to either lose a complete phase (also termed open-phase fault) or to physically maintain the number of phases and current flow, but to lose specific control capabilities on either one or both of the semiconductor of a certain phase. As a result, it is possible to expect that the configuration of the electrical drive vary and that the post-fault electrical drive may be regarded as an entire different system [146].

As it has been stated in numerous previous works, the phase redundancy that multiphase drives possess allows managing faulty operation, depending on the specific electrical machine configuration, without the need of extra equipment. This holds true for any kind of open-circuit and short-circuit faults, where proposed post-fault control techniques exploit the extra degrees of freedom the faulty converter possess when compared to conventional three-phase converters.

Depending on the type of fault and the specific electrical drive topology, different post-fault control strategies, drive configuration and electrical machine winding connections are adopted for post-fault operation.

For instance, the inclusion of auxiliary semiconductors in each or some phase windings was addressed in [147], in order to physically isolate the short-circuit faulty phase (i.e. changing from a short-circuit fault to an open-circuit or open-phase fault), and ensure ripple free output torque with the remaining four healthy phases. As a result, the electrical drive is able to manage different types of

faults, but at the expense of extra electronic equipment. On the other hand, in [148] short-circuit faults are managed in a five-phase drive by controlling the available four healthy phases, maintaining operation at the expense of higher stator phase windings losses and torque ripple. However in a dual three-phase drive [114], this increase in torque ripple, which is mainly due to the symmetric fault condition, can be properly managed by maintaining post-fault operation with one three-phase drive in short-circuit and compensate the braking torque with the healthy three-phase drive [149]. Different winding connections have been also considered for single and phase short circuit faults [150], for a dual three-phase machine, assessing the effect of the harmonics obtained in the machines losses and torque, and evaluating its performance under different working conditions.

A similar approach has been followed for open-phase and open-line faults, where different drive topologies or machine winding connections have been considered. For instance, in [3] a six-phase drive was designed in order to independently control each phase of a three-phase machine under different types of faults and its viability was proved by emulating an open-circuit line fault. While the winding connections of a five-phase machine, considering penta- and star- type winding, was compared in [44]. In this case, fundamental and third-harmonic components are used to control the post-fault operation of the electrical drive, increasing the available torque while reducing torque ripple and losses. It was concluded that penta-winding connection results in an improved fault-tolerance behavior because a higher number of open-circuit phases can be managed (up to a total of three open-phase faults in a five-phase drive), a higher and smoother torque is produced, and even lower losses are obtained when certain types of faults appear.

2.5.4 FAULT-TOLERANT CONTROL TECHNIQUES

Multiphase drive fault-tolerance is achievable through control reconfiguration considering the type of fault, its effect on the electrical drive and certain derating limits in order to ensure that post-fault operation does not result in further drive damage. Regardless of the electrical machine type (either induction or permanent magnet), and number of phases, proper post-fault control exploits the additional degrees of freedom, by setting and controlling the *x-y* plane reference currents [106, 151], preserving the fundamental component of the air-gap magnetic field and ensuring circular flux trajectory [44, 105, 106], [150]-[152].

The number of degrees of freedom available for post-fault operation control purposes, depends not only on the type of fault, electrical machine and power converter configuration, but also on the

number of healthy phases, type of winding connection (star-type, penta-type) and isolated neutral points. For instance, a comparative study was presented in [153], where a six-phase machine with both single and double neutral points where used, demonstrating that in case of a single neutral point, the controller possessed an extra degree of control freedom, when compared to the same machine with two isolated neutrals.

Different control criteria can be achieved, depending on the selected *x-y* current references namely, minimum drive derating [151, 154], minimum copper losses [150, 151, 154, 155, 156] and minimum torque ripple or torque enhancement by third current harmonic injection [150, 157].

Proposed post-fault control techniques are mainly based on FOC strategies with an outer speed or torque control loop and an inner current controller, implementing hysteresis [13, 76, 104], synchronous frame current control with feed-forward compensation [154], and resonant [155, 156] controllers. An important remark which constitutes one of the contributions of this thesis work is that none of these contributions have proven the transition from pre- to post-fault situations and have only shown the post-fault performance of the electrical drive.

2.5.4.1 DRIVE DERATING

Regardless of the type of fault, post-fault control is generally designed to maintain rated flux and ensure certain torque/speed capability and quality [102]. The electrical drive derating level, i.e. setting the electrical drive working condition bellow its rated or designed values, depends on the specific electrical machine and power converter type/ratings, winding connection, DC-Link voltage reserve, type of fault and desired post-fault operation [45, 153]. Drive derating can be achieved following different approaches [102]:

1. Reducing the machines operating point constraints, i.e. torque and/or speed references, and consequently the demanded voltages and currents, without necessarily ensuring that the electrical drive is working at its maximum post-fault capability.
2. Limiting the drives currents to its nominal RMS values. Lowering the amount of torque/speed available for post-fault operation, but aiming to maintain the electrical drive at its maximum achievable working point.
3. Allowing phase currents to be above pre-fault values (within the drives electrical limits), but maintaining copper losses at nominal working condition values.

4. Designing the electrical drive to withstand higher current and voltage ratings than the ones sustained in normal pre-fault operation. By overrating the electrical drive, no derating has to be considered under post-fault operation, however an increase on the overall costs is foreseeable.

As can be expected, if the third approach is considered, the electrical drive derating will be lower than with the second approach. This was demonstrated in [115], on an eleven-phase induction machine under an open-phase fault, where the derating factor was 9% and 14%, respectively, with each approach, considering the same post-fault control technique and criteria.

In case of following the second approach, the current through the available healthy phases is increased up to its maximum capability, while limiting joule losses or thermal stress and maintaining peak phase currents within the drive ratings [103]. This increase in the phase currents requires in turn higher phase voltages which will ultimately demand a higher DC-Link voltage for post-fault operation [158]. A common practice, when designing electrical drives, is to select the DC-Link voltage rating depending on the electrical machines maximum phase voltage. If the electrical drive is designed considering only nominal and/or pre-fault conditions, the electrical drive must be derated [159], in order to maintain its operation within its electrical limits (reducing the achievable torque/speed), while avoiding overmodulation [160, 161] and voltage unbalance [162].

On the other hand, it is possible to maintain pre-fault operating conditions or to reduce the electrical drive derating by considering a proper DC-Link voltage reserve and overrating the electrical components for post-fault operation during the design stage. However, this results in extra costs and it is assumed, for some cases at the design stage, that a derating factor is a better option. For instance, as research presented in [158] suggests, the amount of DC-Link voltage reserved for ensuring proper post-fault operation depends on the electrical machine winding connection, being higher in star-winding than in pentagon-winding machines, accounting for approximately 12.5% and 8.5% for the star and pentagon machines, respectively. These percentages are considerably lower when compared to the overrating currents needed for post-fault operation of an electrical drive under single or double open-phase faults, which have been estimated as 38% in case of a single open-phase fault [151], and more than double for a two open-phase fault [163, 164, 165]. Nonetheless, drive overrating is not always a feasible option and is not adopted for withstanding short-circuit fault situations, where the machines currents must be limited to its maximum phase rated value due to the increased stator losses [149].

Regarding the type of machine, it has been stated in [102, 153] that permanent magnet machines are capable of maintaining less post-fault derating than induction machines due to the fact that for induction machines, the magnetization and torque production are limited by the maximum achievable *d* and *q* current components, while in permanent magnet machines, the maximum phase current does not affect the machines magnetization and torque production varies linearly with the available *q*-current component. Nonetheless, it has been demonstrated that by considering current harmonic injection techniques along with different post-fault control criteria [157], between 55% and 74.3% of nominal torque is achievable with zero torque ripple in a five-phase permanent magnet machine under an open-phase fault.

A similar case is observed when different types of winding connections are used, exploiting the fact that an odd *n*-phase machine allows (*n*+1)/2 winding connections. For instance, it was experimentally verified in [45, 164] that pentagon winding connections offered better post-fault performance, with lower drive derating, higher average torque with lower ripple and higher efficiency than traditional star winding connections. Moreover, it was demonstrated in [153] that star winding connections with single isolated neutral offer higher torque capability (between 47% and 66% of the nominal pre-fault torque, depending on the post-fault criteria) and copper loss minimization than star winding machines with two isolated neutral points. However, if the electrical drive is designed for restrictive applications such as more electric aircrafts, where higher component redundancy is desired and the implementation of an electrical drive with isolated neutrals is mandatory [166, 167], the maximum post-fault achievable torque would be about 43% of the pre-fault nominal torque, by operating the electrical drive under minimum copper loss criteria with the whole faulty converter disconnected, also termed “single VSC” operation [102, 153].

2.5.4.2 POST-FAULT MACHINE MODELING

As it can be observed in Fig. 2.20, the electrical drive configuration is changed after the fault occurrence and consequently the drive model must be revised for control and current reference calculation purposes. Most of the available literature is focused on the drive model considering open-phase faults, where the machines stator winding distribution becomes asymmetrical. As in pre-fault condition, two different approaches can be considered to model the electrical machine namely, phase variable model or VSD.

In the first case, the machines faulty phase or phases are accounted by considering the remaining healthy phases and their spatial distribution within the stator [102]. However, the VSD is preferred for control purposes in order to simplify the machines model and its control implementation. In this case the Clarke transformation (26) used in pre-fault no longer results in independent planes, and depending on the type of fault one or more control degrees of freedom are lost. In consequence, the post-fault current controller must be designed considering the interdependence of the remaining phase currents [155, 156, 153]. On the other hand, a detailed description of the asymmetrical behavior of the electrical machine and the use of reduced order transformation matrices (orthogonal and non-orthogonal), where presented in [154, 168, 169], maintaining the currents and voltages components equal to the available degrees of freedom, thus simplifying the control implementation. In the case of orthogonal matrices the model equations result in non-constant parameters and ellipsoidal α-β current components, while the use of non-orthogonal matrices result in the same pre-fault components and consequently circular α-β currents [102].

2.5.4.3 POST-FAULT CURRENT REFERENCE

Post-fault performance and drive system safe operation depend directly on the proper selection of the current references that will be provided to the controller. If current references are maintained as in pre-fault operation, high torque ripples will be observed, leading to further machine damage [168, 170]. Optimum current reference calculation depends on the specific electrical drive configuration and machine winding connection. For instance, the current references imposed for the "single VSC" operation of a faulty six-phase drive remain symmetrical as in pre-fault operation [153]. However, this is not the case for five-phase two level induction machines, where healthy phase current references are calculated, considering the machines symmetry (healthy phase currents sum is equal to zero), ensuring a rotating air-gap MMF and the cancelation of torque ripple terms, during steady state operation [102]. Most of the proposed current reference calculation methods are implemented off-line, using the machines model and the desired torque reference in order to estimate the desired waveforms. However, a method for online current reference estimation based on the desired torque was presented in [103].

Depending on the control criteria aim, two different approaches are found in the literature [102, 103].

1. Maximum torque or minimum derating method (MT). MT is based on feeding the

machine using balanced currents with equal shape and magnitude, providing a desired reference torque. The healthy phase currents are calculated for the maximum peak value allowed by the drive ratings (nominal RMS value) and with the optimum phase displacement in order to maintain constant torque with minimum ripple and equal copper losses distribution [104, 148, 151, 171, 172]. Even though copper losses are symmetrically distributed among healthy phases, temperature is not and depends on the type of fault and location [103].

2. Minimum loss or minimum copper loss (ML). Contrary to MT, ML is based on feeding unbalanced currents to achieve the desired torque reference, while minimizing overall copper losses. Under minimum copper loss operation the magnitude of phase currents is not considered and consequently unequal RMS phase currents are observed [116, 159, 173].

As can be expected, post-fault performance will depend on the drive derating and the specific implemented control criteria. If phase currents are maintained within rated values, MT will result in higher torque production capability at the expense of higher losses compared to ML, where the asymmetrical current waveforms diminish the torque production. Moreover, if for instance phase currents are not maintained within rated values with ML criteria, the machine would be subject to possible magnetic saturation effects and unequal temperature distribution [102].

Based on these two general control aims, different current waveform references have been studied, exploiting the ability to control not only the fundamental frequency but also higher order current harmonics [102], further improving post-fault capabilities.

Reference currents based on solely the fundamental component or sinusoidal reference currents [102] have been studied considering different machine models and optimization methods [115, 153, 170], for distributed winding induction machines where spatial harmonics can be neglected. In general terms, the α-β current references are calculated in order to provide a desired smooth rotating MMF, while the *x*-*y* current references are determined depending on the specific effect that the fault has on the electrical machine and on the adopted post-fault criteria (i.e. reduce copper losses or ensure maximum torque). Fault occurrence, location and nature affect the machines modeling equations and consequently different transformation matrices are used for the VSD, obtaining either circular or ellipsoidal currents [155, 168, 153, 169]. In case that higher order spatial harmonics are not negligible (i.e. affect torque production), *x*-*y* current components under either ML o MT control criteria generate

low-frequency torque ripple [102]. Nonetheless, this torque pulsation can be reduced by appropriately selecting *x-y* current references, at the expense of higher copper losses and reduced torque derating [155]. Sinusoidal current references have been also studied considering machines with pentagon and pentacle winding connections [45, 164, 165]. Even though similar performance is obtained with one open-circuit fault in star- and penta- connections, the extra degree of freedom of penta-type connections, allow post-fault operation with up to three open-phase faults.

On the other hand reference currents considering both fundamental and higher frequency components, leading to non-sinusoidal currents also termed as multi-frequency reference currents [102], have been proposed to manage post-fault performance of PM machines with trapezoidal Back-EMF or electrical drives with different number of faulty phases [44, 103, 116, 148, 157, 165]. Even though the control becomes much more difficult to implement, proposed research aims to exploit the effect of different current harmonics as an extra degree of freedom in order to improve and optimize post-fault operation. Online and off-line reference current calculation methods have been proposed in the literature [103, 116], based on scalar and vectorial methods [103] and obtaining similar performance. ML and MT criteria have been considered [103, 116, 148, 157], with either one or two open-phase faults. For instance, third order harmonics are considered in [148] to compensate torque pulsations, while reference currents have been optimized in [157, 159] to ensure maximum torque production with minimum ripple and to operate PM machines in the flux-weakening region. Pentagon and pentacle winding connections have also been analyzed in [44, 147, 165], considering phase/line and open/short circuit faults, further proving the improved fault-tolerance capabilities these types of machines possess when compared to traditional star-winding machines [102].

2.5.4.4 POST-FAULT CONTROL TECHNIQUES

Post-fault operation can be sustained either under open- or closed- loop control. While open loop-control results in simpler implementation, the machine torque and currents are subject to significant ripple and unbalance, resulting in excessive vibration and losses [156]. On the other hand closed-loop control offers the capability to improve post-fault torque and current waveforms. The improvement is however obtained at the expense of an increment in the implementation complexity. Unbalanced machine voltages are also required and, depending on the post-fault control criteria, some DC-Link voltage reserve. Notice that the type of controller (i.e. linear, non-linear, predictive), depends on the implemented post-fault criteria, being necessary to meet the following constraints [102]:

1. Current references are no longer constant in a rotating reference frame. Thus controllers with limited bandwidth such as PI's, may lead to incorrect reference current tracking.
2. Due to the machines winding asymmetries, the stator neutral voltage oscillates affecting phase to line voltage matrix (94).
3. Negative sequence voltage components in the α-β plane appear, due to the effect the neutral voltage oscillation has on the phase to line voltage matrix and consequently in the leg to phase voltage matrix (95).

Even though the general FOC structure is preserved, the unbalanced post-fault situation complicates the task of the controllers. For instance, if either MT or ML criteria is adopted, the selected controller for post-fault operation needs to be capable of sinusoidal current reference tracking in the stator reference frame [103, 155]. In order to reduce the implementation complexity, in a best case scenario, the ideal controller would maintain the same structure either on pre- or post-fault operation and only current references would be adjusted depending on the drives working condition or type of fault and the selected constraints regarding the demanded average torque and maximum ripple, copper losses and speed operation [156].

In the following subsections, the controllers found in the research literature, aiming to achieve the aforementioned constraints, will be summarized.

2.5.4.4.1 HYSTERESIS CONTROLLERS

Several research works have proposed the use of hysteresis controllers [44, 103, 104, 116, 147, 157, 165, 174], taking advantage of the high bandwidth such controllers possess and allowing to track the oscillating post-fault current references. Nonetheless the implementation of such controllers comes at the expense of variable switching frequency and its related electromagnetic compatibility constraints, restraining them from its implementation in certain applications.

One example of such controller is presented in Fig. 2.21, based on the scheme presented in [116]. The control scheme is based on an outer speed loop that generates the required torque reference, an optimum current reference generator which is based on different lookup tables considering different types of faults and working conditions and an inner current loop with hysteresis regulators aimed to follow the optimal current references. The stator phase current/voltages and rotor position are not only used for the controller implementation but also to detect the fault occurrence.

Subsequently, the fault information and the torque reference is given to the optimum current reference generator block, which selects the appropriate lookup table. It has to be noted that the optimal current references (stored in lookup tables), are not calculated online, but instead they are calculated off-line considering different torque references and the Back-EMF term at different known working points.

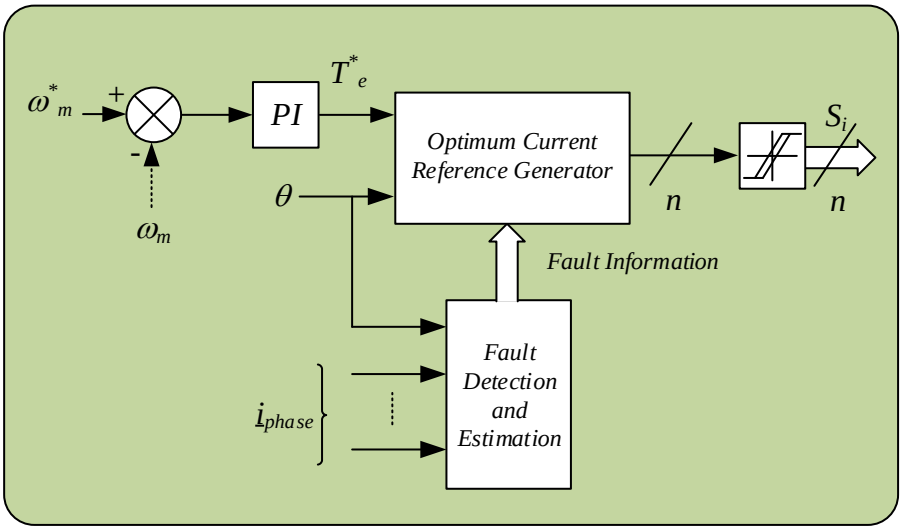

Fig. 2.21.: Post-fault control scheme based on hysteresis controllers.

2.5.4.4.2 ROBUST CONTROLLERS

Robust control techniques have also been proposed for post-fault operation, reducing the effect of an inaccurate drive model after the fault occurrence on the controller performance. In particular, fuzzy logic [169] and sliding-mode [175] techniques have been used for current reference tracking, with standard FOC schemes.

2.5.4.4.3 PROPORTIONAL-INTEGRAL CONTROLLERS

Traditional PI controllers have also been used to manage post-fault operation with the main advantage of maintaining, with minimum changes, the same FOC and PWM pre-fault schemes.

For instance, six phase drives have been analyzed in [168]. A single neutral point IM is used, and current references are estimated considering a specific post-fault decoupled model. The current control depends also on the number of open phases and their position. A double three-phase PM machine with dual three-phase inverters is considered in [176], where stator current is regulated in healthy phases while torque pulsations and copper losses are reduced, and a seven-phase axial flux PM machine is controlled in [156] considering up to two open phases, being the control structure deduced by means of the vectorial multimachine approach.

One of the main concerns when implementing PI controllers in fault-tolerant schemes is their difficulty to follow oscillating currents (*x-y* post-fault sinusoidal current references) due to their small bandwidth. To cope with this problem, a synchronous frame current control with feed-forward compensation terms and a specific fault-dependent drive model was proposed in [154], for a five-phase drive with an interior permanent magnet machine, as shown in Fig. 2.22.

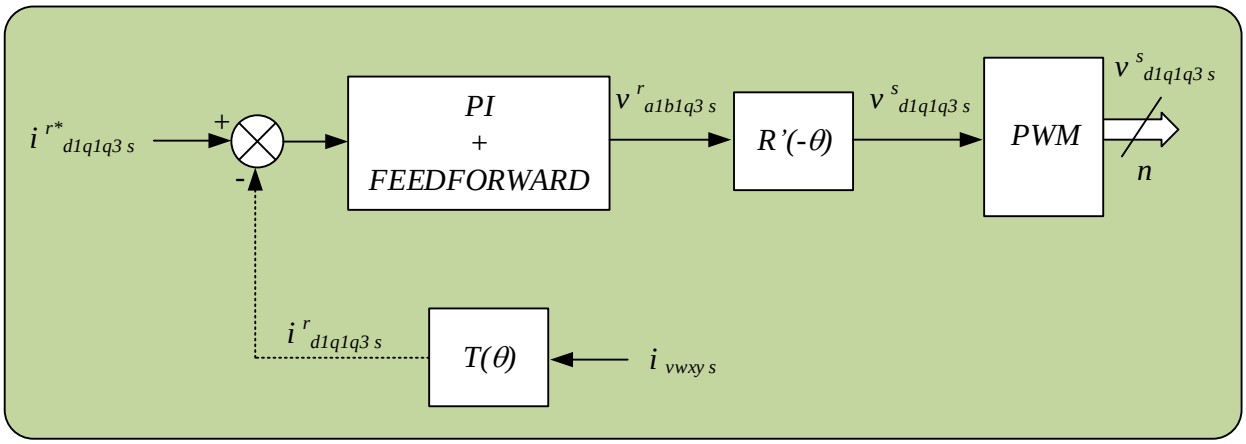

Fig. 2.22.: Post-fault control scheme based on PI controllers.

A modification of the pre-fault transformation matrix (26) is proposed (147), with terms *a* and *b* defined as in (148), aiming to consider the loss of one phase and maintain orthogonality. However, it was demonstrated that (147) provides symmetrical resistive and leakage inductance terms but asymmetrical Back-EMF terms, in the α-β plane. Consequently, the α-β components describe an ellipsoid instead of a circle, affecting the machines equations, including time-variant coefficients. To compensate this effect, a matrix $A(\theta)$ including this time variant terms is defined and used to generate a modified rotating matrix (149), eliminating the pulsating terms in the Back-EMF and providing constant coefficients.

$$[T_c] = \frac{2}{5}\begin{bmatrix} \cos(\theta-\vartheta)+a & \cos(\theta-2\vartheta)+a & \cos(\theta+2\vartheta)+a & \cos(\theta+\vartheta)+a \\ -\sin(\theta-\vartheta)-b & -\sin(\theta-2\vartheta)-b & -\sin(\theta+2\vartheta)-b & -\sin(\theta+\vartheta)-b \\ -\sin(2\vartheta) & \sin(\vartheta) & -\sin(\vartheta) & \sin(2\vartheta) \\ 1 & 1 & 1 & 1 \end{bmatrix} \quad (147)$$

$$a = 0.25\cos(\theta) \ and \ b = \ 0.25\sin(\theta) \quad (148)$$

$$[R'(-\theta)] = [R(-\theta)][A(\theta)] = \begin{bmatrix} 0.5\cos(\theta) & -0.5\sin(\theta) & 0 \\ \sin(\theta) & \cos(\theta) & 0 \\ 0 & 0 & 1 \end{bmatrix} \quad (149)$$

2.5.4.4.4 PROPORTIONAL-RESONANT CONTROLLERS

As stated previously, the limited bandwidth of traditional PI controllers highly degrades the post-fault current control performance due to the inability they possess to track sinusoidal current references. As a result, recent research suggests the use of standard Clarke transformation matrix (26) together with PI and proportional-resonant (PR) controllers. The performance of this controller scheme has been analyzed for machines with an odd number of phases [45, 155, 156], and six-phase machines [153]. It is shown that the number of changes in the control scheme after the fault occurs is kept to a minimum, maintaining the same transformation matrix, using linear controllers and PWM schemes, and providing a constant switching frequency and a simple control structure.

The control scheme proposed in [155] is depicted in Fig. 2.23. Notice that an outer torque and flux control is implemented in a rotor-flux-oriented *d*-*q* reference with traditional PI controllers. The *d*-current reference can be either set to a constant value or determined based on flux reference, while the *q*-current reference is obtained with a PI controller based on the torque error. The remaining available control planes, whose current references are sinusoidal, are controlled through proportional-resonant controllers (one for each frame). Each PR controller is composed of two PI regulators implemented in two counter-rotating reference frames, rotating in the direct and inverse direction of the field-oriented reference frame, in order to properly track both positive and negative sequence currents.

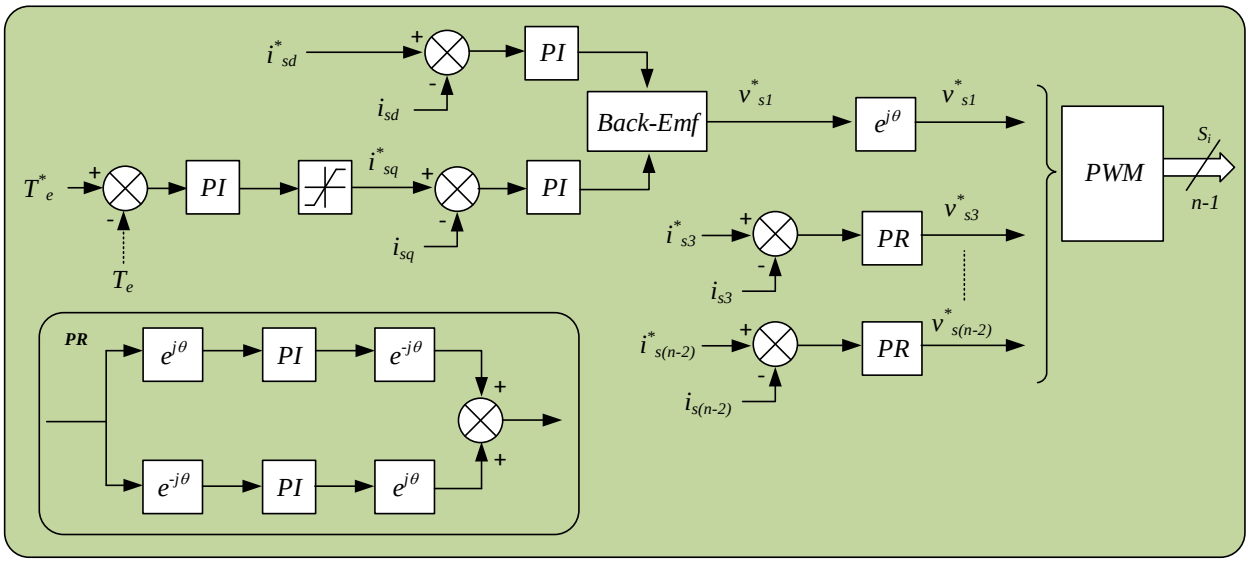

Fig. 2.23.: Post-fault control scheme based on PI and PR controllers.

2.6 SUMMARY

In this chapter the basic concepts of multiphase drives under normal and faulty operation have been presented. It has been shown that multiphase machines possess a number of benefits that makes them ideal for high power, safety-critical applications, where the number of phases results not only in better performance but also in higher reliability. Different types of multiphase machines where presented and special attention was taken on symmetrical five-phase induction machines, whose mathematical model was thoroughly analyzed in phase variables and in stationary/rotating reference frame. Traditional electrical motor drives control techniques were presented showing the evolution they have followed from the three-phase case up to their implementation in multiphase drives under pre- and post-fault conditions. Typical industry controllers such as the FOC and DTC were presented along with the modifications proposed in the literature in order to improve their performance. Moreover, the proposed post-fault controllers based on FOC strategies, implementing robust controllers or hysteresis, PI and PR regulators, were presented for different types of multiphase drives. Finally predictive control techniques were analyzed, differentiating between available schemes and special consideration was taken on finite-control set model-based predictive control, where the discrete-time state-space model of the machine was presented and applied to predictive current control, predictive torque control and restrained search techniques. As a final remark, notice that neither DTC nor Predictive Control techniques are found in the literature regarding post-fault operation. As will be presented in the next chapter, the main contribution of this PhD thesis is the development of a FCS-MPC capable of fault-tolerance operation.

2.7 REFERENCES

[1] E. Levi, "Multiphase Electric Machines for Variable–Speed Applications," *IEEE Transactions on Industrial Electronics*, vol. 55, no. 5, pp. 1893–1909, May 2008.

[2] M.J. Duran, S. Kouro, Wu Bin, E. Levi, F. Barrero, S. Alepuz, "Six-phase PMSG wind energy conversion system based on medium-voltage multilevel converter," *Proceedings of the 2011-14th European Conference on Power Electronics and Applications (EPE 2011)*, pp. 1-10, 2011.

[3] L. Lillo, L. Empringham, P.W. Wheeler, S. Khwan-On, C. Gerada, M.N. Othman, X. Huang, "Multiphase Power Converter Drive for Fault-Tolerant Machine Development in Aerospace Applications," *IEEE Transactions on Industrial Electronics*, vol. 57, no. 2, pp. 575-583, 2010.

[4] C. Chan, "The State of the Art of Electric Hybrid, and Fuel Cell Vehicles," *IEEE Proceedings*, vol. 95, no. 4, April 2007.

[5] M. Zeraoulia, M. E. H. Benbouzid, D. Diallo, "Electric Motor Drive Selection Issues for HEV Propulsion Systems: A Comparative Study," *IEEE Transactions on Vehicular Technology*, vol. 55, no. 6, pp. 1756-1764, 2006.

[6] E. Jung, H. Yoo, S. Sul, H. Choi, Y. Choi, "A Nine-Phase Permanent-Magnet Motor Drive System for an Ultrahigh-Speed Elevator," *IEEE Trans. on Industry Applications*, vol. 48, no. 3, pp. 987-995, 2012.

[7] T.J. McCoy, "Trends in Ship Electric Propulsion," *IEEE Power Engineering Society Summer Meeting*, pp. 343-346, 2002.

[8] A. Tessarolo, "Modeling and Analysis of Multiphase Electric Machines for High-Power Applications" PhD Thesis, University of Padova, 2011.

[9] E. Levi, R. Bojoi, F. Profumo, H. Toliyat, S. Williamson, "Multiphase Induction Motor Drives–A Technology Status Review," *IET Electric Power Applications*, vol. 1, no. 4, pp. 489–516, 2007.

[10] R. Bojoi, "Analysis, Design and Implementation of a Dual Three-Phase Vector Controlled Induction Motor Drive" PhD Thesis, Politecnico Di Torino, 2002.

[11] S. Williamson, A.C. Smith, "Pulsating Torque and Losses in Multiphase Induction Machines," *IEEE Transactions on Industry Applications*, vol. 39, no. 4, pp. 986-993, 2003.

[12] L. Parsa, H.A. Toliyat, "Five-Phase Permanent-Magnet Motor Drives," *IEEE Transactions on Industry Applications*, vol. 41, no. 1, pp. 30-37, 2005.

[13] H. Xu, H.A. Toliyat, L.J.Petersen, "Five-Phase Induction Motor Drives with DSP-Based Control System," *IEEE Transactions on Power Electronics*, vol. 17, no. 4, pp. 524-533, 2002.

[14] A. Iqbal, S.N. Vukosavic, E. Levi, M. Jones, H.A. Toliyat, "Dynamics of a Series-Connected Two-Motor Five-Phase Drive System with a Single-Inverter Supply," *Proc. of IEEE Ind. Appl. Soc. Annual Meeting (IAS)*, pp. 1081-1088, 2005.

[15] A. Iqbal, E. Levi, M. Jones, S.N. Vukosavic, "A PWM Scheme for a Five-Phase VSI Supplying a Five-Phase Two-Motor Drive," in Proc. of Annual Conference of the IEEE Industrial Electronics Society (IECON), pp. 2575-2580, 2006.

[16] D. Dujic, "Development of Pulse-Width-Modulation Techniques for Multi-Phase and Multi-Leg Voltage Source Inverters" PhD Thesis, Liverpool John Moores University, 2008.

[17] H. Toliyat, T. Lipo, J. White, "Analysis of a Concentrated Winding Induction Machine for Adjustables Speed Drive Applications Part 1 (Motor Analysis)," *IEEE Transactions on Energy Conversion*, vol. 6, no. 4, pp. 679–683, 1991.

[18] H. Toliyat, T. Lipo, J. White, "Analysis of a Concentrated Winding Induction Machine for Adjustables Speed Drive Applications Part 2 (Motor Design and Performance)," *IEEE Transactions on Energy Conversion*, vol. 6, no. 4, pp. 684–692, 1991.

[19] L. Pereira, C. Scharlau, L. Pereira, J. Haffner, "General Model of a Five–Phase Induction Machine Allowing for Harmonics in the Air Gap Field," *IEEE Transactions on Energy Conversion*, vol. 21, no. 4, pp. 891–899, 2006.

[20] R. Nelson, P. Krause, "Induction Machine Analysis for Arbitrary Displacement Between Multiple Winding Sets," *IEEE Transactions on Power Apparatus and Systems*, vol. PAS–93, no. 3, pp. 841–848, 1974.

[21] D. Hadiouche, H. Razik, A. Rezzoug, "On the Modeling and Design of Dual–Stator Windings to Minimize Circulating Harmonic Currents for VSI Fed AC Machines," *IEEE Transactions on Industry Applications*, vol. 40, no. 2, pp. 506–515, 2004.

[22] T. Lipo, "A *d–q* Model for Six Phase Induction Machines," *International Conference on Electric Machines*, pp. 860-867, 1980.

[23] R. Bojoi, M. Lazzari, F. Profumo, A. Tenconi, "Digital Field-Oriented Control for Dual Three-Phase Induction Motor Drives," *IEEE Transactions on Industry Applications*, vol. 39, no. 3, pp. 752-760, 2003

[24] R. Bojoi, F. Profumo, A. Tenconi, "Digital Synchronous Frame Current Regulation for Dual Three-Phase Induction Motor Drives," *IEEE 34th Annual Power Electronics Specialists Conference. PESC03*, vol. 3, no., pp.1475-1480 2003.

[25] R. Bojoi, E. Levi, F. Farina, A. Tenconi; F. Profumo, "Dual Three-Phase Induction Motor Drive with Digital Current Control in the Stationary Reference Frame," *IEE Proceedings on Electric Power Applications*, vol. 153, no. 1, pp. 129-139, 2006

[26] R. Bojoi, A. Tenconi, G. Griva, F. Profumo, "Vector Control of Dual-Three-Phase Induction-Motor Drives Using Two Current Sensors," *IEEE Transactions on Industry Applications*, vol. 42, no. 5, pp. 1284-1292, 2006

[27] R. Bojoi, F. Farina, G. Griva, F. Profumo, A. Tenconi, "Direct Torque Control for Dual Three–Phase Induction Motor Drives," *IEEE Transactions on Industry Applications*, vol. 41, no. 6, pp. 1627-1636, 2005.

[28] K. Hatua, V. Ranganathan, "Direct Torque Control Schemes for Split–Phase Induction Machine," *IEEE Transactions on Industry Applications*, vol. 41, no. 5, pp. 1243-1254, 2005.

[29] F. Barrero, M.R. Arahal, R. Gregor, S. Toral, M.J. Duran, "A Proof of Concept Study of Predictive Current Control for VSI Driven Asymmetrical Dual Three-phase AC Machines," *IEEE Transactions on Industrial Electronics*, vol. 56, no. 6, pp. 1937-1954, 2009.

[30] F. Barrero, J. Prieto, E. Levi, R. Gregor, S. Toral, M. Duran, M. Jones, "An Enhanced Predictive Current Control Method for Asymmetrical Six-phase Motor Drives," *IEEE Transactions on Industrial Electronics*, vol. 58, no. 8, pp. 3242-3252, 2011.

[31] Y. Zhao, T.A. Lipo, "Space Vector PWM Control of Dual Three-Phase Induction Machine Using Vector Space Decomposition," *IEEE Transactions on Industry Applications*, vol. 31, no. 5, pp. 1100-1109, 1995.

[32] F. Barrero, M.R. Arahal, R. Gregor, S. Toral, M.J. Durán, "One-step Modulation Predictive Current Control Method for the Asymmetrical Dual Three-Phase Induction Machine," *IEEE Transactions on Industrial Electronics*, vol. 56, no. 6, pp. 1974-1983, 2009.

[33] R. Gregor, F. Barrero, S. Toral, M.J. Duran, M.R. Arahal, J. Prieto, J.L. Mora, "Predictive-SVPWM Current Control Method for Asymmetrical Dual Three-Phase Induction Motor Drives," *IET Electric Power Applications*, vol. 4, no. 1, pp. 26-34, 2010.

[34] J. Prieto, M. Jones, F. Barrero, E. Levi, S. Toral, "Comparative Analysis of Discontinuous and Continuous PWM Techniques in VSI-Fed Five-Phase Induction Motor," *IEEE Transactions on Industrial Electronics*, vol. 58, no. 12, pp. 5324-5335, 2011.

[35] D. Dujic, M. Jones, E. Levi, J. Prieto, F. Barrero, "Switching Ripple Characteristics of Space Vector PWM Schemes for Five-Phase Two-Level Voltage Source Inverters—Part 1: Flux Harmonic Distortion Factors," *IEEE Transactions on Industrial Electronics*, vol. 58, no. 7, pp. 2789-2798, 2011.

[36] M. Jones, D. Dujic, E. Levi, J. Prieto, F. Barrero, "Switching Ripple Characteristics of Space Vector PWM Schemes for Five-Phase Two-Level Voltage Source Inverters—Part 2: Current Ripple," *IEEE Transactions on Industrial Electronics*, vol. 58, no. 7, pp. 2799-2808, 2011.

[37] M. Jones, S. Vukosavic, D. Dujic, E. Levi, "A Synchronous Current Control Scheme for Multiphase Induction Motor Drives," *IEEE Transactions on Energy Conversion*, vol. 24, no. 4, pp. 860-868, 2009.

[38] L. Zheng, J. Fletcher, B. Williams, X. He, "Dual–Plane Vector Control of a Five–Phase Induction Machine for an Improved Flux Pattern," *IEEE Transactions on Industrial Electronics*, vol. 55, no. 5, pp. 1996-2005, 2008.

[39] G. Liliang, J. Fletcher, L. Zheng, "Low–Speed Control Improvements for a Two–Level Five–Phase Inverter–Fed Induction Machine Using Classic Direct Torque Control," *IEEE Transactions on Industrial Electronics*, vol. 58, no. 7, pp. 2744-2754, 2011.

[40] L. Zheng, J. Fletcher, B. Williams, X. He, "A Novel Direct Torque Control Scheme for a Sensorless Five–Phase Induction Motor Drive," *IEEE Transactions on Industrial Electronics*, vol. 58, no. 2, pp. 503-513, 2011.

[41] C. Lim, E. Levi, M. Jones, N. Abd Rahim, W. Hew, "FCS-MPC-Based Current Control of a Five-Phase Induction Motor and its Comparison with PI-PWM Control," *IEEE Transactions on Industrial Electronics*, vol. 61, no. 1, pp.149-163, 2014.

[42] J. Riveros, F. Barrero, E. Levi, M.J. Durán, M. Jones, S. Toral, "Variable-Speed Five-Phase Induction Motor Drive Based on Predictive Torque Control," *IEEE Transactions on Industrial Electronics*, vol. 60, no. 8, pp. 2957-2968, 2013.

[43] S. Sadeghi, G. Lusu, H.A. Toliyat, L. Parsa, "Wide Operational Speed Range of Five-Phase Permanent Magnet Machines by Using Different Stator Winding Configurations," *IEEE Transactions on Industrial Electronics*, vol. 59, no. 6, pp. 2621-2631, 2012.

[44] A. Mohammadpour, L. Parsa, "A Unified Fault-Tolerant Current Control Approach for Five-Phase PM Motors with Trapezoidal Back EMF under Different Stator Winding Connections," *IEEE Transactions on Power Electronics*, vol. 28, no. 7, pp. 3517-3527, 2013.

[45] A.S. Abdel-Khalik, A.S. Morsy, S. Ahmed, A.M. Massoud, "Effect of Stator Winding Connection on Performance of Five-Phase Induction Machines," *IEEE Transactions on Industrial Electronics*, vol. 61, no. 1, pp. 3-19, 2014.

[46] E. Levi, M. Jones, S. Vukosavic, H. Toliyat, "A Novel Concept of Multiphase, Multimotor Vector Controlled Drive System Supplied from a Single Voltage Source Inverter," *IEEE Transactions on Power Electronics*, vol. 19, no. 2, pp. 320-335, 2004.

[47] E. Levi, M. Jones, S.N. Vukosavic, H.A. Toliyat, "Operating Principles of a Novel Multiphase Multimotor Vector-Controlled Drive," *IEEE Transactions on Energy Conversion*, vol. 19, no. 3, pp. 508-517, 2004

[48] E. Levi, M. Jones, S.N. Vukosavic, A. Iqbal, H.A. Toliyat, "Modeling, Control, and Experimental Investigation of a Five-Phase Series-Connected Two-Motor Drive With Single Inverter Supply," *IEEE Transactions on Industrial Electronics*, vol. 54, no. 3, pp. 1504-1516, 2007

[49] E. Levi, S. Vukosavic, M. Jones, "Vector Control Schemes for Series–Connected Six–Phase Two–Motor Drive Systems," *IEE Proceedings Electric Power Applications*, vol. 152, no. 2, pp. 226-238, 2005.

[50] K. Mohapatra, R. Kanchan, M. Baiju, P. Tekwani, K. Gopakumar, "Independent Field–Oriented Control of two Split–Phase Induction Motors from a Single Six–Phase Inverter," *IEEE Transactions on Industrial Electronics*, vol. 52, no. 5, pp. 1372-1382, 2005.

[51] E. Levi, M. Jones, A. Iqbal, S.N. Vukosavic, H.A. Toliyat, "Induction Machine/Syn-Rel Two-Motor Five-Phase Series-Connected Drive," *IEEE Transactions on Energy Conversion*, vol. 22, no. 2, pp. 281-289, 2007

[52] E. Levi, M. Jones, S. Vukosavic, H. Toliyat, "Steady–state modeling of series–connected five–phase and six–phase two–motor drives," *IEEE Transactions on Industry Applications*, vol. 44, no. 5, pp. 1559-1568, 2008.

[53] D. C. White, H. H.Woodson, "Electromechanical Energy Conversion," Wiley, 1959.

[54] P. C. Krause, O. Wasynczuk, S. D. Sudhoff, "Analysis of Electric Machinery and Drive Systems," Wiley-Interscience, 2002.

[55] A. M. Trzynadlowski, "Control of Induction Motors," Elsevier, 2000.

[56] M.J. Duran, J.A. Riveros, F. Barrero, H. Guzman, J. Prieto, "Reduction of Common-Mode Voltage in Five-Phase Induction Motor Drives Using Predictive Control Techniques," *IEEE Transactions on Industry Applications*, vol. 48, no. 6, pp. 2059-2067, 2012.

[57] N. Mohan, T. Underland, W. Robbins, "Power Electronics," Wiley, 2003.
[58] H. Chih-Yi, W. Chao-Peng, Y. Jung-Tai, H. Yeu-Jent, "Torque and Current Control of Induction Motor Drives for Inverter Switching Frequency Reduction," *IEEE Transactions on Industrial Electronics*, vol. 52, no. 5, pp. 1364-1371, 2005.
[59] B.K. Bose, "An Adaptive Hysteresis-Band Current Control Technique of a Voltage-Fed PWM Inverter for Machine Drive System," *IEEE Transactions on Industrial Electronics*, vol. 37, no. 5, pp. 402-408, 1990
[60] G. Singh, K. Nam, S. Lim, "A Simple Indirect Field–Oriented Control Scheme for Multiphase Induction Machine," *IEEE Transactions on Industrial Electronics*, vol. 52, no. 4, pp. 1177-1184, 2005.
[61] K. Takahashi, K. Ohishi, T. Kanmachi, "A New Quick–Response and High–Efficiency Control Strategy of an Induction Motor," *IEEE Transactions on Industry Applications*, vol. IA–22, no. 5, pp. 820–827, 1986.
[62] H. Toliyat, H. Xu, "A Novel Direct Torque Control (DTC) Method for Five–Phase Induction Machines," *Fifteenth Anual IEEE Applied Power Electronics Conference and Exposition, APEC*, vol. 1, pp. 162-168, 2000.
[63] N. Oikonomou, "Control of Medium-Voltage Drives at Very Low Switching Frequency," PhD Thesis, Elektrotechnik, Informationstechnik und Medientechnik der Bergischen Universität Wuppertal, 2008.
[64] J. Holtz, Q. Juntao, J. Pontt, J. Rodriguez, P. Newman, H. Miranda, "Design of Fast and Robust Current Regulators for High-Power Drives Based on Complex State Variables," *IEEE Transactions on Industry Applications*, vol. 40, no. 5, pp. 1388-1397, 2004.
[65] R. Hyung-Min, K. Jang-Hwan, S. Seung-Ki, "Analysis of Multiphase Space Vector Pulse-Width Modulation Based on Multiple d-q Spaces Concept," *IEEE Transactions on Power Electronics*, vol. 20, no. 6, pp. 1364-1371, 2005.
[66] J.W. Kelly, E.G. Strangas, J.M. Miller, "Multiphase Space Vector Pulse Width Modulation," *IEEE Transactions on Energy Conversion*, vol. 18, no. 2, pp. 259-264, 2003.
[67] A. Iqbal, E. Levi, "Space Vector PWM Techniques for Sinusoidal Output Voltage Generation With a Five–Phase Voltage Source Inverter," *Electric Power Components and Systems*, vol. 34, no. 2, pp. 119-140, 2006.
[68] O. Lopez, D. Dujic, M. Jones, F.D. Freijedo, J. Doval-Gandoy, E. Levi, "Multidimensional Two-Level Multiphase Space Vector PWM Algorithm and its Comparison with Multifrequency Space Vector PWM Method," *IEEE Transactions on Industrial Electronics*, vol. 58, no. 2, pp. 465-475, 2011
[69] A. Iqbal, E. Levi, M. Jones, S. Vukosavic, "Generalised Sinusoidal PWM with Harmonic Injection for Multi–Phase VSIs," *IEEE Power Electronics Specialists Conference, PESC37th*, pp. 1-7, 2006.
[70] D. Dujic, G. Grandi, M. Jones, E. Levi, "A Space Vector PWM Scheme for Multifrequency output Voltage Generation with Multiphase Voltage-Source Inverters," *IEEE Transactions on Industrial Electronics*, vol. 55, no. 5, pp. 1943-1955, 2008.
[71] G.S. Buja, M.P. Kazmierkowski, "Direct Torque Control of PWM Inverter-Fed AC Motors - A Survey," *IEEE Transactions on Industrial Electronics*, vol. 51, no. 4, pp. 744-757, 2004.
[72] R. Kianinezhad, R. Alcharea, B. Nahid, F. Betin, G. Capolino, "A Novel Direct Torque Control (DTC) for Six-Phase Induction Motors with Common Neutrals," *International Symposium on Power Electronics, Electrical Drives, Automation and Motion, 2008. SPEEDAM 2008*, pp. 107-112, 2008.
[73] R. Kianinezhad, B. Nahid, F. Betin, G.A. Capolino, "A Novel Direct Torque Control (DTC) Method For Dual Three Phase Induction Motors," *IEEE International Conference on Industrial Technology, 2006. ICIT 2006*, pp. 939-943, 2006.
[74] L. Zheng; J.E Fletcher, B.W. Williams, He Xiangning, "A Novel Direct Torque Control Scheme for a Sensorless Five-Phase Induction Motor Drive," *IEEE Transactions on Industrial Electronics*, vol. 58, no. 2, pp. 503-513, 2011.
[75] D. Casadei, F. Profumo, G. Serra, A. Tani, "FOC and DTC: Two Viable Schemes for Induction Motors Torque Control," *IEEE Transactions on Power Electronics*, vol. 17, no. 5, pp. 779-787, 2002.
[76] L. Parsa, "Performance Improvement of Permanent Magnet AC Motors," PhD Thesis, Texas A&M University, 2005.

[77] Y. Gao, L. Parsa, "Modified Direct Torque Control of Five-Phase Permanent Magnet Synchronous Motor Drives," *Twenty Second Annual IEEE Applied Power Electronics Conference, APEC 2007*, pp. 1428-1433, 2007.

[78] S. Lu, K. Corzine, "Direct Torque Control of Five-Phase Induction Motor using Space Vector Modulation with Harmonics Elimination and Optimal Switching Sequence," *Twenty-First Annual IEEE Applied Power Electronics Conference and Exposition, 2006. APEC '06*, 2006.

[79] Y. Fei, Z. Xiaofeng, Q. Minzhong, D. Chengdong, "The direct torque control of multiphase permanent magnet synchronous motor based on low harmonic space vector PWM," *IEEE International Conference on Industrial Technology, 2008. ICIT 2008*, pp. 1-5, 2008.

[80] L. Parsa, H.A. Toliyat, "Sensorless Direct Torque Control of Five-Phase Interior Permanent-Magnet Motor Drives," *IEEE Transactions on Industry Applications*, vol. 43, no. 4, pp. 952-959, 2007.

[81] J. Riveros, M. Duran, F. Barrero, S. Toral, "Direct Torque Control for Five–Phase Induction Motor Drives with Reduced Common–Mode Voltage," *38th Conference of the IEEE Industrial Electronics Society, IECON*, pp. 3616-3621, 2012.

[82] P. Cortes, M.P. Kazmierkowski, R.M. Kennel, D.E. Quevedo, J. Rodriguez, "Predictive Control in Power Electronics and Drives," *IEEE Transactions on Industrial Electronics*, vol. 55, no. 12, pp. 4312-4324, 2008.

[83] S. Kouro, P. Cortes, R. Vargas, U. Ammann, J. Rodriguez, "Model Predictive Control—A Simple and Powerful Method to Control Power Converters," *IEEE Transactions on Industrial Electronics*, vol. 56, no. 6, pp. 1826-1838, 2009.

[84] J. Rodriguez, R.M. Kennel, J.R. Espinoza, M. Trincado, C.A. C.A. Silva, Rojas, "High-Performance Control Strategies for Electrical Drives: An Experimental Assessment," *IEEE Transactions on Industrial Electronics*, vol. 59, no. 2, pp. 812-820, 2012.

[85] L-H. Hoang, K. Slimani, P. Viarouge, "Analysis and Implementation of a Real-Time Predictive Current Controller for Permanent-Magnet Synchronous Servo Drives," *IEEE Transactions on Industrial Electronics*, vol. 41, no. 1, pp. 110-117, 1994.

[86] M. Hyung-Tae, K. Hyun-Soo, Y. Myung-Joong, "A Discrete-Time Predictive Current Control for PMSM," *IEEE Transactions on Power Electronics*, vol. 18, no. 1, pp. 464-472, 2003.

[87] L. Springob, J. Holtz, "High-Bandwidth Current Control for Torque-Ripple Compensation in PM Synchronous Machines," *IEEE Transactions on Industrial Electronics*, vol. 45, no. 5, pp. 713-721, 1998.

[88] R. S. Arashloo; J. L. Martinez Romeral, M. Salehifar, J. M. Moreno, "Model Predictive Current Control of Five Phase Permanent Magnet Motor," *European Conference on Power Electronics and Applications (EPE), 2013 15th*, pp. 1-6, 2013.

[89] M. Depenbrock, "Direct Self-Control (DSC) of Inverter-Fed Induction Machine," *IEEE Transactions on Power Electronics*, vol. 3, no. 4, pp. 420-429, 1988.

[90] A. Linder, R. Kennel, "Model Predictive Control for Electrical Drives," *IEEE 36th Power Electronics Specialists Conference, 2005. PESC '05*, pp. 1793-1799, 2005.

[91] R. Kennel, A. Linder, M. Linke, "Generalized Predictive Control (GPC)-Ready for use in Drive Applications?," *IEEE 32nd Annual Power Electronics Specialists Conference, 2001. PESC. 2001*, pp. 1839-1844, 2001.

[92] J. Rodriguez, M.P. Kazmierkowski, J.R. Espinoza, P. Zanchetta, H. Abu-Rub, H.A. Young, C.A. Rojas, "State of the Art of Finite Control Set Model Predictive Control in Power Electronics," *IEEE Transactions on Industrial Informatics*, vol. 9, no. 2, pp. 1003-1016, 2013.

[93] M.R. Arahal, F. Barrero, S. Toral, M.J. Durán, R. Gregor, "Multi-Phase Current Control Using Finite–state Model-Predictive Control," *Control Engineering Practice*, vol. 17, no. 5, pp. 579-587, 2009.

[94] J. Martinez, R. Kennel, T. Geyer, "Model Predictive Direct Current Control," *Proceedings IEEE ICIT*, pp. 1808-1813, 2010.

[95] T. Geyer, G. Papafotiou, M. Morari, "Model Predictive Direct Torque Control—Part I: Concept, Algorithm, and Analysis," *IEEE Transactions on Industrial Electronics*, vol. 56, no. 6, pp. 1894-1905, 2009.

[96] T. Geyer, "A Comparison of Control and Modulation Schemes for Medium Voltage Drives: Emerging Predictive Control Concepts Versus Field Oriented Control," *IEEE Energy Conversion Congress and Exposition (ECCE), 2010*, pp. 2836–2843, 2010.

[97] J. Holtz, "The Representation of AC Machine Dynamics by Complex Signal Flow Graphs," *IEEE Transactions on Industrial Electronics*, vol. 42, no. 3, pp. 263-271, 1995.

[98] H. Miranda, P. Cortes, J. Yuz, J. Rodriguez, "Predictive Torque Control of Induction Machines Based on State-Space Models," *IEEE Transactions on Industrial Electronics*, vol. 56, no. 6, pp. 1916-1924, 2009.

[99] J.A. Riveros, J. Prieto, F. Barrero, S. Toral, M. Jones, E. Levi, "Predictive Torque Control for Five-Phase Induction Motor Drives," *36th Annual Conference on IEEE Industrial Electronics Society IECON 2010*, pp. 2467-472, 2010.

[100] M. J. Duran, J. Prieto, F. Barrero, S. Toral, "Predictive Current Control of Dual Three-Phase Drives using Restrained Search Techniques," *IEEE Transactions on Industrial Electronics*, vol. 58, no. 8, pp. 3253-3263, 2011.

[101] A. Consoli, "Special Section on Robust Operation of Electrical Drives," *IEEE Transactions on Power Electronics*, vol. 27, no. 2, pp. 472-478, 2012.

[102] F. Barrero, M. J. Duran, "Recent Advances in the Design, Modeling and Control of Multiphase Machines," *IEEE Transactions on Industrial Electronics*, vol. -, no. -, pp. -, 2015.

[103] X. Kestelyn, E. Semail, "A Vectorial Approach for Generation of Optimal Current References for Multiphase Permanent-Magnet Synchronous Machines in Real Time," *IEEE Transactions on Industrial Electronics*, vol. 58, no. 11, pp. 5057-5065, 2011.

[104] L. Parsa, H. A. Toliyat, "Fault-Tolerant Interior-Permanent-Magnet Machines for Hybrid Electric Vehicle Applications," *IEEE Transactions on Vehicular Technology*, vol. 56, no. 4, pp. 1546-1552, 2007.

[105] X. Huang, A. Goodman, C. Gerada, Y. Fang, Q. Lu, "Design of a Five-Phase Brushless DC Motor for a Safety Critical Aerospace Application," *IEEE Transactions on Industrial Electronics*, vol. 59, no. 9, pp. 3532-3541, 2012.

[106] H.S. Che, E. Levi, M. Jones, M.J. Duran, W.P. Hew, N.A. Rahim "Operation of a Six-Phase Induction Machine Using Series-Connected Machine-Side Converters," *IEEE Transactions on Industrial Electronics*, vol. 61, no. 1, pp. 164-176, 2014.

[107] A. Stefani, "Induction Motor Diagnosis in Variable Speed Drives," PhD Thesis, Department of Electrical Engineering, University of Bologna, 2010.

[108] Pinjia Zhang, Yi Du, T.G. Habetler, Bin Lu, "A Survey of Condition Monitoring and Protection Methods for Medium-Voltage Induction Motors," *IEEE Transactions on Industry Applications*, vol. 47, no. 1, pp. 34-46, 2011.

[109] A. H. Bonnett, C. Yung, "Increased Efficiency Versus Increased Reliability," *IEEE Industry Applications Magazine*, vol. 14, no. 1, pp. 29-36, 2008.

[110] S. Nandi, H. A. Toliyat, and X. Li, "Condition Monitoring and Fault Diagnosis of Electrical Motors - A Review," *IEEE Transactions on Energy Conversion*, vol. 20, pp. 719-729, 2005.

[111] A. M. da Silva, "Induction Motor Fault Diagnostic and Monitoring Methods" MSc Thesis, Marquette University, 2006.

[112] P. Vas, "Parameter Estimation, Condition Monitoring, and Diagnosis of Electrical Machines," Oxford, U.K.: Clarendon, 1993.

[113] L. Zarri, M. Mengoni, Y. Gritli, A. Tani, F. Filippetti, G. Serra, D. Casadei, "Detection and Localization of Stator Resistance Dissymmetry Based on Multiple Reference Frame Controllers in Multiphase Induction Motor Drives," *IEEE Transactions on Industrial Electronics*, vol. 60, no. 8, pp. 3506-3518, 2013.

[114] M. Barcaro, N. Bianchi, F. Magnussen, "Faulty Operations of a PM Fractional-Slot Machine with a Dual Three-Phase Winding," *IEEE Transactions on Industrial Electronics*, vol. 58, no. 9, pp. 3825-3832, 2011.

[115] A.S. Abdel-Khalik, M.I. Masoud, S. Ahmed, A. Massoud, "Calculation of Derating Factors Based On Steady-State Unbalanced Multiphase Induction Machine Model Under Open Phase(s) And Optimal Winding Currents," *Elsevier Electric Power System Research*, vol. 106, pp. 214-225, 2014.

[116] S. Dwari, L. Parsa, "An Optimal Control Technique for Multiphase PM Machines Under Open-Circuit Faults," *IEEE Transactions on Industrial Electronics*, vol. 55, no. 5, pp. 1988-1995, 2008.
[117] D. Foito, J. Maia, V.F. Pires, J.F. Martins, "Fault Diagnosis In Six-Phase Induction Motor Using A Current Trajectory Mass Center," *Elsevier Measurement*, vol. 51, no. 1, pp. 164-173, 2014.
[118] M. Salehifar, R.S. Arashloo, J.M. Moreno-Equilaz, V. Sala, L. Romeral, "Fault Detection and Fault Tolerant Operation of a Five Phase PM Motor Drive Using Adaptive Model Identification Approach," *IEEE Journal of Emerging and Selected Topics in Power Electronics*, vol. 2, no.2, pp. 212-223, 2014.
[119] H. Henao, C. Demian, and G. A. Capolino, "A frequency-domain detection of stator winding faults in induction machines using an external flux sensor," *IEEE Transactions on Industry Applications*, vol. 39, no. 5, pp. 1272–1279, 2003.
[120] H. A. Toliyat, T. A. Lipo, "Transient analysis of cage induction machines under stator, rotor bar and end ring faults," *IEEE Transactions on Energy Conversion*, vol. 10, no. 2, pp. 241–247, 1995.
[121] M. E. H. Benbouzid, "A Review of Induction Motors Signature Analysis as a Medium for Faults Detection," *IEEE Transactions on Industrial Electronics*, vol. 47, no. 5, pp. 984-993, 2000.
[122] B. Akin, Choi Seungdeog, U. Orguner, H.A. Toliyat, "A Simple Real-Time Fault Signature Monitoring Tool for Motor-Drive-Embedded Fault Diagnosis Systems," *IEEE Transactions on Electronics*, vol. 58, no. 5, pp. 1990-2001, 2011.
[123] G.F.H. Beng, X. Zhang, D.M. Vilathgamuwa, "Sensor Fault-Resilient Control of Interior Permanent-Magnet Synchronous Motor Drives," *IEEE/ASME Transactions on Mechatronics*, vol. 20, no. 2, pp. 855-864, 2015.
[124] S.M. Bennett, R.J. Patton, S. Daley, "Rapid Prototyping of a Sensor Fault Tolerant Traction Control System," *IEE Colloquium on Fault Diagnosis in Process Systems* (Digest No: 1997/174), 1997.
[125] Hainan Wang, S. Pekarek, B. Fahimi, "Multilayer Control of an Induction Motor Drive:A Strategic Step for Automotive Applications," *IEEE Transactions on Power Electronics*, vol. 21, no. 3, pp. 676-686, 2006.
[126] D. Chakraborty, V. Verma, "Speed and Current Sensor Fault Detection and Isolation Technique for Induction Motor Drive Using Axes Transformation," *IEEE Transactions on Industrial Electronics*, vol. 62, no. 3, pp. 1943-1954, 2015.
[127] C. Hung-Chi, H. Chih-Hao, C. Da-Kai, "Position Sensorless Control for Five-Phase Permanent-Magnet Synchronous Motors," *IEEE/ASME International Conference on Advanced Intelligent Mechatronics* (AIM2014), 2014.
[128] A.S. Morsy, A.S. Abdel-khalik, S. Ahmed, A.M. Massoud, "Sensorless Speed Control of a Five-Phase Induction Machine Under Open-Phase Condition", *The Journal of Engineering, IET Open Access*, 2014.
[129] T. A. Najafabadi, F. R. Salmasi, P. J. Maralani, "Detection and Isolation of Speed-, DC-Link Voltage-, and Current-Sensor Faults Based on an Adaptive Observer in Induction-Motor Drives," *IEEE Transactions on Industrial Electronics*, vol. 58, no. 5, pp. 1662-1672, 2011.
[130] F. Zidani, M. E. H. Benbouzid, D. Diallo, A. Benchaib, "Active Fault-Tolerant Control of Induction Motor Drives in EV and HEV Against Sensor Failures Using a Fuzzy Decision System," *IEEE International Conference on Electric Machines and Drives*, IEMDC'03., vol. 2, pp. 677-683 vol. 2, 2003.
[131] D. Diallo, M. E. H. Benbouzid, A. Makouf, "A Fault-Tolerant Control Architecture for Induction Motor Drives in Automotive Applications," *IEEE Transactions on Vehicular Technology*, vol. 53, no. 6, pp. 1847-1855, 2004.
[132] M. E. H. Benbouzid, D. Diallo, M. Zeraoulia, "Advanced Fault-Tolerant Control of Induction-Motor Drives for EV/HEV Traction Application: from Conventional to Modern and Intelligent Control Techniques," *IEEE Transactions on Vehicular Technology*, vol. 56, no. 2, pp. 519-528, 2007.
[133] B. Tabbache, N. Rizoug, M. E. H. Benbouzid, A. Kheloui, "A Control Reconfiguration Strategy for Post-Sensor FTC in Induction Motor Based EVs," *IEEE Transactions on Vehicular Technology*, vol. 62, no. 3, pp. 965-971, 2013.
[134] A. Raisemche, M. Boukhnifer, C. Larouci, D. Diallo, "Two Active Fault Tolerant Control Schemes of Induction Motor Drive in EV or HEV," *IEEE Transactions on Vehicular Technology*, vol. 63, no. 1, pp. 19-29, 2014.

[135] X. Shi, M. Krishnamurthy, "Survivable Operation of Induction Machine Drives With Smooth Transition Strategy for EV Applications," *IEEE Journal of Emerging and Selected Topics in Power Electronics*, vol. 2, no. 3, pp. 609-617, 2014.
[136] Y.-S. Jeong, S.-K. Sul, S. E. Schulz, N. R. Patel, "Fault Detection and Fault-Tolerant Control of Interior Permanent-Magnet Motor Drive System for Electric Vehicle," *IEEE Transactions on Industrial Applications*, vol. 41, no. 1, pp. 46-51, 2005.
[137] K.-S. Lee, J.-S. Ryu, "Instrument Fault Detection and Compensation Scheme for Direct Torque Controlled Induction Motor Drives," *IEE Proceedings Control Theory and Applications*, vol. 150, no. 4, pp. 376-382, 2003.
[138] M. E. Romero, M. M. Seron, J. A. D. Dona, "Sensor Fault-Tolerant Vector Control of Induction Motors," *IET Control Theory & Applications*, vol. 4, no. 9, pp. 1707-1724, 2010.
[139] F. R. Salmasi, T. A. Najafabadi, "An Adaptive Observer with Online Rotor and Stator Resistance Estimation for Induction Motors With One Phase Current Sensor," *IEEE Transactions on Energy Conversion*, vol. 26, no. 3, pp. 959-966, 2011.
[140] X. Zhang, G. Foo, M. D. Vilathgamuwa, K. J. Tseng, B. S. Bhangu, C. Gajanayake, "Sensor Fault Detection, Isolation and System Reconfiguration Based on Extended Kalman Filter for Induction Motor Drives," *IET Electric Power Applications*, vol. 7, no. 7, pp. 607-617, 2013.
[141] A. B. Youssef, S. K. E. Khil, I. S. Belkhodja, "State Observer-Based Sensor Fault Detection and Isolation, and Fault Tolerant Control of a Single-Phase PWM Rectifier for Electric Railway Traction," *IEEE Transactions on Power Electronics*, vol. 28, no. 12, pp. 5842-5853, 2013.
[142] B. Tabbache, M. E. H. Benbouzid, A. Kheloui, J. M. Bourgeot, "Virtual-Sensor-Based Maximum-Likelihood Voting Approach for Fault-Tolerant Control of Electric Vehicle Powertrains," *IEEE Transactions on Vehicular Technology*, vol. 62, no. 3, pp. 1075-1083, 2013.
[143] J. Holtz, "Sensorless Control of Induction Machines-With or Without Signal Injection," *IEEE Transactions on Industrial Electronics*, vol. 53, no. 1, pp. 7-30, 2006.
[144] Z. Q. Zhu, L. M. Gong, "Investigation of Effectiveness of Sensorless Operation in Carrier-Signal-Injection-Based Sensorless-Control Methods," *IEEE Transactions on Industrial Electronics*, vol. 58, no. 8, pp. 3431-3439, 2011.
[145] W. Cao, B. Mecrow, G. Atkinson, J. Bennett, D. Atkinson, "Overview of Electric Motor Technologies Used for More Electric Aircraft (MEA)," *IEEE Transactions on Industrial Electronics*, vol. 59, no. 9, pp. 3523-3531, 2012.
[146] F. Meinguet, N. Ngac-Ky, P. Sandulescu, X. Kestelyn, E. Semail, "Fault-Tolerant Operation of an Open-end Winding Five-Phase PMSM Drive With Inverter Faults," *in proc. of the 39th Annual Conference of the IEEE Industrial Electronics Society* (IECON 2013), 2013.
[147] A. Mohammadpour, L. Parsa, "Global Fault-Tolerant Control Technique for Multi-Phase Permanent-Magnet Machines," *IEEE Transactions on Industry Applications*, vol. 51, no. 1, pp. 178-186, 2015.
[148] N. Bianchi, S. Bolognani, M.D. Pré, "Strategies for the Fault-Tolerant Current Control of a Five-Phase Permanent-Magnet Motor," *IEEE Transactions on Industry Applications*, vol. 43, no. 4, pp. 960-970, 2007.
[149] M.O.E. Aboelhassan, T. Raminosoa, A. Goodman, L. de Lillo, C. Gerada, "Performance Evaluation of a Vector-Control Fault-Tolerant Flux-Switching Motor Drive," *IEEE Transactions on Industrial Electronics*, vol. 60, no. 8, pp. 2997-3006, 2013.
[150] L. Alberti, N. Bianchi, "Experimental Tests of Dual Three-Phase Induction Motor Under Faulty Operating Condition," *IEEE Transactions on Industrial Electronics*, vol. 59, no. 5, pp. 2041-2048, 2012.
[151] J. R. Fu, T.A. Lipo, "Disturbance Free Operation of a Multiphase Current Regulated Motor Drive with an Opened Phase," *IEEE Transactions on Industry Applications*, vol. 30, no. 5, pp. 1267-1274, 1994.
[152] Y. Zhao, T.A. Lipo, "Modeling and Control of a Multi-Phase Induction Machine with Structural Unbalance Part II. Field-Oriented Control and Experimental Verification," *IEEE Transactions on Energy Conversion*, vol. 11, no. 3, pp. 578-584, 1996.
[153] H.S. Che, M.J. Duran, E. Levi, M. Jones, W.P. Hew, N.A. Rahim, "Postfault Operation of an Asymmetrical Six-Phase Induction Machine with Single and Two Isolated Neutral Points," *IEEE Transactions on Power Electronics*, vol. 29, no. 10, pp. 5406-5416, 2014.

[154] H.M. Ryu, J.W. Kim, S.K. Sul, "Synchronous-Frame Current Control of Multiphase Synchronous Motor Under Asymmetric Fault Condition Due to Open Phases," *IEEE Transactions on Industry Applications*, vol. 42, no. 4, pp. 1062-1070, 2006.

[155] A. Tani, M. Mengoni, L. Zarri, G. Serra, D. Casadei, "Control of Multi-Phase Induction Motors with an Odd Number of Phases Under Open-Circuit Phase Faults," *IEEE Transactions on Power Electronics*, vol. 27, no. 2, pp. 565-577, 2012.

[156] F. Locment, E. Semail, X. Kestelyn, "Vectorial Approach-Based Control of a Seven-Phase Axial Flux Machine Designed for Fault Operation," *IEEE Transactions on Industrial Electronics*, vol. 55, no. 10, pp. 3682-3691, 2008.

[157] S. Dwari, L. Parsa, "Fault-Tolerant Control of Five-Phase Permanent-Magnet Motors with Trapezoidal Back EMF," *IEEE Transactions on Industrial Electronics*, vol. 58, no. 2, pp. 476-485, 2011.

[158] A. Abdel-Khalik, A. Morsy , S. Ahmed, A. Massoud, "Effect of Stator Winding Connection on Performance of Five-phase Induction Machines," *IEEE Transactions on Industrial Electronics*, vol. 61, no. 1, pp. 3-19, 2014.

[159] Z. Sun, J. Wang, G.W. Jewell, D. Howe, "Enhanced Optimal Torque Control of Fault-Tolerant PM Machine Under Flux-Weakening Operation," *IEEE Transactions on Industrial Electronics*, vol. 57, no. 1, pp. 344-353, 2010.

[160] M.J. Durán, J. Prieto, F. Barrero, "Space Vector PWM With Reduced Common-Mode Voltage for Five-Phase Induction Motor Drives Operating in Overmodulation Zone," *IEEE Transactions on Power Electronics*, vol. 28, no. 8, pp. 4030-4040, 2013.

[161] G. Carrasco, C. Silva, "Space Vector PWM Method for Five-Phase Two-Level VSI with Minimum Harmonic Injection in the Over Modulation Region," *IEEE Transactions on Industrial Electronics*, vol. 60, no. 5, pp. 2042-2053, 2013.

[162] J. M. Apsley, "Derating of Multiphase Induction Machines due to Supply Imbalance," *IEEE Transactions on Industrial Applications*, vol. 46, no. 2, pp. 798–805, 2010.

[163] L. Zheng, J. E. Fletchert, B. W.Williams, "Current Optimization for a Multi-Phase Machine Under an Open Circuit Phase Fault Condition," *in Proceedings of 3rd IET International Conference on Power Electronics, Machines and Drives*, 2006.

[164] A.S. Abdel-Khalik, S Ahmed, A.A. Elserougi, A.M. Massoud, "Effect of Stator Winding Connection of Five-Phase Induction Machines on Torque Ripples Under Open Line Condition," *IEEE/ASME Transactions on Mechatronics*, vol. 20, no. 2, pp. 580-593, 2015.

[165] A. Mohammadpour, S. Sadeghi, L. Parsa, "A Generalized Fault-Tolerant Control Strategy for Five-Phase PM Motor Drives Considering Star, Pentagon, and Pentacle Connections of Stator Windings," *IEEE Transactions on Industrial Electronics*, vol. 61, no. 1, pp. 63-75, 2014.

[166] J.W. Bennett, B.C. Mecrow, D.J. Atkinson, G.J. Atkinson, "Safety-Critical Design of Electromechanical Actuation Systems in Commercial Aircraft," *IET Electric Power Applications*, vol. 5, no. 1, pp. 37-47, 2011.

[167] J.W. Bennett, G.J. Atkinson, B.C. Mecrow, D.J. Atkinson, "Fault-Tolerant Design Considerations and Control Strategies for Aerospace Drives," *IEEE Transactions on Industrial Electronics*, vol. 59, no. 5, pp. 2049-2058, 2012.

[168] R. Kianinezhad, B. Nahid-Mobarakeh, L. Baghli, F. Betin, GA. Capolino, "Modeling and Control of Six-Phase Symmetrical Induction Machine Under Fault Condition Due to Open Phase," *IEEE Transactions on Industrial Electronics*, vol. 55, no. 5, pp. 1966-1977, 2008.

[169] M.A. Fnaiech, F. Betin, G.A. Capolino, F. Fnaiech, "Fuzzy Logic and Sliding-Mode Controls Applied to Six-Phase Induction Machine With Open Phases," *IEEE Transactions on Industrial Electronics*, vol. 57, no. 1, pp. 354-364, 2010.

[170] F. Baudart, B. Dehez, E. Matagne, D. Teleu-Nedelcu, P. Alexandre, F. Labrique, "Torque Control Strategy of Polyphase Permanent-Magnet Synchronous Machines with Minimal Controller Reconfiguration Under Open-Circuit Fault of One Phase," *IEEE Transactions on Industrial Electronics*, vol. 59, no. 6, pp. 2632-2644, 2012.

[171] H. A. Toliyat, "Analysis and Simulation of Five-Phase Variable-Speed Induction Motor Drives Under Asymmetrical Connections," *IEEE Transactions on Power Electronics*, vol. 13, no. 4, pp. 748-756, 1998.

[172] J. Figueroa, J. Cros, P. Viarouge, "Polyphase PM Brushless DC Motor for High Reliability Application," *in Proceedings of the 10th European Conference on Power Electronics and Applications*, (EPE 2003), 2003.

[173] J. Wang, K. Atallah, D. Howe, "Optimal Torque Control of Fault-Tolerant Permanent Magnet Brushless Machines," *IEEE Transactions on Magnetics*, vol. 39, no. 5, pp. 2962-2964, 2003.

[174] A. Mohammadpour, S. Mishra, L. Parsa, "Fault-Tolerant Operation of Multiphase Permanent-Magnet Machines Using Iterative Learning Control," *IEEE Journal of Emerging and Selected Topics in Power Electronics*, vol. 2, no. 2, pp. 201-211, 2014.

[175] F. Betin, G.A. Capolino, "Shaft Positioning for Six-Phase Induction Machines with Open Phases Using Variable Structure Control," *IEEE Transactions on Industrial Electronics*, vol. 59, no. 6, pp. 2612-2620, 2012.

[176] M.A. Shamsi-Nejad, B. Nahid-Mobarakeh, S. Pierfederici, F. Meibody-Tabar, "Fault Tolerant and Minimum Loss Control of Double Star Synchronous Machines Under Open Phase Conditions," *IEEE Transactions on Industrial Electronics*, vol. 55, no. 5, pp. 1956-1965, 2008.

CHAPTER: 3

CONTRIBUTIONS

3.1 INTRODUCTION

This Doctoral thesis work is focused on the extension of finite-control set model-based predictive control, for multiphase drives, to the fault-tolerant operation while ensuring efficient and controlled post-fault operation. In order to obtain an accurate system model, suitable for a FCS-MPC strategy, research work has been conducted in the mathematical study of the electrical machine equations under pre- and post-fault conditions considering different types of faults, providing further insight of the effect fault conditions have on the system behavior. Simulation models of a five-phase induction machine under two different types of faults namely, open-phase (produced by either an open-circuit line or phase fault) and IGBT-gating failure faults, where developed in order to design and test the FCS-MPC controller and their results were presented in several international conferences. Obtained results paved the way for the implementation and experimental validation of the proposed fault-tolerant strategy based on predictive control techniques on the laboratory test-rig, leading to two of the article contributions presented later on in this chapter. Subsequently, a fault-tolerant scheme based on linear controllers was designed based on research available in the state of the art literature and a comparison between the proposed predictive technique and a proportional resonant fault-tolerant controller was conducted through simulation and experimental tests under an open-phase fault, leading to both an international conference and a journal paper publication.

The contributions of this Thesis are presented in three different journal papers published in the *IEEE Transactions on Industrial Electronics*, between the years 2013/2015. Next, a summary of each journal paper is presented, highlighting their most important aspects. Subsequently, each journal paper is included.

3.2 FAULT-TOLERANT FCS-MPC FOR MULTIPHASE DRIVES UNDER AN OPEN-PHASE FAULT

In the first journal paper entitled, "Speed Control of Five-Phase Induction Motors with Integrated Open-Phase Fault Operation using Model-Based Predictive Current Control Techniques", a novel predictive controller for post-fault operation of a five-phase drive under an open-phase fault, based on FCS-MPC is shown (Fig. 3.1).

As stated previously, FCS-MPC performance highly depends on the accuracy of the system model and consequently a mathematical model of the multiphase drive under faulty operation must be considered. A detailed model of the multiphase induction drive with an open-phase is developed and the fault effect on the machines modeling equations are stated. For instance, an open-phase fault results in asymmetrical stator/rotor impedance terms leading in turn to non-circular stator currents in the α-β plain (Fig. 3.2b). Moreover, the faulty phase current is zero while the phase voltage is now determined by the Back-EMF term. Consequently, the machines neutral voltage oscillates and the leg-to-phase voltage matrix must be modified in order to consider this effect. To cope with these asymmetries a modified Clarke transformation matrix has been proposed (150), maintaining rotor/stator impedance and Back-EMF terms circular in the α-β plain (Fig. 3.2c).

The main advantage of the proposed matrix when compared to the one proposed in previous research works is that its implementation leads to symmetrical terms without the need of a modified rotating matrix, reducing the amount of changes that are needed for post-fault operation.

$$[T_{c\_mod}] = \frac{2}{5}\begin{bmatrix} \cos(\vartheta)-1 & \cos(2\vartheta)-1 & \cos(3\vartheta)-1 & \cos(4\vartheta)-1 \\ \sin(\vartheta) & \sin(2\vartheta) & \sin(3\vartheta) & \sin(4\vartheta) \\ \sin(2\vartheta) & \sin(4\vartheta) & \sin(6\vartheta) & \sin(8\vartheta) \\ 1 & 1 & 1 & 1 \end{bmatrix} \tag{150}$$

As stated previously, the machines neutral voltage oscillates under post-fault operation. This effect has to be considered in order to provide an accurate system model to the predictive controller and ensure that the appropriate voltage vector is selected. As a consequence, notice that the Back-EMF term of the faulty phase is now considered in the voltage matrix equation (151), second term.

$$\begin{bmatrix} v_{bs} \\ v_{cs} \\ v_{ds} \\ v_{es} \end{bmatrix} = \frac{V_{dc}}{4}\begin{bmatrix} 3 & -1 & -1 & -1 \\ -1 & 3 & -1 & -1 \\ -1 & -1 & 3 & -1 \\ -1 & -1 & -1 & 3 \end{bmatrix}\begin{bmatrix} S_b \\ S_c \\ S_d \\ S_e \end{bmatrix} - \frac{L_m\frac{di_{s\alpha}}{dt}+L_m\frac{di_{r\alpha}}{dt}}{4}[I_4] \tag{151}$$

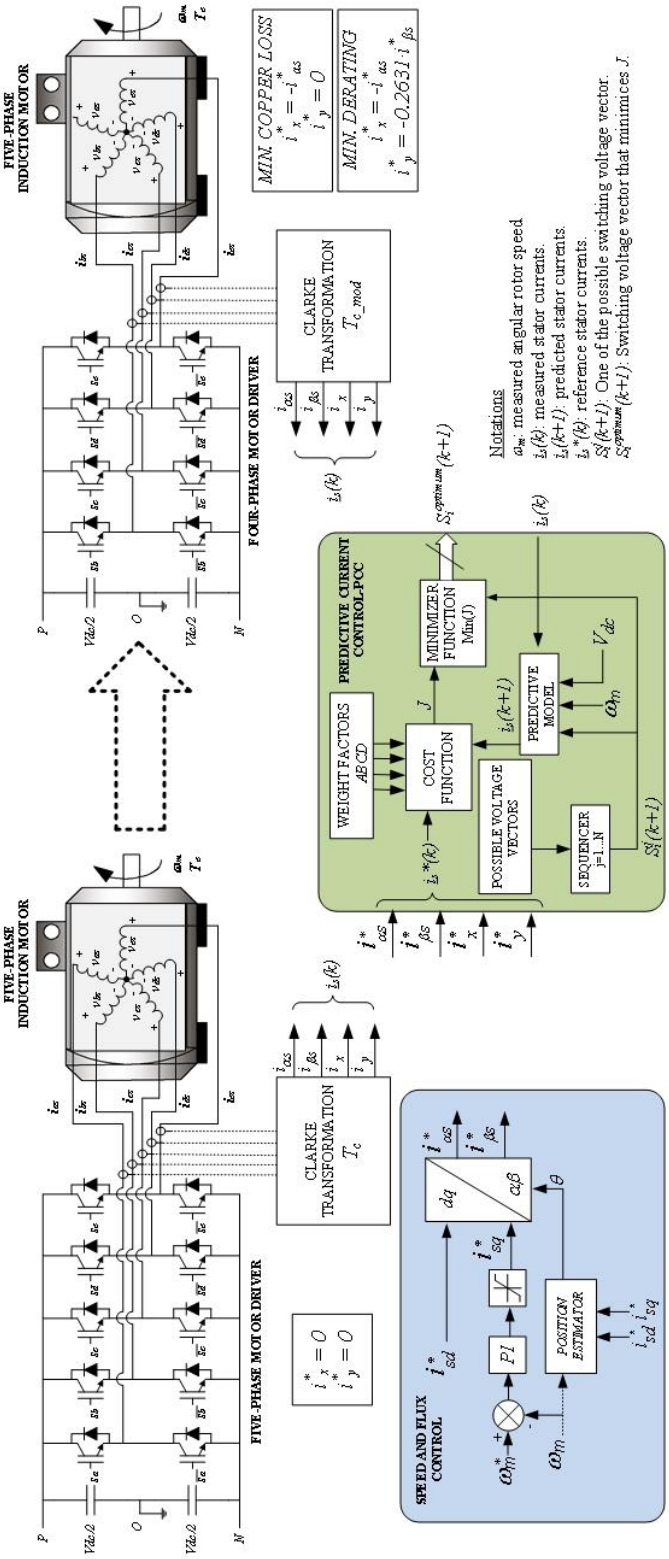

Fig. 3.1.: Pre- and post- fault drive topology and proposed control scheme based on an outer speed and flux loop and an inner open-phase fault-tolerant FCS-MPC current control.

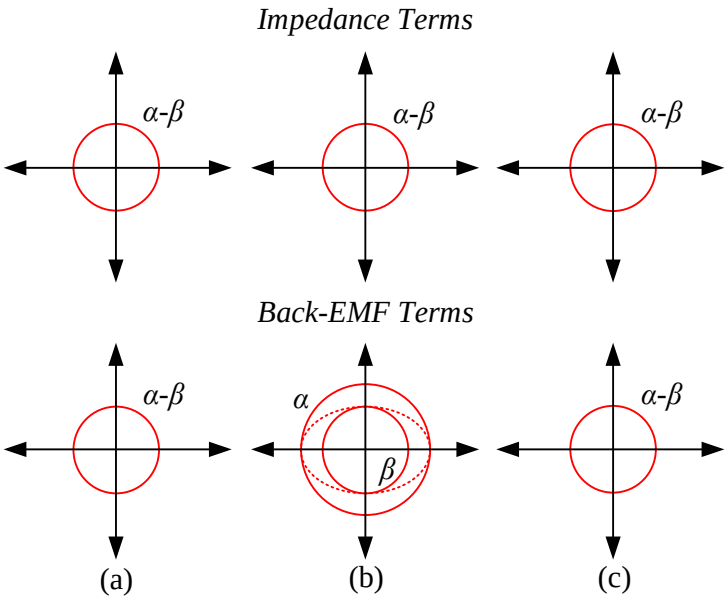

Fig. 3.2.: Mapping of the α-β components for the five-phase system under normal (a) and open-phase fault operation implementing the traditional Clarke transformation (b) and the modified Clarke transformation (c).

Subsequently, the mathematical model was used in order to design a post-fault FCS-MPC scheme. The controller is formed by an outer speed control loop and an inner predictive current controller. The predictive current controller was designed and implemented both for pre- and post-fault implementation, in order to test and prove the capability of the proposed controller to manage either pre- or post- fault operation and its transition. Notice that the FCS-MPC cost function *J* (152) is the same for either pre- or post-fault operation and that only the weight factor *C* for the *x*-current component is modified between working states, being zero under post-fault operation. Two main control criteria were adopted for post-fault operation namely, minimum copper loss and minimum derating, by appropriately selecting post-fault current references, as shown in Fig. 3.1 right hand side, being in both cases the *x*-current fixed to $-i_{s\alpha}$, while the *y*-current component is set either to zero for minimum copper loss or -26.31% of the β-current component for minimum derating. Obtained results allowed concluding that by implementing minimum derating, the electrical drive is capable of achieving an extra 8% of torque than with minimum copper losses, being possible to maintain a post-fault torque of 56% of the nominal torque with minimum copper loss criteria and 64% with minimum derating.

$$J = A|\overline{i_{s\alpha}}| + B|\overline{i_{s\beta}}| + C|\overline{i_{sx}}| + D|\overline{i_{sy}}| \quad (152)$$

where *A*, *B*, *C*, *D* are the cost function weight factor and each α-β-x-y current term is defined as:

$$\overline{i_{s\alpha}} = i^*_{s\alpha}(k+1) - \hat{\imath}_{s\alpha}(k+1),\ \overline{i_{s\beta}} = i^*_{s\beta}(k+1) - \hat{\imath}_{s\beta}(k+1) \quad (153)$$

$$\overline{i_{sx}} = i_{sx}^{*}(k+1) - \hat{\imath}_{sx}(k+1),\ \overline{i_{sy}} = i_{sy}^{*}(k+1) - \hat{\imath}_{sy}(k+1) \quad (154)$$

As a final remark, even though fault detection is not considered within the present work, the effect of fault detection delay is considered for some experimental tests. Considering the available data in the literature, a transition time of 40 ms between pre- and post-fault operation was considered, concluding that even though the predictive controller provides an almost instantaneous proper post-fault operation once the fault is detected, during the fault detection phase, the controller completely loses control capabilities due to the inaccuracies in the system model.

3.3 IGBT-GATING FAULT EFFECT IN FAULT-TOLERANT MULTIPHASE INDUCTION DRIVES

In the second journal paper entitled, "IGBT-Gating Failure Effect on a Fault-Tolerant Predictive Current Controlled 5-Phase Induction Motor Drive", a second type of fault of multiphase drives was studied. The effect an IGBT-gating failure, causing the non-commutation of both semiconductors in one phase of the electrical drive, leading to the loss of controllability, is analyzed from theoretical and experimental perspectives. It was demonstrated that under such type of fault, the faulty phase free-wheeling diodes (D_1 and D_2) are able to conduct in different instants, connecting the faulty phase to the negative (N) or the positive (P) rail of the converter, if the conditions in (155)-(157) are met, leading to non-controlled currents. Consequently, a constant change of the electrical drive configuration, from a four-phase system (five-phase drive with an open-phase fault) to a four-phase drive plus one non-controlled phase (Fig. 3.3), is observed. Moreover, the non-controlled current through the faulty phase introduces an additional non-controlled oscillation in the stator neutral voltage, which must be accounted for control purposes.

$$D_1 - ON: V_{D1} = v_{as} + V_{CM} - 0.5V_{DC} \geq V_{\gamma} \quad (155)$$

$$D_2 - ON: V_{D2} = v_{as} + V_{CM} + 0.5V_{DC} \leq -V_{\gamma} \quad (156)$$

$$V_{CM} = V_{sN} - \frac{V_{DC}}{2} = \frac{1}{5}(V_{aN} + V_{bN} + V_{cN} + V_{dN} + V_{eN}) - \frac{V_{DC}}{2} \quad (157)$$

where V_{D1} and V_{D2} is the voltage across each free-wheeling diode, v_{as} is the faulty phase voltage, V_{γ} is the diode forward conduction voltage, V_{sN} is the voltage between the machines neutral point (s) to the negative rail of the converter, given by the sum of each leg voltage ($i = a, b, c, d, e$) to N, and V_{CM} is the common-mode voltage (CMV) that relates the motor neutral voltage to the DC-link mid-point.

Traditionally, when this type of fault occurs, the complete faulty phase is disconnected from

the electrical machine, reconfiguring the electrical drive to work as in an open-phase fault. However, this strategy requires additional electric components in the VSI in order to physically disconnect the converter phase from the electrical machine, increasing the cost and complexity of the power converter. The IGBT-gating fault management through control means, reduces this extra cost and complexity, at the expense of an additional non-controlled oscillation in the stator neutral voltage.

Even though predictive controllers require an accurate system model for their implementation, the constant and instantaneous change of the electrical drive configuration, makes an accurate system model description a high-computational cost task, making its implementation much more complex and depending on the type of microprocessor used for the specific application, inviable. Nonetheless, by analyzing the available post-fault voltage vectors under an open-phase fault, it was concluded that the effect of the non-controlled phase in the available four-phase system, results in a small deviation of the available vectors either to the left or the right side depending on the diode that is conducting. Consequently, it was foreseeable that the developed FCS-MPC fault-tolerant controller could withstand IGBT-gating failures at the expense of a certain downgrade in its performance.

The controller operation under this type of fault was demonstrated experimentally considering different working states (i.e. steady state, speed reversal and pre- and post-fault transition), with minimum copper loss and minimum derating criteria, considering different load torques and for some tests a fault detection delay of 40 ms. In order to measure the performance decay the same working points where tested under an IGBT-gating fault and an open-phase fault, giving further insight on the effect of not considering the four-phase plus one non-controlled phase in the controllers electrical drive model.

On the overall, as experimental results demonstrate, the free-wheeling diode stator currents slightly reduce the torque production and increase copper losses, maintaining the basic features of the post-fault operation controlled system. A small reduction of the post-fault available torque is observed when working at maximum post-fault ratings, being further affected if fault detection delay is considered. However, if the electrical drive is not driven at its maximum post-fault working point the effect is neglectable. Consequently, the degradation in the control performance is limited and can be considered as an external perturbation of the controller or even an acceptable tradeoff for not implementing an accurate system model with its transition between the four-phase system and four-phase system with one non-controlled phase.

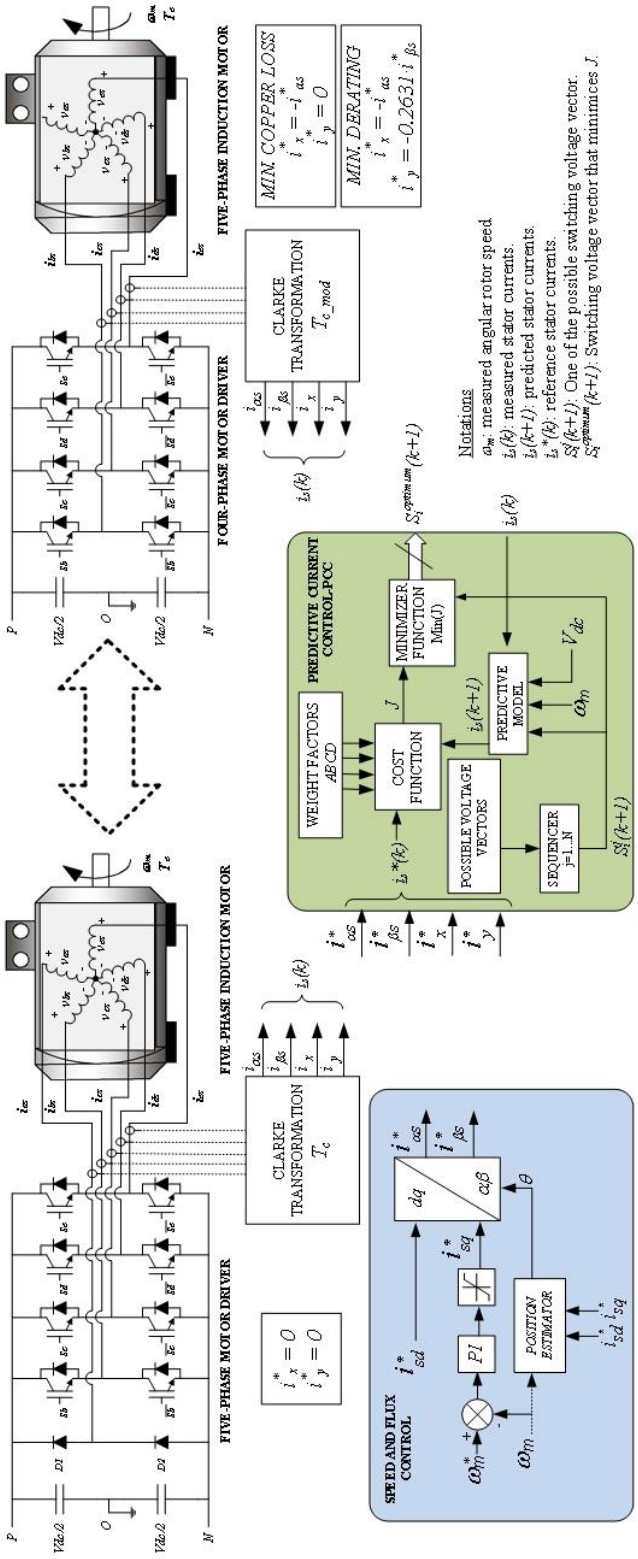

Fig. 3.3.: Electrical drive topology reconfiguration under an IGBT-Gating failure and control scheme based on an outer speed and flux loop and an inner fault-tolerant FCS-MPC current control.

3.4 PERFORMANCE ANALYSIS OF FAULT-TOLERANT FCS-MPC AND LINEAR CONTROL TECHNIQUES

Finally, the third journal paper entitled, "Comparative Study of Predictive and Resonant Controllers in Fault-Tolerant Five-phase Induction Motor Drives", analyzes the performance of two open-phase fault-tolerant control schemes, based on linear and predictive control techniques, for five-phase induction machines, through a set of experimental tests (i.e. steady state, reversal and pre- to post-fault transition). Furthermore, provided tests are conducted at maximum post-fault ratings with either minimum copper loss (T_L=0.56*T_n) or minimum derating criteria (T_L=0.64*T_n), and consider steady state operation and control transition from pre- to post-fault, with and without fault detection delay of 40 ms.

Even though both controllers are capable of post-fault operation, maintaining a sinusoidal MMF while achieving minimum losses, maximum torque per-ampere and reducing torque vibrations, its implementation is completely different due to the machine asymmetric effect on the control strategy. For instance, when a FCS-MPC control strategy is implemented (Fig. 3.1), the electrical model of the machine must be revised in order to account for the faulty phase and provide accurate predictions. Consequently, a modified Clarke transformation is considered in order to compensate the faulty machine asymmetries' in the α-β subspace and the faulty phase counter electromotive force must be considered for the voltage vector estimation. On the other hand if a linear control strategy is implemented (Fig. 3.4), the electrical machine model and vector space decomposition remains as in pre-fault, due to the fact that the asymmetry in the impedance terms on the α-β plane does not have any effect on the controller performance and that there is no need to consider the faulty phase back-emf in the voltage equilibrium equations. Nonetheless, the type of controller is changed from traditional PI to PR controllers, in order to handle the oscillating post-fault *x*-*y* current references. In order to compare the controller's performance under the same conditions, both control schemes are based, as schematically shown in Fig. 3.1 and Fig. 3.4, either on pre- or post-fault operation, on an outer speed and flux control loop implemented in a rotor-flux-oriented *d*-*q* reference frame with conventional PI controllers. The *d*-current reference is set to a constant value and the *q*-current reference is determined by a PI controller based on the speed error. Under pre-fault operation, *x*-*y* current references are zero, thus PI controllers are used to follow the current references in the linear

inner control scheme, while the traditional Clarke transformation, voltage matrix and the cost function considering both *x* and *y* current error are considered for the inner current predictive controller scheme. When the open-phase fault occurs, each inner control scheme is modified in order to achieve post-fault operation.

Test results allow concluding that speed control in post-fault operation with inner fault-tolerant schemes implemented based either on FCS-MPC (Fig. 3.1) or PR (Fig. 3.4) controllers is viable with similar performance. Moreover, both control methods ensure proper post-fault current reference tracking, either with the minimum copper loss or the minimum derating criteria at maximum post-fault ratings, maintaining the electrical drive within its maximum post-fault current limits. As expected from predictive methods, the speed response is faster than with the PR controller, but at the expense of higher torque and current ripple. However they are more affected in the transition from pre- to post-fault modes of operation due to the high dependence on the model accuracy, which is highly deviated during the fault detection delay.

Regarding the implementation of each control scheme, it must be noted that the number of changes required to adapt the control structure to the faulty situation is higher when FCS-MPC are used when compared to PR control because of the necessity to consider the neutral point voltage oscillation and modify the Clarke transformation matrix. Nonetheless, it must be stated that in order to ensure a proper post-fault drive operation, the different PI constants must be correctly tuned, increasing the complexity during its implementation and limiting the behavior of the electrical drive only for the operating point for which the regulators have been tuned.

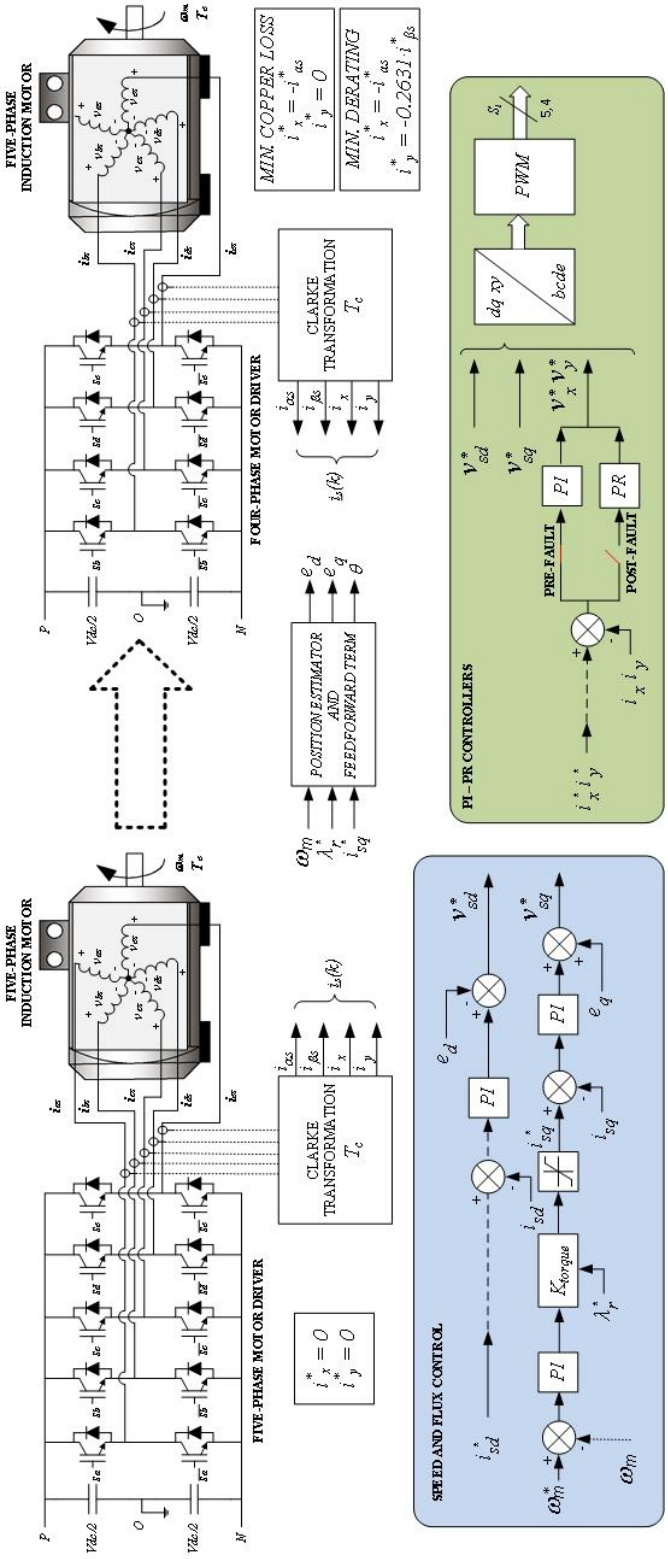

Fig. 3.4.: Pre- and post- fault drive topology and implemented control scheme based on an outer speed and flux loop and an inner open-phase fault-tolerant PR controller.

3.5 JOURNAL PAPERS

This section contains the following journal papers:

Journal paper 1:

Title: Speed Control of Five-Phase Induction Motors with Integrated Open-Phase Fault Operation using Model-Based Predictive Current Control Techniques.

Authors: H. Guzman, M. J. Duran, F. Barrero, B. Bogado, S. Toral.

Publication: *IEEE Transactions on Industrial Electronics.*

DOI: 10.1109/TIE.2013.2289882.

Journal paper 2:

Title: IGBT-Gating Failure Effect on a Fault-Tolerant Predictive Current Controlled 5-Phase Induction Motor Drive.

Authors: H. Guzman, F. Barrero, M. J. Duran.

Publication: *IEEE Transactions on Industrial Electronics.*

DOI: 10.1109/TIE.2014.2331019.

Journal paper 3:

Title: Comparative Study of Predictive and Resonant Controllers in Fault-Tolerant Five-phase Induction Motor Drives.

Authors: H. Guzman, M. J. Duran, F. Barrero, L. Zarri, B. Bogado, I. Gonzalez Prieto, M. R. Arahal.

Publication: *IEEE Transactions on Industrial Electronics.*

DOI: 10.1109/TIE.2015.2418732.

JOURNAL PAPER 1

Title: Speed Control of Five-Phase Induction Motors with Integrated Open-Phase Fault Operation using Model-Based Predictive Current Control Techniques.

Authors: H. Guzman, M. J. Duran, F. Barrero, B. Bogado, S. Toral.

Publication: *IEEE Transactions on Industrial Electronics.*

Volume: 61

Issue: 9

Pages: 4474 - 4484

Year: 2014

DOI: 10.1109/TIE.2013.2289882.

Summary:

Fault-tolerance is one of the most interesting features in standalone electric propulsion systems. Multiphase induction motor drives are presented like a better alternative to their three-phase counterparts because of their capability to withstand faulty situations, ensuring the post-fault operation of the drive. Finite-control set model-based predictive control (FCS-MPC) has been introduced in the last decade like an interesting alternative to conventional controllers for the electrical torque and current regulation of multiphase drives. However, FCS-MPC strategies for multiphase drives with the ability to manage pre- and post-fault operations have not been addressed at all. This paper proposes a fault tolerant speed control for five-phase induction motor drives with the ability to run the system before and after an open-phase fault condition using a FCS-MPC strategy. Experimental results are provided in order to validate the functionality of the proposed control method, maintaining rated currents and ensuring fast and ripple-free torque response.

JOURNAL PAPER 2

Title: IGBT-Gating Failure Effect on a Fault-Tolerant Predictive Current Controlled 5-Phase Induction Motor Drive.

Authors: H. Guzman, F. Barrero, M. J. Duran.

Publication: *IEEE Transactions on Industrial Electronics.*

Volume: 62

Issue: 1

Pages: 15 - 20

Year: 2015

DOI: 10.1109/TIE.2014.2331019.

Summary:

Multiphase machine drives are gaining importance in high reliability applications due to their fault-tolerance capability and their ability to cope with the post-fault operation without any extra electronic components. Predictive current controllers have been recently proposed for managing post-fault operation of these drives when an open phase fault is considered. However, the faulty situation assumes zero stator current while free-wheeling diodes can continue conducting in a non-controlled mode. This work analyses the post-fault operation of the five-phase drive when the free-wheeling diodes of the faulty phase are still conducting. Experimental results are provided using a conventional IGBT-based multiphase power converter to quantify the effect of the free-wheeling diodes, when an IGBT-gating fault occurs, on the model-based predictive current controlled drive.

JOURNAL PAPER 3

Title: Comparative Study of Predictive and Resonant Controllers in Fault-Tolerant Five-phase Induction Motor Drives.

Authors: H. Guzman, M. J. Duran, F. Barrero, L. Zarri, B. Bogado, I. Gonzalez Prieto, M. R. Arahal.

Publication: *IEEE Transactions on Industrial Electronics.*

Volume: PP

Issue: 99

Pages: 1 - 1

Year: 2015

DOI: 10.1109/TIE.2015.2418732.

Summary:

One of the most attractive features of multiphase machines is the fault-tolerant capability due to the higher number of phases. Different post-fault control strategies based on hysteresis, PI-resonant and predictive techniques have been recently proposed. They all proved their capabilities to withstand fault situations and to preserve the fundamental component of the air-gap field, while achieving minimum losses, maximum torque per-ampere and reducing torque vibrations. Nonetheless, due to their recent introduction, no thorough study has yet appeared comparing the performance of these controllers. In this paper two open-phase fault-tolerant control schemes are experimentally compared in a real five-phase induction machine. The controllers being compared are based on PI-resonant and predictive control techniques, respectively. The experiments include pre- and post-fault situations. Obtained results show that both control methods offer nearly the same performance. When compared, predictive control provides faster control response and superior performance at low speed operation but is found to be less resilient to fault detection delays and to have higher current ripple. Regarding the controller implementation, it is shown that the transition from pre- to post- fault operation involves modelling the non-linear effects observed when an open-phase fault occurs for the predictive controller, and the proper retuning of the PI trackers for the PI-resonant controller, in order to ensure post-fault operation.

3.6 SUMMARY

In this chapter, the contributions that constitute this Doctoral thesis have been presented. Conducted research on the fault-tolerance capability of multiphase drives consisting on the mathematical study of the electrical machine equations under pre- and post- fault conditions under different types of faults and the development/comparison of control strategies that are capable of ensuring post-fault operation, have resulted in the publication of three journal papers in the *IEEE Transactions on Industrial Electronics*, between the years 2013 and 2015, consisting on the proposal of a novel fault-tolerant technique for open-phase faults based on a FCS-MPC current control, the study of the proposed controller under an IGBT-Gating failure on both semiconductors of a converters phase and finally the comparison of the fault-tolerant FCS-MPC with proportional-resonant controllers. It is proved not only that controlled post-fault operation without extra hardware is feasible with multiphase drives, but also that predictive control techniques such as FCS-MPC can be extended to such type of operation obtaining similar performance as with traditional linear controllers.

CHAPTER: 4

CONCLUSIONS AND FUTURE WORK

4.1 CONCLUSIONS

The main conclusions drawn from this Doctoral Thesis work can be summarized as:

1. Controlled post-fault operation of multiphase drives is feasible without extra hardware.
2. During an open-phase fault, the machine modeling equations must be revised in order to account for the loss of the faulty phase. In the first place, one control degree of freedom is lost and it is necessary to implement a modified Clarke transformation in order to provide symmetrical impedances and Back-EMF terms in the α-β subspace. Secondly, the faulty phase current is zero while its voltage is given by its Back-EMF term, which must be considered in the leg-to-phase voltage matrix, providing a different stator phase voltage matrix than in pre-fault operation.
3. Depending on the specific application constraints and type of multiphase drive, different post-fault control criteria can be successfully applied, aiming to reduce copper losses or to provide maximum torque.
4. Finite-Control Set Model-Based Predictive Control can be successfully extended to withstand post-fault operation. Moreover, the fast reference tracking of controlled variables inherent of predictive controllers makes the controller reconfiguration from pre- to post-fault operation one of the main advantages of this type of controllers when compared to fault-tolerant schemes based on linear controllers.
5. Due to the inherent necessity of FCS-MPC to account for an accurate system model, fault detection delay represents the main drawback of this technique for industrial applications, where obtained results show that during this period of time the fault-tolerant FCS-MPC controller loses complete control capability.

6. Under the same working conditions, the proposed fault-tolerant FCS-MPC controller is capable of ensuring post-fault operation also under an IGBT-Gating fault with minimum torque reference deviation. Even though the predictive controller is designed considering the multiphase drive equations under an open-phase fault, the effect of an IGBT-Gating failure is mainly observed in a small deviation of the post-fault available voltage vectors under an open-phase fault. Consequently, although an accurate system model that accounts both obtained drive states is not considered, the predictive controller design is much simpler at the expense of a slightly lower post-fault achievable torque.
7. Linear control schemes based on PI and PR controllers can be successfully implemented for steady state operation (either under pre- or post-fault operation), and the transition between working states, without the need to consider the fault effect on the electrical drive modeling equations.
8. Contrary to the proposed fault-tolerant FCS-MPC, linear control schemes based on PI and PR controllers, are not highly affected under the unavoidable fault detection delay and consequently offer better system behavior during pre- to post-fault transition.
9. Once the fault is detected, the FCS-MPC control is capable of achieving post-fault references faster than the linear controller, at the expense of higher current and torque ripple.
10. The main drawback of fault-tolerant schemes based on PR controllers is that the different PI constants must be correctly tuned, increasing the complexity during its implementation and limiting the behavior of the electrical drive only for the operating point for which the regulators have been tuned.

4.1.1 SUMMARY OF ADDITIONAL RESEARCH WORK

Table I contains a summary of the presented conference works, journal papers, filed patent applications, book chapters and research projects developed during the doctoral thesis period but that were not considered as the main contributions of the research investigation conducting to the PhD degree.

Table I. Summary of additional achievements during the Doctoral thesis.

	Number
Conference Works	7
Journal Papers	3
Patents	1
Book Chapters	2
Participation in R&D Projects	3
Codirected Bachelor Thesis	2

4.2 FUTURE WORK

Proposed future work can be divided in the following topics:

1. Model-based fault detection techniques. Taking advantage of the accurate model designed in order to implement FCS-MPC controllers, a possible future work may consist on appropriately detecting the fault occurrence by comparing the electrical drive measured currents with the expected ones based on the information given by the predictive model.
2. The post-fault operation analysis considering different types of controllers that have been not considered up until now. The extension of traditional DTC control schemes to fault-tolerance operation. The knowledge of the electrical drive model under abnormal operation and the available voltage vectors under either an open-phase fault or an IGBT-Gating failure, makes the implementation of DTC with fault-tolerant capability a feasible option for future work.
3. FCS-MPC parameter sensibility under post-fault operation. Parameter deviation can highly affect predictive controller's performance. It is foreseeable that under different types of faults, the parameter deviation may degrade the proposed fault-tolerant FCS-MPC performance in different percentage.
4. The analysis and extension of the fault-tolerant FCS-MPC to the operation of multiphase drives based on permanent magnet machines' with non-sinusoidal electromotive forces. Further increasing the post-fault mathematical model complexity and the controllers' constraints.

5. FCS-MPC fault-tolerant operation at the machines' rated speed and under flux weakening mode. Further improving the controller for real implementation in electrical transport vehicles.

CAPÍTULO: 5

RESUMEN EN ESPAÑOL DE LA TESIS DOCTORAL

5.1 MOTIVACIÓN DE LA TESIS DOCTORAL

Las máquinas eléctricas son una de las principales tecnologías que hacen posible las energías renovables y los vehículos eléctricos. La necesidad constante de incrementar la capacidad de potencia para generar más energía o para impulsar vehículos cada vez más grandes, ha motivado la investigación y el desarrollo en el área de las máquinas multifásicas las cuales, gracias a su número de fases, permiten no sólo manejar más potencia con menos pulsaciones de par y contenido armónico en la corriente que las máquinas trifásicas convencionales [1], sino que también permiten obtener una mayor tolerancia a fallos, aumentando el interés de su implementación en aplicaciones donde la fiabilidad juega un papel importante por razones económicas y de seguridad.

Aunque hasta el día de hoy la implementación de sistemas multifásicos está lejos de ser convencional en la industria, es posible pensar que con la implementación de generadores eólicos cada vez más grandes y el interés que existe por desarrollar aviones, barcos y vehículos eléctricos (aplicaciones con un alto estándar de seguridad y fiabilidad), las máquinas y sistemas multifásicos, tendrán un papel importante en el futuro.

Los recientes trabajos de investigación en el área de sistemas multifásicos se centran en el desarrollo de técnicas que permitan explotar las características específicas y especiales de las máquinas multifásicas, viendo el incremento en el número de fases no como un aumento en la complejidad de implementación, sino como un mayor número de grados de libertad tanto en el diseño como en el control, que pueden mejorar sus prestaciones y fiabilidad, haciéndolas más atractivas para su uso en aplicaciones industriales. Es así como se han desarrollado técnicas de control que permitan operar a alta velocidad o alto par, tolerancia a diferentes tipos de fallos y máquinas con diferentes conexionados de devanados o con sistemas formados por múltiples variadores y máquinas.

La presente tesis doctoral se centra en el estudio de las máquinas multifásicas ante diferentes tipos de fallos, así como en el desarrollo y comparación de estrategias de control capaces de asegurar una correcta operación en situación de post-falta (en este sentido, se considerará el caso más habitual de fallo en este tipo de sistema, consistente en una fase abierta).

5.2 OBJETIVOS

5.2.1 OBJETIVO GENERAL

La extensión del control predictivo para máquinas multifásicas (específicamente el control predictivo de estados finitos basado en modelo) a la operación tolerante a fallos, aprovechando la capacidad de tolerancia a fallos que las máquinas multifásicas poseen, asegurando su funcionamiento de una manera eficiente y controlada.

5.2.2 OBJETIVOS ESPECÍFICOS

- Investigar sobre las máquinas multifásicas, sus ventajas y desventajas, así como sobre su posible aplicación industrial en vehículos eléctricos y en sistemas de generación eólica.
- Analizar el efecto que tienen diferentes tipos de faltas en el sistema multifásico y desarrollar nuevos e interesantes modelos matemáticos del accionamiento multifásico con diferentes tipos de fallos.
- Estudio de diferentes técnicas de control de accionamientos multifásicos en condiciones de pre- y post- falta.
- Identificar las limitaciones del accionamiento multifásico ante un fallo, considerando una máquina de inducción de cinco fases alimentada por un convertidor de dos niveles, y proponer diferentes técnicas de control de faltas, con el fin de asegurar al máximo la optimización de energía.
- Estudiar y analizar las estrategias de control predictivo tradicionales para máquinas de tres fases y extenderlas a las máquinas multifásicas y la tolerancia a fallos.
- Implementar, comparar y valorar el funcionamiento de técnicas tolerantes a fallos basadas en controles de tipo lineal y predictivo, ante diferentes condiciones de operación.

5.3 ORGANIZACIÓN DEL DOCUMENTO

Esta tesis doctoral está organizada siguiendo las directivas dadas por la Universidad de Málaga para la presentación de una tesis doctoral por compendio de artículos científicos. El documento está dividido en tres partes principales. En la primera parte, se presentan la motivación y los objetivos de este trabajo de investigación (*Chapter 1*), junto con las generalidades y el estado del arte de los variadores y las máquinas multifásicas (*Chapter 2*), donde se presenta un estudio de las publicaciones científicas en el campo del modelado y el control en pre- y post- falta. En la segunda parte, se presentan las contribuciones de esta tesis doctoral (*Chapter 3*). Las primeras dos contribuciones están basadas en la propuesta de un control tolerante a fallos mediante técnicas de control predictivo basado en modelo para máquinas de inducción de cinco fases ante una falta de fase abierta (*Journal paper 1*) y el posterior estudio de dicho control ante el fallo del disparo de los IGBT's de una fase (*Journal paper 2*). La tercera contribución está basada en el análisis comparativo entre el control predictivo tolerante a fallos propuesto y un control tolerante a fallos basado en reguladores resonantes, permitiendo identificar las ventajas y desventajas que posee cada tipo de control frente a un fallo de fase abierta (*Journal paper 3*). Por último, en la tercera parte de este documento (*Chapter 4*) se presenta un resumen de los artículos científicos, trabajos de congreso, patentes y participación en proyectos de investigación realizados durante la realización de esta tesis doctoral (pero que no fueron incluidos como contribuciones principales de la tesis), junto con las conclusiones y trabajo futuro.

5.4 ACCIONAMIENTOS MULTIFÁSICOS: GENERALIDADES, MODELADO Y CONTROL

Los accionamientos multifásicos, basados en máquinas eléctricas con más de tres fases, fueron propuestos hace aproximadamente 50 años. Sin embargo, sólo han sido analizados por parte de la comunidad científica durante los últimos años, gracias al desarrollo de semiconductores con mayor capacidad de potencia y alta frecuencia de conmutación, tales como los IGBT's, y a la aparición de unidades microelectrónicas de control con elevada capacidad de procesamiento, tales como los DSP's y las FPGA's [1], permitiendo controlar de manera eficiente y apropiada sistemas con máquinas multifásicas. Esto ha permitido que los accionamientos multifásicos se hayan propuesto recientemente en aplicaciones de alto rendimiento, alta potencia y fiabilidad, tales como la generación de energía eólica [2], el sector aeroespacial [3] y la propulsión de vehículos eléctricos [4, 5], o en el desarrollo

de ascensores de velocidad ultra rápida empleando una máquina de imanes permanentes de nueve fases controlada por tres convertidores trifásicos [6]. Otros ejemplos de aplicaciones de alta potencia, fiabilidad y capaces de cumplir con estándares industriales, viables y basados en accionamientos multifásicos aparecen en el ámbito de la propulsión naval [7, 8] y en la refrigeración de una instalación de gas natural licuado (LNG por sus siglas en inglés). En el primer caso, como ejemplos de aplicaciones de máquinas multifásicas, un motor de inducción de 20 MW con quince fases y con tres neutros independientes, controlado por tres convertidores de cinco fases de la empresa Alstom es incorporado a un prototipo desarrollado por la marina de Estados Unidos [7]. Mientras que en el segundo caso, se diseña y se emplea para el sistema de refrigeración de una instalación de LNG, un motor de doce fases, 45 MW, 7200 voltios con cuatro neutros independientes, controlado por cuatro convertidores de tipo cascada multinivel trifásicos con IGBT's [8].

Algunas de las ventajas de los accionamientos multifásicos, al ser comparados con accionamientos trifásicos convencionales, son [1, 9, 10, 11]:

1. Mejor distribución espacial de la fuerza magnetomotriz (MMF por sus siglas en inglés) en el entrehierro de la máquina [9], reduciendo las pérdidas en el cobre en el rotor.
2. Menor contenido de armónicos en las corrientes del estator.
3. Menores pulsaciones de par. Las máquinas multifásicas son menos susceptibles a las pulsaciones de par a baja frecuencia, causadas por los armónicos de orden $(2n \pm 1)$ en una máquina de n-fases.
4. Menor contenido de armónicos en la corriente del DC-Link.
5. Mejor distribución de potencia por fase. Para una potencia nominal dada, la corriente nominal por cada fase disminuye conforme aumentan el número de fases.
6. Mayor número de grados de libertad en el control permitiendo:
    a. Accionamientos con alta capacidad de par. En máquinas multifásicas con devanados concentrados, es posible utilizar los componentes armónicos de bajo orden de las corrientes (tercer armónico en una máquina de cinco fases, tercero y quinto en una máquina de siete fases) para incrementar la capacidad de producción de par [12, 13].
    b. Accionamientos con múltiples motores. Al conectar en serie los devanados del estator de un grupo de máquinas multifásicas con devanados distribuidos, es

posible controlar independientemente con sólo un convertidor de potencia, diferentes números de máquinas [14, 15].

c. Accionamientos tolerantes a fallos. Más fiables que las máquinas trifásicas. En el caso de un fallo en una máquina trifásica, la máquina puede continuar funcionando como una máquina monofásica pero necesita equipo externo para arrancar y para controlar las oscilaciones de par. Por otra parte, una máquina de n-fases con una o más de sus fases en condición de fallo (dependiendo del número total de fases *n* y sus características constructivas), puede continuar generando un campo rotatorio sin requerir equipo externo siempre y cuando el número de fases abiertas no sea mayor a $(n-3)$, a cambio de una menor capacidad de par y de corriente.

Las máquinas multifásicas se clasifican tradicionalmente dependiendo de la distribución de sus devanados como concentrados o distribuidos, o en función de la disposición de sus devanados como simétricas o asimétricas. Los accionamientos electromecánicos de tipo multifásico de devanados concentrados generan un flujo de campo con un alto contenido armónico cuando se les aplica una tensión de estator sinusoidal, el cual puede ser utilizado para aumentar la capacidad de producción de par eléctrico, frente a una distribución casi sinusoidal de la fuerza magnetomotriz conseguida con el bobinado distribuido donde los armónicos en el flujo sólo generan pérdidas electromagnéticas. Por otra parte, las máquinas simétricas están formadas por devanados desplazados $2\pi/n$ entre sí, mientras que las máquinas asimétricas están formadas por grupos de devanados independientes desplazados entre ellos un ángulo eléctrico π/n.

Del mismo modo, las máquinas multifásicas se pueden clasificar por el número par o impar de fases que poseen [17, 18, 19] y si el número de fases que poseen es múltiplo de tres [20, 21, 22]. Entre las máquinas con un número par de fases, las máquinas de seis fases son las más usadas en el ámbito científico. Este tipo de máquinas pueden tener una distribución asimétrica (30°) o simétrica (60°) de devanados y uno o dos neutros. Sin embargo, la estructura más común se basa en dos juegos de devanados trifásicos asimétricos con dos neutros independientes, accionamientos usualmente denominados como máquinas con doble devanado trifásico asimétrico. Este tipo de máquinas han sido ampliamente investigadas, siendo posible encontrar trabajos centrados en su modelado [22], técnicas de control específicas (basadas en control orientado en campo [23, 24, 25, 26], control directo de par [27, 28] o control predictivo [29, 30]) o estrategias de modulación [31, 32, 33]. Por el contrario,

las máquinas con un número impar de fases (no múltiplo de tres) son a veces preferidas por su estructura simétrica. Este tipo de máquinas se construyen con devanados en configuración estrella, un único neutro y con devanados concentrados o distribuidos. El caso más habitual dentro de este grupo es el caso de la máquina de cinco fases, para las cuales se puede encontrar en la literatura científica diferentes tipos de técnicas de modulación y control, basadas en modulación por ancho de pulsos con portadora o modulación con vectores espaciales [34, 35, 36], control de campo orientado [13, 37, 38], control directo de par [39, 40] y control predictivo [41, 42], que buscan sacar provecho de las ventajas de las máquinas multifásicas, manteniendo tensiones sinusoidales o no sinusoidales, dependiendo del tipo de distribución de los devanados y modo de funcionamiento.

Más aún, dependiendo de si el número de fases de la máquina es un número primo o no, es posible realizar diferentes conexiones en los devanados del estator, obteniendo máquinas con un neutro, múltiples neutros o con configuración poligonal. El efecto de la conexión de los devanados del estator bajo diferentes puntos de operación ha sido analizado en [43, 44, 45], donde se ha demostrado que es posible obtener diferentes prestaciones de operación de par/velocidad dependiendo del tipo de conexión de la máquina. Una máquina de n-fases puede ser conectada de $((n+1)/2)$, configuraciones diferentes. Por ejemplo, una máquina de cinco fases puede ser conectado en configuración estrella, pentágono y poligonal. Dependiendo del tipo de conexión, la magnitud de la corriente y tensión que cae en los devanados, para una misma tensión de DC-Link y capacidad de potencia, varía. Es así como la tensión que cae sobre el devanado es mayor en las configuraciones de tipo poligonal o pentágono que en estrella, mientras que las corrientes son mayores en la conexión en estrella seguidas por la configuración en pentágono y poligonal, respectivamente. Debido a esto, la configuración en estrella permite obtener un alto par con baja velocidad, mientras que la configuración en pentágono proporciona menor par que la configuración en estrella pero con una mayor velocidad y la configuración poligonal proporciona una operación de alta velocidad pero a menor par que en los casos anteriores.

Como se demuestra en [46, 47] es posible controlar múltiples máquinas multifásicas conectadas en serie desde un único convertidor de potencia, considerando ciertos cambios en el orden de las fases para desacoplar el par y flujo generados en las máquinas por las corrientes impuestas. Las configuraciones de los accionamientos multimotor han sido estudiadas con máquinas de cinco y seis fases [48, 49, 50], y considerando topologías con máquinas de diferente número de fases o tipo de máquina [51, 52]. Al implementar múltiples bucles de control de campo orientado (FOC por sus siglas

en inglés), uno por cada par de corrientes según la descomposición en espacios vectoriales (VSD por sus siglas en inglés), es posible aprovechar los grados de control adicionales que las máquinas multifásicas poseen y controlar, por ejemplo, dos máquinas independientes con un único variador de cinco fases. La disposición de los devanados entre las máquinas se realiza de tal forma que la corriente en ejes d-q de una de las máquinas representa la corriente en coordenadas x-y para otra, en la que su valor no tiene influencia en la producción de par, y viceversa. Es así como las corrientes d-q son utilizadas para controlar la producción de par y flujo en la primera máquina mientras que las corrientes en x-y son usadas, de manera similar, para la producción de par y flujo en la segunda máquina. Cabe resaltar que la configuración multimotor genera un incremento en las perdidas en el cobre y no posee tolerancia a fallos, debido a que los grados de libertad necesarios para la operación post-falta son empleados para controlar independientemente cada una de las máquinas. Asimismo la configuración de variadores multimotor es sólo válida para accionamientos con bobinados distribuidos y no es posible con máquinas de devanados concentrados, en los que las corrientes en x-y generarían par y, por consiguiente, no sería posible controlar independientemente cada máquina.

En general, se puede decir que los accionamientos multifásicos constituyen una tecnología interesante, formada por un gran número de máquinas y convertidores de potencia, y con características especiales que las hacen interesantes en aplicaciones industriales concretas como pueden ser los casos del transporte eléctrico y la generación de energía, lo que justifica el interés actual por esta tecnología a nivel de investigación, y en la búsqueda de estándares industriales y de seguridad válidos que permitan aprovechar los beneficios de este tipo de máquinas a precios competitivos de mercado.

5.5 CONTRIBUCIONES

Esta tesis doctoral se centra en la extensión del control predictivo de estados finitos basado en modelo (FCS-MPC por sus siglas en inglés) para accionamientos multifásicos a la operación tolerante a fallos, asegurando un funcionamiento eficiente y controlado en situación post-falta. Con el fin de contar con un modelo preciso del sistema en situación de falta, adecuado para una estrategia FCS-MPC, se realizaron trabajos de investigación en el estudio matemático de las ecuaciones del modelo de la máquina en condiciones de pre- y post- falta considerando diferentes tipos de faltas, permitiendo establecer el efecto que las condiciones de fallo tienen en el comportamiento del sistema. Se

desarrollaron modelos de simulación de una máquina de inducción de cinco fases, considerando faltas de fase abierta y en el disparo de los IGBT's de una fase, permitiendo el diseño y validación del controlador FCS-MPC tolerante a fallos, donde los resultados obtenidos fueron presentados en diversos congresos internacionales. La posterior implementación y validación experimental del control tolerante a fallos propuesto (en la bancada de pruebas del laboratorio), dio lugar a la publicación de dos de los artículos científicos presentados en esta tesis. Del mismo modo, se desarrolló un control tolerante a fallos basado en controladores lineales (de tipo resonante), teniendo en cuenta los esquemas propuestos en publicaciones científicas recientes y se realizó una comparativa entre el control tolerante a fallos basado en FCS-MPC y el controlador resonante ante un fallo de fase abierta, mediante resultados de simulación y experimentales, dando lugar a la publicación en un congreso internacional y en un artículo de revista científica.

Las principales contribuciones de esta tesis han sido aceptadas y se han publicado como trabajos de investigación en la revista científica *IEEE Transactions on Industrial Electronics* entre los años 2013/2015. A continuación, se realiza un resumen de cada uno de los artículos publicados, resaltando sus aspectos más importantes.

5.5.1 CONTROL TOLERANTE A FALLOS BASADO EN FCS-MPC PARA ACCIONAMIENTOS MULTIFÁSICOS ANTE UN FALLO DE FASE ABIERTA

En el primer artículo científico titulado, "Speed Control of Five-Phase Induction Motors with Integrated Open-Phase Fault Operation using Model-Based Predictive Current Control Techniques", se presenta un nuevo control predictivo basado en FCS-MPC para la operación post-falta de un accionamiento de cinco fases ante el fallo de una fase abierta (Fig. 3.1).

El funcionamiento del control basado en FCS-MPC depende en gran medida de la precisión del modelo del sistema utilizado y, por consiguiente, del modelo matemático del accionamiento multifásico en situación de falta considerado. Se desarrolló un modelo detallado del accionamiento multifásico con una fase abierta y se establecieron los efectos del fallo en las ecuaciones del modelo de la máquina de inducción de cinco fases. Se estableció que el fallo de una fase abierta genera términos asimétricos en las impedancias del estator y del rotor (en el plano α-β), generando a su vez corrientes no circulares de estator en el plano α-β (Fig. 3.2b). En este caso la corriente en la fase en fallo es cero, mientras que su tensión es ahora dada por el término de la fuerza contra electromotriz

(Back-EMF por sus siglas en inglés). Por consiguiente, la tensión del neutro de la máquina oscila y la matriz de tensiones de fase debe ser modificada de tal forma que considere este efecto.

Para manejar los términos asimétricos, se ha propuesto una matriz modificada de Clarke (150) que mantiene los componentes de impedancia de rotor/estator y Back-EMF circulares en el plano α-β (Fig. 3.2c). La principal ventaja que presenta la utilización de la matriz propuesta (150), al compararla con diferentes trabajos de investigación publicados hasta la fecha, es que su implementación permite obtener términos simétricos sin la necesidad de contar con una matriz de rotación modificada, simplificando su implementación y reduciendo el número de cambios a realizar en el control para la operación post-falta.

$$[T_{c\_mod}] = \frac{2}{5}\begin{bmatrix} \cos(\vartheta)-1 & \cos(2\vartheta)-1 & \cos(3\vartheta)-1 & \cos(4\vartheta)-1 \\ \sin(\vartheta) & \sin(2\vartheta) & \sin(3\vartheta) & \sin(4\vartheta) \\ \sin(2\vartheta) & \sin(4\vartheta) & \sin(6\vartheta) & \sin(8\vartheta) \\ 1 & 1 & 1 & 1 \end{bmatrix} \tag{150}$$

Del mismo modo es necesario tener en cuenta en el modelo del accionamiento multifásico la oscilación de la tensión del punto neutro durante la operación post-falta, con el fin de asegurar que el controlador FCS-MPC cuenta con un modelo detallado del sistema que le permita elegir el vector de tensión apropiado. Para ello, el término de la Back-EMF de la fase en fallo es incluida en la matriz de tensiones (151), dada por el segundo término y dependiente de la corriente de estator y rotor en el eje α.

$$\begin{bmatrix} v_{bs} \\ v_{cs} \\ v_{ds} \\ v_{es} \end{bmatrix} = \frac{V_{dc}}{4}\begin{bmatrix} 3 & -1 & -1 & -1 \\ -1 & 3 & -1 & -1 \\ -1 & -1 & 3 & -1 \\ -1 & -1 & -1 & 3 \end{bmatrix}\begin{bmatrix} S_b \\ S_c \\ S_d \\ S_e \end{bmatrix} - \frac{L_m\frac{di_{s\alpha}}{dt}+L_m\frac{di_{r\alpha}}{dt}}{4}[I_4] \tag{151}$$

Una vez desarrollado el modelo matemático del sistema en situación de fallo, se diseñó el control basado en FCS-MPC. El controlador diseñado está formado por un bucle externo de velocidad y un bucle interno predictivo en corriente. El controlador predictivo en corriente fue diseñado e implementado para trabajar en situaciones de pre- y post- falta, con el fin de demostrar su capacidad de funcionar en pre- o post- falta y de gestionar el sistema durante el transitorio asociado a la aparición del fallo. Cabe resaltar que la función de coste *J* es la misma en situación de pre- o post- falta:

$$J = A|\overline{\overline{\imath_{s\alpha}}}| + B\left|\overline{\overline{\imath_{s\beta}}}\right| + C|\overline{\overline{\imath_{sx}}}| + D\left|\overline{\overline{\imath_{sy}}}\right| \tag{152}$$

Donde los términos *A*, *B*, *C*, *D* representan el peso de cada variable en la función de coste y cada término de corriente en los ejes α-β-x-y, se definen como:

$$\overline{\overline{\imath_{s\alpha}}} = i^*_{s\alpha}(k+1) - \hat{\imath}_{s\alpha}(k+1),\ \overline{\overline{\imath_{s\beta}}} = i^*_{s\beta}(k+1) - \hat{\imath}_{s\beta}(k+1) \tag{153}$$

$$\overline{\overline{i_{sx}}} = i_{sx}^{*}(k+1) - \hat{i}_{sx}(k+1),\ \overline{\overline{i_{sy}}} = i_{sy}^{*}(k+1) - \hat{i}_{sy}(k+1) \quad (154)$$

Únicamente el factor *C* para la corriente en la componente *x* debe ser modificado, siendo igual a cero durante la operación post-falta. Se adoptaron dos criterios de control para el funcionamiento post-falta, "*Minimum Copper Loss*" y "*Minimum Derating*", denotados como ML y MD, respectivamente. Según el criterio seleccionado, las referencias de corriente en post-falta cambian, tal y como se presenta en la Fig. 3.1, donde se muestra que en ambos criterios la referencia de corriente del eje *x* queda fija a $-i_{s\alpha}$, mientras que la referencia de corriente en el eje *y* es cero para el criterio de ML y -26.31% de la componente de corriente en el eje β para el de MD. Los resultados obtenidos permiten concluir que la implementación del criterio MD permite al accionamiento eléctrico generar un par eléctrico máximo un 8% superior al alcanzado con el criterio de ML, siendo el par máximo alcanzable en post-falta con el criterio de ML un 56% del par nominal de la máquina en pre-falta y un 64% con el criterio de MD.

Cabe resaltar, que aunque la detección de faltas no se ha considerado en esta tesis doctoral, el efecto que tiene el retraso entre el momento en que sucede la falta, su detección y la reconfiguración del control para el funcionamiento post-falta, se ha considerado en algunos de los ensayos experimentales realizados. Teniendo en cuenta el tiempo estimado en que se demora un sistema en detectar un fallo, según la literatura científica disponible hasta el momento, se tomó un tiempo de transición entre pre- y post- falta de 40 ms. Los resultados obtenidos permiten concluir que aunque el controlador predictivo ofrece una adecuada operación post-falta si ésta es detectada de manera casi instantánea, el controlador pierde por completo la capacidad de control durante el tiempo de transición debido a la diferencia que existe entre el modelo utilizado en el FCS-MPC y el sistema físico en situación de fallo.

5.5.2 FALLO EN EL DISPARO DE LOS IGBT'S EN ACCIONAMIENTOS DE INDUCCIÓN MULTIFÁSICOS TOLERANTES A FALLOS

En el segundo artículo científico titulado "IGBT-Gating Failure Effect on a Fault-Tolerant Predictive Current Controlled 5-Phase Induction Motor Drive", se analiza un segundo tipo de fallo en el accionamiento multifásico. El efecto que tiene el fallo en el disparo de los dos IGBT's de una misma fase, perdiendo su capacidad de encender y por lo tanto la controlabilidad de una rama, es analizada desde el punto de vista teórico y experimental. Se demostró que los diodos de libre

circulación de la fase en fallo (D_1 y D_2) son capaces de conducir en diferentes instantes de tiempo durante este tipo de faltas, conectando la fase en fallo al bus negativo (*N*) o positivo (*P*) del convertidor si las condiciones (155)-(157) se cumplen. Este efecto genera la circulación de corrientes no controladas en la fase en fallo. Como consecuencia, la topología del accionamiento eléctrico estará cambiando constantemente, pasando de un sistema de cuatro fases (variador de cinco fases con una fase abierta) a un sistema con cuatro fases controladas y una no controlada (Fig. 3.3), generándose debido al fallo una oscilación en la tensión de neutro del estator que debe ser considerada en la estrategia de control.

$$D_1 - ON: V_{D1} = v_{as} + V_{CM} - 0.5V_{DC} \geq V_\gamma \quad (155)$$

$$D_2 - ON: V_{D2} = v_{as} + V_{CM} + 0.5V_{DC} \leq -V_\gamma \quad (156)$$

$$V_{CM} = V_{sN} - \frac{V_{DC}}{2} = \frac{1}{5}(V_{aN} + V_{bN} + V_{cN} + V_{dN} + V_{eN}) - \frac{V_{DC}}{2} \quad (157)$$

Donde V_{D1} y V_{D2} representan la tensión que cae sobre cada uno de los diodos de libre circulación, V_γ la tensión de conducción del diodo, v_{as} es la tensión entre el punto medio de la rama y el neutro de la máquina, V_{sN} es la tensión entre el punto neutro de la máquina (*s*) y el bus negativo del convertidor, dado por la suma de la tensión a la salida de la rama del inversor ($i = a, b, c, d, e$) con respecto a *N*, y V_{CM} es la tensión de modo común (CMV) que relaciona la tensión entre el punto neutro de la máquina y el punto medio del DC-Link.

En general, cuando este tipo de faltas ocurren, la fase en fallo es desconectada de la máquina eléctrica, reconfigurando el variador multifásico para funcionar con el fallo de fase abierta. Sin embargo, esta estrategia requiere de componentes eléctricos adicionales en el convertidor para poder desconectar físicamente la fase del convertidor de la máquina eléctrica que falló, incrementando el coste y la complejidad del convertidor de potencia. Se propone por el contrario la gestión de este tipo de faltas mediante técnicas de control, reduciéndose así complejidad y costes extra, a cambio de la aparición de una oscilación no controlada en la tensión del neutro del estator.

Como se ha comentado anteriormente, los controladores de tipo predictivo necesitan un modelo detallado del sistema a controlar. Por tanto, el cambio en la configuración de la topología del accionamiento eléctrico durante la gestión del fallo hace que la descripción del sistema cambie en función de la presencia o no del mismo, siendo más compleja y aumentando el coste computacional de la estrategia de control. Sin embargo, al analizar los vectores de tensión disponibles en situación post-falta se puede concluir que el efecto que tiene la fase no controlada resulta en una pequeña desviación de los vectores disponibles después del fallo de fase abierta, bien a la izquierda o a la

derecha, dependiendo del diodo de libre circulación que esté conduciendo. Por ello, el uso del controlador FCS-MPC tolerante a fallos de fase abierta, podría ser utilizado también para controlar el accionamiento multifásico durante fallos en los disparos de los IGBT's de una fase a cambio de una pequeña disminución en sus prestaciones.

La capacidad de controlar este tipo de faltas mediante el controlador FCS-MPC tolerante a fallos se demostró experimentalmente considerando diferentes puntos de operación (i.e. estado estable, cambio en la velocidad de referencia y la transición de pre- a post- falta) y los criterios de ML y MD, bajo diferentes valores de par de carga y en algunos ensayos con retrasos en la detección y reconfiguración a post-falta de 40 ms. Con el fin de determinar la disminución de las prestaciones del controlador, se realizaron ensayos en los mismos puntos de operación considerando faltas de fase abierta y de disparo en los IGBT's, permitiendo determinar el efecto que tiene el no considerar un modelo detallado del sistema en el FCS-MPC en el caso del fallo en los disparos de los IGBT's.

En general, se deduce que la corriente no controlada a través de los diodos de libre circulación reduce ligeramente el par de carga máximo alcanzable, incrementando las pérdidas en el cobre. Más aún, esta reducción en el par de carga máximo alcanzable en post-falta es mayor si se considera el tiempo de transición entre la detección del fallo y la reconfiguración del control. Sin embargo, si el accionamiento multifásico no se encuentra trabajando en el máximo punto de operación en post-falta, el efecto es despreciable. Como consecuencia, la degradación en las prestaciones del control es limitada y puede ser considerada como aceptable si se considera el coste computacional y el aumento en la complejidad de implementación de un modelo detallado del accionamiento con fallo en los disparos de los IGBT's.

5.5.3 Análisis Comparativo entre Controles Tolerantes a Fallos Basados en FCS-MPC y Controles Lineales

Finalmente, en el tercer artículo científico titulado "Comparative Study of Predictive and Resonant Controllers in Fault-Tolerant Five-phase Induction Motor Drives" se realiza un análisis comparativo entre el control tolerante a fallos basado en FCS-MPC con un control lineal de tipo resonante ante un fallo de fase abierta, mediante una serie de ensayos experimentales (i.e. estado estable, cambio en la velocidad de referencia y transición entre pre- y post- falta). Los ensayos realizados se llevaron a cabo operando el accionamiento multifásico con el máximo para de carga

post-falta establecido según cada criterio de control, siendo este de (T_L=0.56*T_n) para el criterio de ML y de (T_L=0.64*T_n) para el criterio de MD, considerando además la operación en estado estable y la transición de pre- a post- falta con y sin retraso en la detección y reconfiguración del control después de la falta.

Aunque los dos controladores son capaces de asegurar una correcta operación post-falta, manteniendo una MMF circular, alcanzando mínimas perdidas y máximo par por amperio y reduciendo las vibraciones del par, su implementación es completamente diferente debido a los efectos que tienen las asimetrías en las ecuaciones de la máquina en post-falta en cada estrategia de control. En el caso del control basado en FCS-MPC (Fig. 3.1), el modelo del accionamiento multifásico debe ser modificado para incluir el efecto que tiene el fallo en las ecuaciones del sistema de forma tal que el controlador pueda proporcionar predicciones más precisas. Por consiguiente, se utiliza una transformación modificada de Clarke para compensar las asimetrías de la máquina en el espacio α-β y la fuerza contra electromotriz es considerada para la estimación del vector de tensión. Por otro lado, si se implementa la estrategia basada en control lineal (Fig. 3.4), el modelo de la máquina eléctrica y la descomposición de vectores espaciales se mantienen como en pre-falta debido a que la asimetría en las impedancias de la máquina en el espacio α-β no afectan el funcionamiento del controlador y no es necesario considerar la Back-EMF en las ecuaciones de tensión. Sin embargo, es necesario implementar reguladores de tipo resonante (PR por sus siglas en inglés) para poder controlar las referencias de corriente oscilantes en el eje *x*-*y*.

Con el fin de comparar el funcionamiento de los controladores bajo las mismas condiciones de funcionamiento, se implementaron como se muestra en la Fig. 3.1 y Fig. 3.4, tanto en pre- como en post- falta, con un bucle externo de control (FOC) de velocidad y flujo en el eje *d*-*q* con reguladores PI convencionales. La referencia de corriente en *d* se fija a un valor constante y el valor de referencia en *q* es determinado por un controlador PI basado en el error entre la velocidad medida y la de referencia. Durante el funcionamiento pre-falta, las referencias de corriente en *x*-*y* son cero, utilizándose controladores PI en el esquema de control para estas componentes. En el caso del controlador predictivo y pre-falta, se emplean la matriz de transformación de Clarke, la matriz de tensión convencional y la función de coste que considera las corrientes en *x*-*y*. Cuando sucede el fallo, el bucle de control interno de cada esquema de control es modificado de forma tal que pueda operar en situación de post-falta, utilizando reguladores PR para las componentes *x*-*y* en el control lineal y modificando el esquema FCS-MPC según lo presentado en la sección 5.5.1.

Los resultados obtenidos permiten concluir que los dos controladores tolerantes a fallo aseguran una correcta operación post-falta ofreciendo características similares. Ambos aseguran además un buen seguimiento de corriente implementando los criterios de ML o de MD, en sus respectivos puntos máximos de operación. Como era de esperar, la respuesta del controlador predictivo es mucho más rápida a costa de un mayor rizado en el par y en la corriente. Sin embargo, su funcionamiento se ve mucho más afectado en la transición de operación de pre- a post- falta debido a las diferencias que existen entre el modelo implementado en el control y el sistema físico durante la transición.

En cuanto a la implementación, cabe resaltar que el número de cambios necesarios para adaptar el control a la operación en post-falta es mucho mayor con el control basado en FCS-MPC que con el basado en PR, debido a la necesidad de considerar la oscilación de la tensión en el punto neutro de la máquina y de modificar la matriz de transformación de Clarke. No obstante, también debe tenerse en cuenta que para obtener un correcto funcionamiento con el esquema basado en PR, los diferentes reguladores deben ser ajustados para cada punto de operación, aumentando el tiempo necesario para su puesta en marcha y limitando los puntos de trabajo del sistema a aquellos puntos para los cuales se han ajustado los reguladores.

5.6 CONCLUSIONES

Las principales conclusiones de esta tesis doctoral son:

1. La operación controlada post-falta de un accionamiento multifásico es viable sin necesidad de equipos electrónicos adicionales.
2. Durante un fallo de fase abierta las ecuaciones de la máquina deben ser modificadas con el fin de incluir el efecto que tiene la pérdida de una fase. En primer lugar, se pierde un grado de libertad en el control y es necesario implementar una matriz modificada de la transformada de Clarke con el fin de obtener términos de impedancia y Back-EMF simétricos en el espacio α-β. Del mismo modo, la corriente en la fase en fallo es cero, mientras que la tensión está dada por el término de la Back-EMF, que debe ser considerado en la matriz de tensiones de fase, obteniéndose una matriz diferente a la utilizada en situación de pre-falta.

3. Dependiendo de las características específicas de la aplicación y del tipo de accionamiento multifásico, se pueden implementar diferentes criterios de control, permitiendo reducir las pérdidas en el cobre u obtener el máximo par durante la operación en post-falta.
4. El control basado en FCS-MPC puede ser implementado para la operación post-falta. La velocidad con que los controladores predictivos son capaces de seguir las variables de referencia hace que la reconfiguración del sistema de pre- a post- falta sea una de las grandes ventajas que presenta esta técnica al compararse con controladores de tipo lineal, cuya respuesta es más lenta.
5. Debido a la necesidad del control basado en FCS-MPC de contar con un modelo detallado del sistema a controlar, el retraso en la detección del fallo representa una importante desventaja de esta técnica a tener en cuenta en su implementación en aplicaciones industriales puesto que, según se deduce de los resultados obtenidos, durante este periodo de tiempo el controlador pierde por completo la capacidad de controlar el accionamiento multifásico.
6. Ante las mismas características de funcionamiento, el controlador tolerante a fallos de fase abierta basado en FCS-MPC puede también controlar el accionamiento durante el fallo en el disparo de los IGBT's de una fase sin forzar la total apertura de la misma, a cambio de una ligera disminución en el par máximo alcanzable. Aunque el controlador predictivo está diseñado considerando las ecuaciones matemáticas del sistema durante el fallo de una fase abierta, el efecto que tiene el fallo en los disparos de los IGBT's de una fase se puede ver como una pequeña desviación de los vectores espaciales de tensión que se tienen durante el fallo de fase abierta (la fase no está abierta en realidad, al seguir conectado el diodo de libre circulación en anti paralelo al IGBT). Por tanto, aunque no se cuente con un modelo detallado del accionamiento ante este tipo de fallo, la operación controlada del accionamiento es posible y su efecto sólo se nota en la reducción del máximo par alcanzable.
7. Los controladores lineales basados en reguladores de tipo PI y PR pueden ser implementados satisfactoriamente para la operación en estado estable (en pre- o post-falta) y la transición entre pre- y post- falta, sin la necesidad de considerar el efecto que tiene la falta en el modelo matemático del accionamiento multifásico.

8. Al contrario de lo que se observa en los controladores tolerantes a fallos basados en FCS-MPC, los controladores lineales no se ven ampliamente afectados por el retraso entre la detección del fallo y la reconfiguración del sistema y, por consiguiente, ofrecen un mejor funcionamiento durante la transición de pre- a post- falta.
9. Una vez que la falta es detectada, el controlador basado en FCS-MPC es capaz de seguir las variables de referencia mucho más rápido que los controladores lineales, a cambio de un mayor rizado en la corriente y el par.
10. La mayor desventaja de los controladores tolerantes a fallos basados en PR es que las constantes de los diferentes reguladores PI deben ser ajustadas, aumentando la complejidad de su implementación y limitando el funcionamiento del accionamiento multifásico a los puntos de operación para los cuales han sido ajustados los reguladores.

5.7 RESUMEN DE TRABAJOS DE INVESTIGACIÓN ADICIONALES

La Tabla I contiene un resumen de los artículos de conferencia, revista científica, patentes, capítulos de libro y proyectos de investigación en los que ha participado el doctorando a lo largo del periodo de desarrollo de esta tesis doctoral. Algunos de estos trabajos no han sido incluidos en este documento por no considerarse propiamente contribuciones del doctorando.

Tabla I. Resumen de trabajos realizados durante la tesis doctoral.

	Número
Artículos de Conferencia	7
Artículos en Revista Científica	6
Patentes	1
Capítulos de Libro	2
Participación en Proyectos de I+D	3
PFC codirigidos	2

5.8 TRABAJO FUTURO

Como trabajo futuro relacionado con esta tesis se plantean los siguientes temas:

1. Detección de faltas mediante técnicas basadas en modelo. Aprovechando el modelo matemático detallado desarrollado para implementar el control FCS-MPC post-falta, un posible trabajo futuro puede ser detectar un fallo en el accionamiento multifásico al comparar las corrientes medidas en la máquina con las esperadas, según la información proporcionada por el modelo predictivo.
2. El análisis de la situación de falta con otras estrategias de control no analizadas hasta la fecha. En particular, la extensión del esquema de control DTC tradicional a la operación post-falta. El conocimiento del modelo del accionamiento multifásico y de los vectores espaciales de tensión disponibles en post-falta, bien sea bajo una falta de fase abierta o de fallo en los disparos de los IGBT's de una fase, hace de la implementación del DTC una opción viable en un futuro cercano.
3. Estudio de la sensibilidad de los parámetros de la máquina en el control pre- y post-falta basado en FCS-MPC. Es previsible que la desviación de los parámetros del modelo de predicción degrade el comportamiento del controlador en situación normal, en fallo y durante la transición entre ambos. El análisis de esta degradación o sensibilidad es un tema que es necesario analizar para conocer la viabilidad de estos controladores en aplicaciones reales.
4. El análisis y extensión del control FCS-MPC tolerante a fallos a la operación de accionamientos multifásicos basados en máquinas de imanes permanentes con fuerza electromotriz no sinusoidal. Aumentando la complejidad del modelo matemático en situación post-falta y las consideraciones a tener en cuenta en la estrategia de control.
5. Operación del control FCS-MPC tolerante a fallos a la velocidad nominal de la máquina y en la región de debilitamiento de campo. Mejorando las características del control para su implementación en aplicaciones de vehículos eléctricos.